CYANOBACTERIAL CIRCADIAN CLOCK

IN VITRO AND IN VIVO

By

Ximing Qin

Dissertation

Submitted to the Faculty of the

Graduate School of Vanderbilt University

in partial fulfillment of the requirements

for the degree of

DOCTOR OF PHILOSOPHY

In

BIOLOGICAL SCIENCES

December, 2010

Nashville, Tennessee

Approved:

Professor Douglas G. McMahon

Professor Daniel Kaplan

Professor Brandt Eichman

Professor Hassane Mchaourab

Professor Carl H. Johnson

To my amazing parents

and

To my beloved wife, Yunfei, infinitely supportive

ACKNOWLEDGEMENTS

This work would not have been possible without the financial support from the National Institute of General Medical Sciences, GM067152, to Dr. Carl Johnson, whom I feel especially indebted to. Dr. Carl Johnson is the mentor not only guiding my Ph.D. thesis research, but also encouraging and inspiring my exploration in biological sciences. His pioneering work of solving the mystery of the circadian clockwork in cyanobacteria, hard-working attitude, and extensive knowledge of sciences are an important part of the treasures I have learned during my graduate studies. Furthermore, I appreciate his critical reading and correcting the manuscript of the thesis.

I am grateful to all of those who gave me guidance and advice on my academic studies and life in general. I would like to thank my committee members, Drs. Douglas McMahon, Daniel Kaplan, Brandt Eichman, and Hassane Mchaourab, for their being supportive and constructive. Also, I acknowledge with gratitude my colleagues in the Johnson lab, especially Dr. Tetsuya Mori for training me on biochemistry and Dr. Yao Xu for teaching me genetics. I also appreciate the help from undergraduate students: Brian Torxler and Cathy Zhang.

Chapter II and III are directly derived from published papers. I should mention many individuals for their assistance and contributions. Specifically, I would like to thank Drs. Ping Zou and Hassane Mchaourab for their helps on fluorescent anisotropy, Dr. Dewight Williams for the electron microscopy, Drs. Mori and Xu for their reagents and

materials. I need to express my special thanks to Dr. Mark Byrne. In both *in vivo* and *in vitro* studies, Dr. Mark Byrne constructed the mathematical models and ran the simulations. Also, I thank many comments and discussions from Drs. Rekha Pattanayek, Martin Egli and Phoebe Stewart.

Finally, I would not have finished my graduate studies without the strong support from my parents, Jucai Qin and Yuzhi Jin, and my beloved wife, Dr. Yunfei Zhang. Nothing has been more important than their understanding, support, and encouragement. I owe much to my wife, who always stands by and shares with me on the journey of pursuing my goals.

TABLE OF CONTENTS

LIST OF TABLES

LIST OF FIGURES

CHAPTER I

INTRODUCTION

This thesis is focused on studying the mechanism by which the core circadian clockwork of the cyanobacterium *Synechococcus elongatus* PCC 7942 works, including (i) elucidating the essential pattern of dynamic protein-protein interactions among three identified core clock Kai proteins, namely KaiA, KaiB and KaiC, and (ii) defining the relationship between the traditional TTFL (transcription translation feedback loop) model and the PTO (post translational oscillator) model within this strain. Circadian rhythms are the intrinsic clocks that organisms use to measure time and anticipate changes in environment such as light and temperature. The clock has been found to exist in prokaryotic and eukaryotic organisms, from cyanobacteria to vertebrates.

Prokaryotic cyanobacteria are the simplest organisms that show robust circadian rhythms (Johnson et al., 2008b). In **Chapter I**, I will introduce a brief history of the studies about the circadian rhythm in cyanobacteria and the advantages of using bioluminescence reporters in the model organism *Synechococcus elongatus* (*S. elongatus* in the following text) PCC 7942. A cluster of three genes, *kaiA*, *kaiB* and *kaiC*, was identified as essential to the clock of this strain (Ishiura et al., 1998). Surprisingly, the proteins encoded by those genes were discovered to reconstitute a 24 hour rhythm of phosphorylation of the KaiC protein in test tubes in the presence of ATP (Nakajima et al.,

2005). Various methods have been applied to study the physical protein-protein interactions among the three Kai proteins *in vivo* and *in vitro*, which will be described in this chapter.

Protein interactions play important roles in many physiological processes, including the circadian clock. In mammals, the clock proteins CRY and PER form functional dimers. Also, the clock-related transcriptional factors (BMAL1 and CLOCK in mice, CYC and CLK in *Drosophila*, WC-1 and WC-2 in *Neuropora*) all form complexes to activate the expression of clock controlled genes. These transcriptional factors all contain PAS domains. None of the Kai proteins share similar structures with those known eukaryotic clock proteins, but the Kai proteins interact in a similar way as do the clock proteins of eukaryotes. Besides the methods and results described in **Chapter I**, I apply Native PAGE (poly-acrylamide gel electrophoresis), plus site-directed mutagenesis to study the dynamic and site-dependent interactions among the Kai proteins in **Chapter II**, and demonstrate solid evidence for KaiA being sequestrated during the daily rhythm.

Biochemical and biophysical studies have shed light on the mechanisms by which the three Kai proteins generate robust circadian rhythms *in vitro* in a simple test tube. However, the eventual goal is to understand the circadian system *in vivo*. The TTFL model (see later in this chapter) was originally proposed for this prokaryotic system, but clearly the PTO (see later in this chapter) is a self-sustained pacemaker that can operate independently of the TTFL. In **Chapter III**, detailed information leads to the conclusion that the PTO is the core pacemaker while the TTFL is a slave oscillator that quickly

damps when the PTO stops.

A robust ~24 hr period is one of the three fundamental properties of a circadian clock. The circadian rhythms, either the phosphorylation of KaiC protein or the bioluminescence, are based on large populations of proteins. If individual proteins are oscillating out of phase with each other, the overall rhythm in the population will not be robust. Monomer exchange has been proposed as the mechanism to synchronize the KaiC protein populations. In **Chapter IV**, I will describe the monomer exchange phenomenon within the core KaiABC clockwork.

The Circadian Rhythm in Cyanobacteria

General knowledge about circadian rhythms

As with us humans who wear accurate wristwatches (or their cellular phones) to organize our daily activities for better performance, many organisms have evolved an endogenous circadian clock to adjust their metabolic activities or to anticipate daily environmental events, such as day/night switches or temperature changes. For example, this endogenous clock regulates the sleep/wake, body temperature and endocrine cycles of human beings (Dunlap et al., 2004).

Circadian rhythms have three diagnostic characteristics. First, in a constant environment, the circadian clock will "free-run" with a period about 24 hours in duration. Second, the clock can entrain to an appropriate environmental cycle (usually a light/dark

or temperature cycle). For example, our daily activities adjust to the new time zone if we travel across several time zones. The final characteristic is that the period of the free-running rhythm is "temperature compensated" within the physiological range, which means the period lengths are similar when measured at different constant ambient temperatures. The first experiment that indicated circadian rhythms are endogenous came from the French astronomer, Jean Jacques d'Ortours deMairan in 1729. He observed that a species of *Mimosa* maintained ~24 rhythms of leaf movement even in darkness for several days (see Page 10 in chapter I of Dunlap et al., 2004). To reflect those oscillations that "free-run" with a period about 24 hours, the word *circadian* was coined from two Latin words **circa** "about" plus **dies** "a day" (Dunlap et al., 2004).

Circadian rhythms in cyanobacteria

Before 1985, it was believed that circadian rhythms were exclusively found among eukaryotes (Johnson 2004). However, many strains of cyanobacteria have the ability to fix nitrogen, which is severely inhibited by the presence of oxygen. Cyanobacteria (chlorophyll containing prokaryotic bacteria) are autotrophic photo-synthetic species that produce oxygen when illuminated. In the search to answer how those two contradictory processes could co-exist within the cells, a rhythm of nitrogenase activity was found in continuous light (LL) from studies in a filamentous cyanobacterium *Oscillatoria* sp. in which the nitrogenase activity peaked in the subjective night (Stal and Krumbein, 1985). Also, a temporal separation of photosynthesis (in the day) and nitrogen

fixation (in the night) was reported from studies in the unicellular marine cyanobacteria *Synechococcus* spp. Miami BG43511 and 43522 (Mitsui et al., 1986). Huang and colleagues further demonstrated that the cyanobacteria clearly exhibit circadian rhythms of nitrogen fixation (Grobbelaar et al., 1986) and amino acid uptake (Chen et al., 1991). Also, they isolated circadian mutants from the studies in the cyanobacterium *Synechococcus* RF-1 (Huang et al., 1993a). The next step was to employ advantageous genetic methods to investigate the fundamental basis for circadian rhythms in the cyanobacteria.

Luciferase reporters in cyanobacteria to probe the circadian rhythms

The unicellular freshwater species *S. elongatus* PCC 7942 is a good model organism to study genetically. It was shown that this organism (originally named *Anacystis nidulans* R2) can be easily transformed with exogenous DNA (Shestakov & Khyen, 1970). Other characteristics that allow genetic manipulation are: it can recombine DNA at homologous sites, receive DNA by conjugation from *E.coli* at high efficiency, express reporter genes, and it has a genome that is relatively small (Golden et al., 1997). The chromosome has recently been completely sequenced and contains approximately 2.7 megabases; around 2600 candidate protein-encoding genes have been identified (Holtman et al., 2005; NC_007604.1 in NCBI GenBank).

Pioneering studies of introducing reporter genes into cyanobacteria were initiated by Drs. Takao Kondo, Masahiro Ishiura, Susan Golden and Carl Johnson back in the

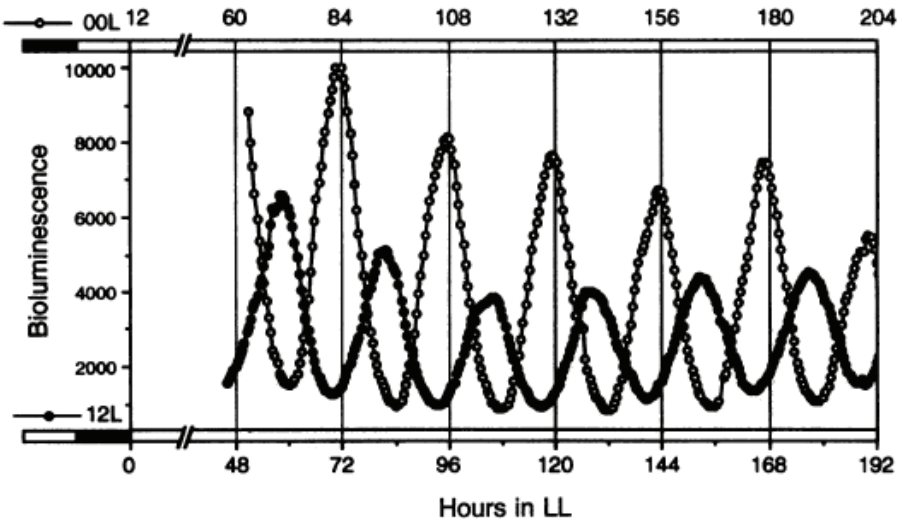

Figure 1-1. Circadian bioluminescence rhythms of the reporter P_{psbAI}::*luxAB* in cyanobacteria *S. elongatus* PCC 7942 (Kondo et al., 1993). Cells were cultured at 30° C and entrained with LD cycles. Open and closed circles represent cultures entrained 12 hr out of phase. (Copyright 1993 National Academy of Sciences, USA)

early 1990s (Ditty et al., 2009). *S. elongatus* PCC 7942 was successfully transformed with a construct in which the *Vibrio harveyi* luciferase gene set *luxAB* was expressed under the control of the promoter for a *Synechococcus* photosystem II gene, *psbAI* (Kondo et al., 1993). This reporter strain was named AMC149. As illustrated in **Figure 1-1**, AMC149 shows robust circadian bioluminescence rhythms, which can be entrained by 24 hr LD cycles (LD12:12). The bioluminescence rhythms fulfill the three diagnostic characteristics of a circadian clock: persistence, entrainability, and temperature compensation (Kondo et al., 1993). Advantages of using a bioluminescence reporter system are: first, bioluminescence has a low background, especially for biomaterials that are auto-fluorescent (in this case cyanobacteria having chlorophyll); second, the relatively high turn-over rate of luciferase makes it a good reporter for dynamic studies;

third, the overt bioluminescence can be monitored automatically and repeatedly without perturbing the organism. With the accomplishment of constructing bioluminescence reporting cyanobacterial strains, the molecular mechanisms underlying the circadian clocks can be dissected with automated monitoring systems.

By using the reporter strains, several important discoveries have been accomplished. Dr. Takao Kondo invented an automated turntable CCD-camera system that is affectionately called in the Johnson lab the "Kondotron" to record the bioluminescence from single colonies on agar plates (Kondo and Ishiura, 1994). This discovery facilitated the screening of mutant strains since an agar plate can contain up to 1,000 mutagenized colonies, and the Kondotron can screen 12 plates in a single experiment. Over 150,000 clones of cells that were chemically mutagenized with ethyl methanesulfonate (EMS) were screened, and a variety of mutants (periods ranging between 16 to 60 hours) were identified (Kondo et al., 1994). With the automated device, circadian rhythms still can be observed in cells with a doubling time of 5 to 10 hours (Kondo et al., 1997). Although a given cell can divide three or four times within one circadian cycle, Dr. Tetsuya Mori has shown that the cell division is gated by the circadian clock such that division is forbidden in the early subjective night phase of LL (Mori et al., 1996). By randomly inserting the promoter-less *luxAB* into the chromosome, a global circadian gene expression pattern was revealed, which indicates all promoters are globally regulated (Liu et al., 1995)

Identification of the core clock genes in cyanobacteria

After over 100 *S. elongatus* mutants were screened (Kondo et al., 1994), rescue experiments performed by using a library of wild-type *S. elongatus* DNA mapped a cluster of three adjacent genes, named *kaiA*, *kaiB*, and *kaiC* (Ishuira et al., 1998). These three genes are clustered on the chromosome and comprise two operons, *kaiA* and *kaiBC*. The former gene is under the control of its own promoter, P_{kaiA}, while the latter two genes are under the control of one promoter, P_{kaiBC}, as a bicistronic operon. Deletion of the entire cluster or loss of any of these genes causes arrhythmia in cyanobacteria. KaiA consists of 284 amino acids, KaiB, 102 amino acids, and KaiC, 519 amino acids. The AMC149 strain in which the original *kaiABC* cluster was replaced with a kanamycin-resistance gene was named ΔKaiABC. Reinsertion of the cluster of *kaiABC* at neutral site II (NSII) into ΔKaiABC completely restored the rhythmicity (Ishuira et al., 1998).

Biochemical functions of the core clock proteins

KaiC has two domains that are similar to each other (Iwasaki et al., 1999). Each half of the KaiC protein contains an ATP-/GTP-binding motif (P loop or Walker's motif A, with the consensus sequence G/AXXXXGKT/S), a Walker's motif B, and two putative catalytic glutamates. In addition, two DXXG motifs that are highly conserved in the GTPase superfamily are found in the N terminal domain of KaiC (Nishiwaki et al., 2000). Indeed, KaiC binds ATP and can autophosphorylate itself *in vitro* (Nishiwaki et al., 2000; Iwasaki et al., 2002). In our lab, we have demonstrated that purified KaiC forms a

hexameric ring in the presence of ATP (Mori et al., 2002). KaiC phosphorylation is stimulated *in vitro* by KaiA (Iwasaki et al., 2002; Williams et al., 2002). On the other hand, KaiB antagonizes the effects of KaiA on KaiC auto-phosphorylation (Williams et al., 2002; Kitayama et al., 2003). KaiC can dephosphorylate *in vitro*; this dephosphoryation is inhibited by KaiA, which is also antagonized by KaiB (Xu et al., 2003). These effects can also be observed *in vivo* (Iwasaki et al., 2002; Xu et al., 2003). Not only is KaiC phosphorylated *in vivo*, but the phosphorylation of KaiC also oscillates with a circadian pattern *in vivo* (Iwasaki et al., 2002). Phosphorylation on the residues S431, T432, and T426 was identified within the crystal structure of KaiC and by mutagenetic analyses (Xu et al., 2004), and the residues S431 and T432 were also identified as the main phosphorylation sites by mass spectroscopy (Nishiwaki et al., 2004). Mutation of any of these phosphorylation sites to alanine abolished rhythmicity *in vivo* (Xu et al., 2004; Nishiwaki et al, 2004).

The schematic of general biochemical functions of Kai proteins is shown in **Figure 1-2**. The KaiC protein is both an autokinase and an autophosphatase. When the KaiC protein itself is incubated in the presence of ATP, the phosphorylation status of KaiC is dependent on the balance of autokinase and autophosphatase activities. Phosphorylation of the KaiC protein causes a mobility shift in SDS-PAGE gels. As shown in **Figure 1-2A**, the autokinase activity dominates at 4ºC, resulting in hyper-phosphorylated KaiC, while the autophosphatase activity dominates at 30ºC, resulting in hypo-phosphorylated KaiC. When binary incubations or ternary mixtures among the three

Kai proteins are incubated with ATP, KaiA can stimulate the autokinase activity or inhibit the autophosphatase activity, while KaiB can antagonize the function of KaiA (**Figure 1-2B**).

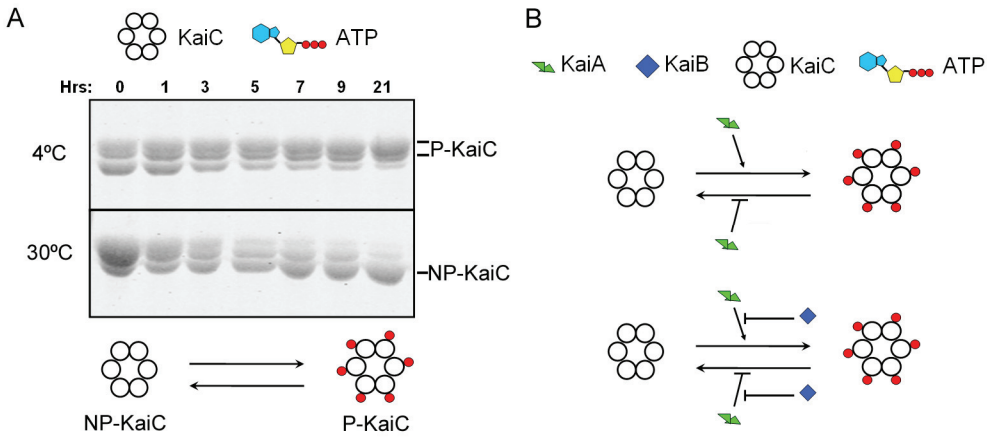

Figure 1-2. The general biochemical functions of Kai proteins. The two triangles (green), diamond (blue), and ring of six circles represent KaiA, KaiB and KaiC respectively. The ATP is drawn as an adenine ring (cyan) with a ribose ring (yellow) and three phosphates (red). **(A)** KaiC is incubated alone with ATP. The balancing of autokinase and autophosphatase is temperature dependent. KaiC is hyper-phosphorylated at 4 ºC (upper gel) and hypo-phosphorylated at 30 ºC (lower gel). **(B)** When proteins are incubated at 30 ºC, KaiA stimulates the autokinase activity or inhibits the autophosphatase activity (upper scheme), and KaiB antagonizes the function of KaiA (lower scheme).

TTFL model proposed in cyanobacteria

The first clock gene, *per*, was identified in *Drosophila* (Reddy et al., 1984). After that, several other clock genes were identified in various eukaryotic organisms. The transcriptional and translational feedback loop (TTFL) model was proposed to explain the oscillation of mRNA and proteins of clock genes (Hardin et al., 1990). In this model, promoters of clock genes are under the control of positive transcriptional factors, whose

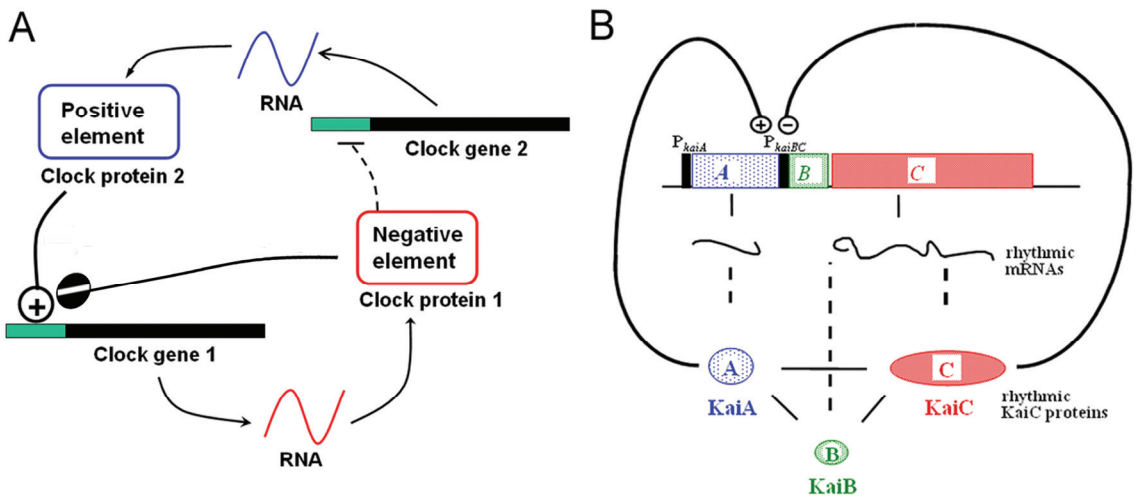

Figure 1-3. TTFL models proposed for the generation of circadian rhythms. (A) A general TTFL model applied to any organism. The positive element(s) activates the expression of clock control genes, among which the negative element(s) will either inhibit the positive element(s) by repressing the expression of the positive element(s) or repress the negative element(s) own expressions. **(B)** Originally proposed TTFL model in cyanobacteria (Ishuira et al., 1998). The positive element KaiA activates the expression of the promoter P_{kaiBC}, and the negative element KaiC represses it.

function is inhibited by the post-translationally modified clock proteins. In other words, the protein products of the clock genes negatively feed back on their own expression in an auto-regulatory feedback loop. **Figure 1-3A** shows the schematic of a general TTFL model.

In *S. elongatus*, the transcripts of *kaiA* and *kaiBC* are rhythmic (Ishuira et al., 1998), and the abundance of KaiB and KaiC proteins is also rhythmic (Xu et al., 2000; Iwasaki et al., 2002). The bioluminescence reporter gene *luxAB* is rhythmically expressed under the control of the promoter P_{kaiBC}. With an IPTG inducible promoter, P_{trc}, the overexpression of the *kaiA* gene enhances the transcription of *kaiBC*, while *kaiC* overexpression represses it (Ishuira et al., 1998). This phenomenon of negative regulation

by the KaiC protein and positive regulation by the KaiA protein fits the TTFL model (**Figure 1-3B**), which was originally proposed for eukaryotes. As in the case of the E-box in the upstream region of clock controlled genes for the binding of BMAL1-CLOCK complexes in eukaryotes (Ripperger & Schibler, 2006), the TTFL model in **Figure 1-3B** for cyanobacteria clock would be predicted to be dependent on P_{kaiBC}. However, the promoter of *kaiBC* is not essential for the generation of proper circadian rhythms. One of the early observations that was not consistent with a core TTFL oscillator in cyanobacteria was that when the *kaiBC* coding regions were put downstream of a non-specific heterologous promoter that was active in *S. elongatus*, the clock was still able to operate (Xu et al., 2003, see below).

PTO model

Although an autoregulatory TTFL was thought to be essential for any organism to have circadian rhythms, the KaiC phosphorylation rhythm in *S. elongatus* still "ticks" in DD (Tomita et al., 2005). This is significant because *S. elongatus* is an autotrophic photosynthetic species and most of its metabolic activities, including RNA and protein synthesis are suppressed under DD conditions (Tomita et al., 2005). Therefore, how could a TTFL operate in DD when transcription/translation is suppressed? In DD, clock protein levels are maintained at constant levels, which again is not as indicated by the TTFL model. Also, the authors shut down transcription and translation in LL by adding inhibitory drugs (rifampicin or chloramphenicol), but the KaiC phosphorylation rhythm

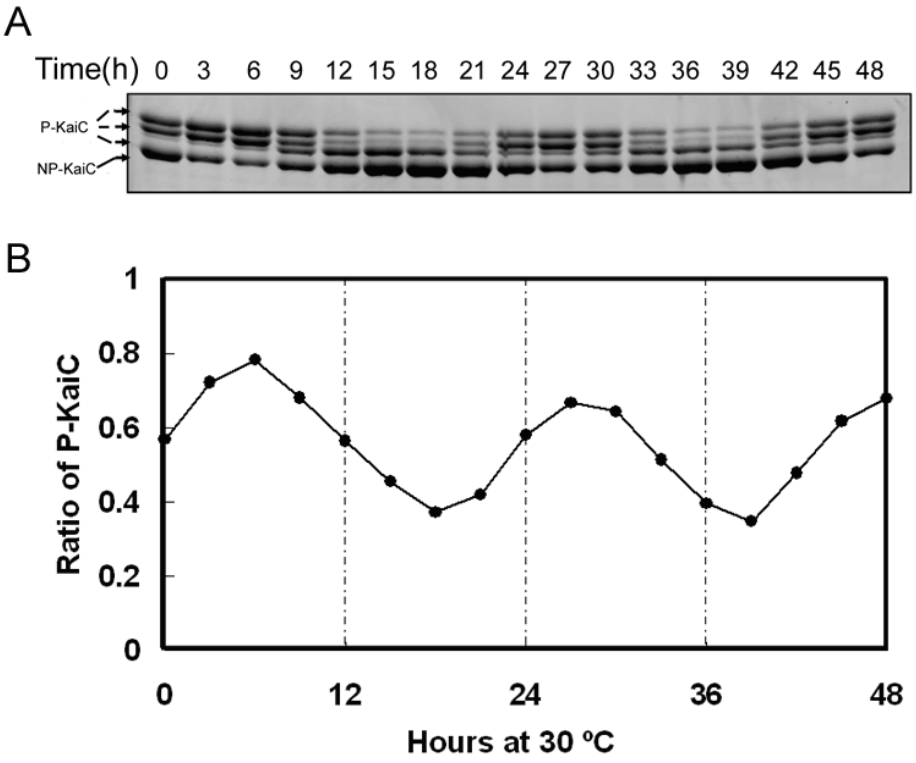

Figure 1-4. Circadian phosphorylation of KaiC in the *in vitro* KaiABC reaction. (A) SDS-PAGE image of a time-course reaction shows a robust KaiC phosphorylation rhythm. The upper three bands are the phosphorylated KaiC (P-KaiC), and the lowest band is the non-phosphorylated KaiC (NP-KaiC). **(B)** Analysis of P-KaiC ratio as the function of incubation time, with the mixture of KaiA, KaiB and 1mM ATP.

still persisted (Tomita et al., 2005). Therefore, the phosphorylation cycle without transcription and translation retained fundamental properties of circadian clocks.

Surprisingly, it was subsequently demonstrated that the three purified Kai proteins can generate a robust circadian KaiC phosphorylation rhythm *in vitro* when mixed together with 1 mM of ATP (Nakajima et al., 2005). Those authors used a A:B:C stoichiometric ratio of 1:1:4 (by weight) and ~1.5:2:1 (by molar concentration) based on that of Kai concentrations *in vivo* (Kitayama et al., 2003). This *in vitro* reconstituted KaiC phosphorylation rhythm is temperature compensated and the period is ~22 hours at 30 ºC.

Mutations in *kaiC* that can shorten or lengthen the period *in vivo* (Ishuira et al., 1998) had a similar affect on the KaiABC oscillator reconstituted *in vitro* (Nakajima et al., 2005). As shown in **Figure 1-4**, our lab is capable of reproducing the *in vitro* KaiC phosphorylation rhythm and pursuing further investigations. Those two important discoveries have deeply affected the field of chronobiology. Nakajima and coworkers concluded that this post translational oscillation of KaiC phosphorylation is the core clock ticking in cyanobacteria (Nakajima et al., 2005).

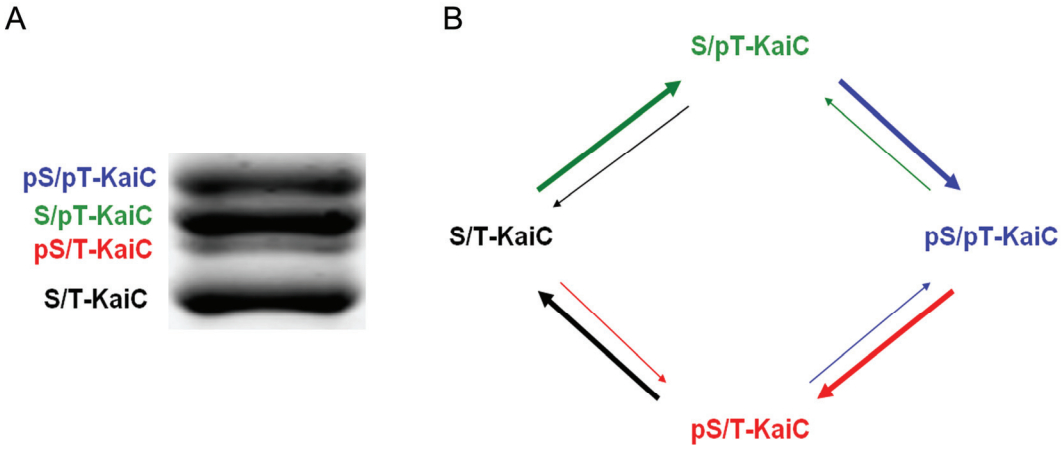

Figure 1-5. The sequential phosphorylation model of the *in vitro* KaiABC oscillator (modified from Nishiwaki et al., 2007; Rust et al., 2007). (A) KaiC resolves with a four-band pattern in 10% SDS-PAGE. S and T are the phosphorylation sites S431 and T432. From top to bottom, as identified by using MS, the bands are doubly phosphorylated (pS/pT), phosphorylated on T432 (S/pT), phosphorylated on S431 (pS/T), non-phosphorylated KaiC (S/T) respectively. **(B)** KaiC undergoes the cycle of phosphorylation as depicted in the schematic.

More recently, experiments using mass spectroscopy (MS) have led to a sequential phosphorylation model being proposed for this *in vitro* rhythm (Nishiwaki et al., 2007; Rust et al., 2007). As illustrated in **Figure 1-5** and the SDS-PAGE image in

Figure 1-4A, during the phosphorylation phase KaiC phosphorylates first on residue T432, then becomes doubly phosphorylated on both T432 and S431. Then KaiC converts to a dephosphorylation phase, in which the dephosphorylation starts on T432-P, followed by the dephosphorylation of S431-P, which results in the return to non-phosphorylated KaiC.

Dual KaiC-based oscillators in cyanobacteria

As discussed above, Nakajima et al. (2005) considered that the KaiABC oscillator was the self-sustrained core pacemaker, implying that transcription & translation were involved only in the output. In this view, the oscillation observed *in vitro* would have an *in vivo* correlate, namely a post-translational oscillator (PTO), which functions as the pacemaker *in vivo*. However, Kitayama and coworkers questioned that conclusion and suggested instead that a TTFL can drive the circadian system in cyanobacteria without a functional PTO (Kitayama et al., 2008). First, those authors reported that over-expression of KaiA, resulting in constitutively hyper-phosphorylated KaiC (a "clamp" of KaiC phosphorylation status), allows circadian rhythms of gene expression as monitored by luciferase reporters *in vivo*. Moreover, they reported that a mutant KaiC ($KaiC^{EE}$, meaning S431E and T432E) mimicking constitutive hyperphosphorylation on S431 and T432 could support a long-period circadian rhythm *in vivo.* Because cyanobacterial cells apparently exhibited self-sustrained oscillations when the KaiABC oscillator was inactivated by clamping the phosphorylation status of KaiC, these two experimental

approaches led Kitayama and coworkers to conclude that a TTFL could operate independently of the PTO at optimal growth temperatures. These results therefore opened the possibility that the KaiABC oscillator (PTO) was not an obligatory core pacemaker in cyanobacteria. As described in detail in **Chapter III**, further investigations were performed to understand the relationship between TTFL and PTO in the model organism *S. elongatus*.

Structural Studies on Kai Proteins

Kai protein structures

Remarkable progress was achieved on the structures of the Kai proteins in the circadian clock field in the years of 2004/2005. These three proteins are the only full-length structures of circadian proteins from any organism, including the eukaryotic proteins (for PER, structures of only the PAS domains are known (Yildiz et al., 2005)). The C-terminal domain structure of KaiA from *Thermosynechococcus elongatus* (*T. elongatus*) BP-1 was solved by solution NMR (Vakonakis et al., 2004; PDB-ID **1Q6A**). The full length structures of KaiA from *S. elongatus* (Ye et al., 2004; PDB-ID **1R8J**) and from the cyanobacterium *Anabaena* sp PCC 7120 (Garces et al., 2004; PDB-ID **1R5Q**) were solved by X-ray crystallography. The *S. elongatus* KaiA protein is composed of two independently folded domains (connected by a linker) that homo-dimerize at the C-terminal domain. The C-terminal domain is also considered to associate with KaiC

(Vakonakis and LiWang, 2004). Crystallographic structures of KaiB from *T. elongatus* BP-1 (Iwase et al., 2005; PDB-ID **1VGL**) and from *Synechocystis* sp. PCC 6803 (Hitomi et al., 2005; PDB-ID **1WWJ**) indicate that KaiB can form a dimer of homo-dimers (therefore, a tetramer). KaiB from *Anabaena* has an alpha-beta motif that is composed of 2 α-helices and 3 β-sheets and shows close resemblance to the alpha-beta motif of thioredoxin (Garces et al., 2004; PDB-ID **1R5P**). From a study on the cyanobacterium *Anabaena* sp., it was determined that KaiA and KaiB share some structural similarities, which may suggest that KaiB antagonizes KaiA function on KaiC phosphorylation by competition for the same binding site (Garces et al., 2004). Representative structures of KaiA and KaiB are shown in **Figure 1-6A&B**.

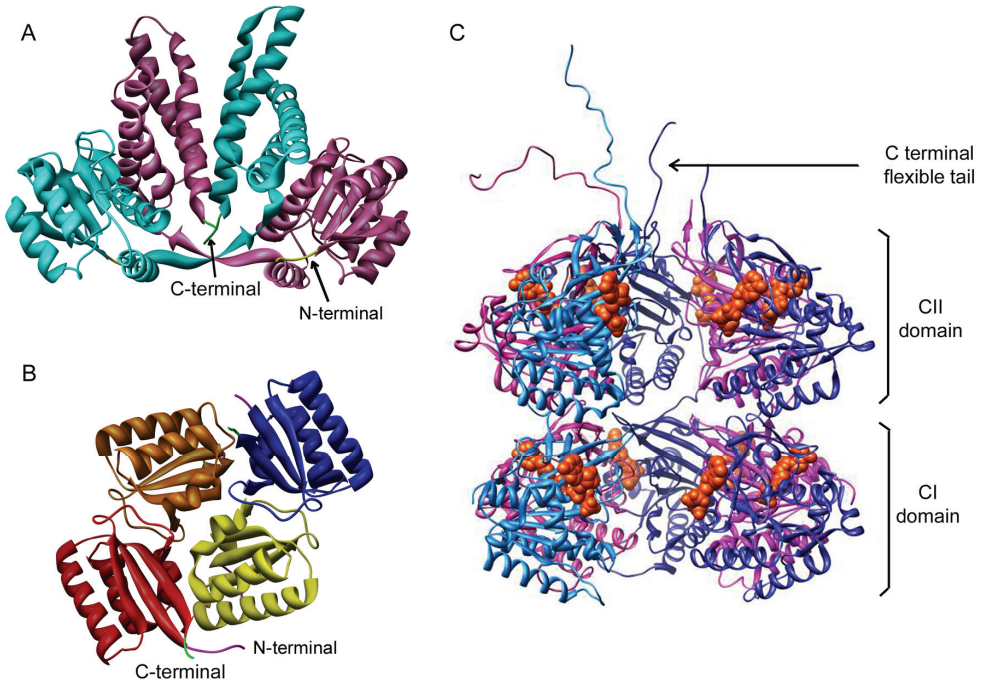

Figure 1-6. The structure of Kai proteins. (A) *S. elongatus* KaiA (PDB-ID **1R8J**) forms a dimer, composed of two domains and an intermediate linker. **(B)** *Synechocystis* sp. KaiB (PDB-ID **1WWJ**) forms

an asymmetric tetramer. **(C)** *S. elongatus* KaiC (PDB-ID **2GBL**) forms a double-donut shape hexamer, composed of CI and CII domains, and a flexible C-termial tail. The facing subunit of the hexamer is removed to emphasize the channel in the middle. The C-terminal tail is very important for the function of KaiC. The ATP molecules are bound at the interface of each KaiC subunit, and highlighted with orange. (Structures constructed by using Chimera, UCSD)

Our lab collaborated with the Egli lab to crystallize the KaiC protein from *S. elongatus* and we solved the structure at 2.8 Å resolution (Pattanayek et al., 2004; PDB-ID **1TF7**). The overall structure is about 100 x 100 Å. KaiC forms double-donut shape hexamers with twelve ATP molecules bound at the interfaces between subunits, six each in the N- and C-terminal rings. KaiC has a KaiCI (CI) and a KaiCII (CII) domain which share similar conformations, but the CII side of the hexamer differs in that it has protruding C-terminal peptide "tentacles" (Pattanayek et al. 2006; PDB-ID **2GBL**), that were missing in the initial 3-D structure model because of their high flexibility (see **Figure 1-6C**). Analysis of the primary sequence indicated that the KaiC protein belongs to the DnaB/RecA superfamily of proteins (Leipe et al., 2000).

Structural studies on Kai protein complexes

Static high resolution X-ray 3-D structures of protein complexes can contribute much to the understanding of the basis of a biochemical/biophysical process. Unfortunately, there are no crystal structures so far of KaiB-KaiC, KaiA-KaiC or KaiA-KaiB-KaiC protein complexes. However, studies from solution NMR and electron microscopy (EM) have given clues about these protein complexes.

Vakonakis and LiWang have determined the NMR solution structure of the complex between the C-terminal domain of KaiA and a 30 amino acid peptide derived from the C-terminal tail of KaiC from *T. elongatus* BP-1 (Vakonakis and LiWang 2004, and PDB-ID **1SUY**). KaiA forms a homo-dimer, and the intersubunit dimerization angle changes upon the formation of the KaiA-peptide complexes as compared with the free state of KaiA (Vakonakis and LiWang 2004).

In collaboration with the Stewart lab, we applied negative-strain EM analysis to analyze the protein complexes of KaiA-KaiC (Pattanayek et al., 2006), KaiB-KaiC (Pattanayek et al., 2008) and KaiA-KaiB-KaiC throughout the cycle of the *in vitro* KaiABC oscillator (Mori et al., 2007). In the KaiA-KaiC complex, KaiA binds exclusively to the CII half of the KaiC hexamer in two configurations: 'tethered' and 'engaged' (Pattanayek et al., 2006). EM images reveal that in the 'tethered' status, KaiA is about 35 Å from the CII of KaiC, which indicates that KaiA pulls the C-terminal peptide away from KaiC. This result is consistent with the NMR study of the complex formed by KaiA and the KaiC-derived C-terminal peptide, which is L-shaped in the complex (Vakonakis and LiWang 2004). In the KaiB-KaiC complex, EM images indicate that KaiB binds to KaiC at the same site where KaiA binds in the 'engaged' state, which then suggests how KaiB may serve to antagonize the effect of KaiA by competitively preventing the binding between KaiA and KaiC. However, both KaiA and KaiB may bind to the KaiC hexamer when the KaiA dimer is bound to an extended C-terminal tail of KaiC in the 'tethered' status, as we observed in the KaiA-KaiB-KaiC complex (Mori et

al., 2007). However, given the limited resolution of EM structures over 20 Å, further investigations (for example by cryo-EM) need to be carried out.

Studies on Protein-Protein Interactions

Protein-protein interactions in other clock model organisms

In *Drosophila*, TIM may regulate the entry of PER into the nucleus by forming a heterodimer (Gekakis et al., 1995). In mammals, the clock protein mCRY, but not mTIM, forms a functional dimer with mPER before it enters the nucleus (Reppert and Weaver, 2001). In different organisms, the positive clock-related transcriptional factors, mBMAL1/mCLOCK in mice (Reppert and Weaver, 2001), CYC/CLK in *Drosophila* (Lee et al., 1999), and WC-1/WC-2 in *Neurospora* (Cheng et al., 2002), all form heterodimeric complexes to activate the expression of clock controlled genes. Moreover, they all contain PAS domains, which are involved in protein-protein interactions (Huang et al., 1993b). In both *Drosophila* and mammals, Casein kinase I interacts with PER to regulate its phosphorylation and entry into nucleus (Kloss et al., 1998; Vielhaber et al., 2000).

Yeast two-hybrid methodology to identify interactions

Soon after the *kai* gene cluster was cloned and found to be essential for the generation of circadian rhythms in *S. elongatus* PCC 7942 (Ishiura et al., 1998), physical

interactions among the three Kai proteins were investigated by using the yeast two-hybrid system (Iwasaki et al., 1999). By expressing any of the Kai proteins as a fusion with either a DNA-binding protein, LexA, or the transcriptional activation domain of VP16, the authors identified both heterotypic interactions (KaiA-KaiB, KaiA-KaiC and KaiB-KaiC) and homotypic interactions (KaiB-KaiB and KaiC-KaiC) in doubly transformed yeast cells using β-galactosidase as a reporter. The interactions between KaiA and KaiB proteins are much weaker than the other combinations. However, in the presence of KaiC, a strong signal was detected for KaiA-KaiB interactions in the yeast two-hybrid assay. Today, looking back to these data, one can see that it already indicated the necessity of KaiB·KaiC protein complexes for recruiting KaiA (see later in this chapter and especially **Chapter II**). Also, two potential KaiA-binding domains in KaiC were identified by using the same technique except that only 60-110 amino acid fragments of the KaiC protein were expressed in the yeast (Taniguchi et al., 2001). The two fragments were residues 206-263 and residues 418-519, which later could be mapped in the KaiC crystal structure (Pattanayek et al., 2004; **Figure 1-6C**) at the waist between the CI and CII domains (residues 206-263) and on the surface of the CII domain (residues 418-519).

Pull-down assays

The yeast two-hybrid system is a powerful biochemical tool for investigating protein-protein interactions, especially for large scale screening. However, this system

has disadvantages. First, expressing exogenous proteins in yeast can bring false positive or negative results; second, the assay cannot tell whether the interaction between two elements is direct or indirect; last, and very importantly, no dynamic information can be derived from the assay. Besides the yeast two-hybrid assay, Kai protein pull-down assays have been performed both *in vivo* and *in vitro*.

The first *in vivo* pull-down assay (from cell extracts) was done by tagging each Kai protein with a His_6- tag at the N-terminus and introducing it back to the ΔKaiABC strain, confirming the interactions among the Kai proteins that had been suggested by the two-hybrid assay (Iwasaki et al., 1999). Later, the Kondo research group used anti-KaiC serum to co-immunoprecipitate the protein complexes associated with KaiC in time-course experiments, and did immunoblots against KaiA or KaiB proteins (Kageyama et al., 2003; Kitayama et al., 2003). The authors found that KaiA and KaiB bound to KaiC more abundantly during the subjective night, which is in the phase of KaiC dephosphorylation *in vivo* (Iwasaki et al., 2002). However, at that time, there was no clue about the relationship between KaiC phosphorylation and the formation of protein complexes. The authors speculated that the protein complexes could have modulated the phosphorylation state of the KaiC protein (Kageyama et al., 2003; Kitayama et al., 2003). More investigations started to show that KaiC was undergoing a circadian change of phosphorylation on S431 and T432 (Nishiwaki et al., 2000; Xu et al., 2003; Iwasaki et al., 2002; Pattanayek et al., 2004). C-terminal Flag-KaiA was used to demonstrate that KaiA preferably binds to phosphorylated KaiC and that the

phosphorylation of KaiC is important for formation of KaiA·KaiB·KaiC complexes *in vivo* (Iwasaki et al., 2004).

Considering the fact that the abundance of the KaiC protein is increasing during the early subjective night *in vivo*, an increase of the formation of the three Kai protein complexes is plausible. A complementary series of biochemical experiments was done *in vitro* by the pioneering work started in the Kondo laboratory. By immobilizing the GST fusion form of each of the Kai proteins, followed by incubation with ^{35}S-labeled KaiA or KaiC, or His_6-tagged KaiB, Iwasaki et al. confirmed what they had observed in yeast cells (Iwasaki et al., 1999). The binding between KaiB and KaiC was reported in another species, *Anabaena sp* PCC 7120, by using Ni-NTA agarose to co-precipitate protein complexes for N-terminal His_6-tagged KaiC (Garces et al., 2004). Interestingly, mutation of the Arg23 to Ala in KaiB (in *S. elongatus* it is Arg22) significantly reduced the affinity of KaiB to KaiC (Garces et al., 2004, and **Chapter II**). *S. elongatus* KaiA is composed of three domains, the N-terminal domain (1-135), the central linker domain and the C-terminal domain (175-284). The C-terminal domain of KaiA (GST-KaiA) bound to full-length KaiC protein (Uzumaki et al., 2004). In 2005, an astonishing publication demonstrated that the KaiC phosphorylation circadian rhythm could be reconstituted in the presence of ATP *in vitro* (Nakajima et al., 2005). This discovery has changed the direction of studying protein interactions among the Kai proteins; in the simpler *in vitro* system, the interactions can be addressed more quantitatively, more dynamically, and more specifically in comparison with KaiC phosphorylation status.

In the *in vitro* KaiABC system, by using C-terminal tagged KaiA-Flag, KaiB-His_6, and WT-KaiC, two-step pull-down assays demonstrated that the KaiA-KaiC, KaiA-KaiB-KaiC, and KaiB-KaiC complexes associate and dissociate in a circadian pattern (Kageyama et al., 2006). Among these protein complexes, KaiB-KaiC complexes showed the most robust circadian rhythm while the other two complexes fluctuated weakly (Kageyama et al., 2006). Single pull-downs between either KaiA-flag/KaiC or KaiB-His_6/KaiC demonstrated that the interaction between KaiA and KaiC is rapid and saturates with 10% of total KaiC, while the interaction between KaiB and KaiC peaks after about a 4-6 hour incubation (and involves about 20% of total KaiC). Further examination of the effect of KaiC phosphorylation status on the formation of complexes showed that KaiA associates equally with both P-KaiC (phosphorylated KaiC) and NP-KaiC (nonphosphorylated KaiC), but KaiB preferably associated with P-KaiC (Kageyama et al., 2006). And for the first time, monomer exchange between KaiC hexamers was observed by using N-terminal tagged Flag-KaiC and His_6-KaiC proteins (Kageyama et al., 2006). Based upon further work in the Kondo and Johnson labs, the monomer exchange phenomenon has been proposed to be a mechanism to synchronize the phosphorylation status of the individual KaiC proteins in the population of molecules, thereby allowing the *in vitro* reaction to oscillate for many cycles (Mori et al., 2007; Ito et al., 2007, and **Chapter IV**).

Gel filtration chromatography

Another powerful tool to study protein interactions and the size of protein complexes is gel filtration chromatography. Combined with time-course experiments, gel filtration has been applied to both *in vivo* soluble protein extracts (Kageyama et al., 2003) and the *in vitro* KaiABC oscillator system (Kageyama et al., 2006). Results from LD and LL conditions are similar for the *in vivo* protein extracts: clock-related proteins are more abundant during night (or subjective night), occurring as 400-600 kDa protein complexes, and they separate during day (or subjective day). Gel filtration studies on *kaiC*-null strains indicated that the KaiC protein is the core of the large complexes (Kageyama et al., 2003). Although the gel filtration results from *in vivo* studies are fuzzy due to the whole cell protein extract, the results from the *in vitro* system clearly demonstrate that Kai proteins are forming heteromultimeric complexes of 500-600 kDa (Kageyama et al., 2006). Quantitative analysis of the *in vitro* gel filtration results indicated that the KaiC hexamer formed heterocomplexes with KaiA during the phosphorylation phase and with KaiB during the dephosphorylation phase (Kageyama et al., 2006). Gel filtration also was used to determine the quaternary structure of the KaiB protein, either a tetramer at ~55 kDa (Iwase et al., 2005) or a dimer at ~25 kDa (Garces et al., 2004; Kageyama et al., 2006).

Blue native poly-acrylamide gel electrophresis (BN-PAGE)

BN-PAGE, in which proteins are mixed with Coomassie Blue dye and

electrophoresed in a native gel, has been used to isolate supramolecular associations of multiprotein complexes while avoiding the use of chemical crosslinking or biochemically engineered tags. The principle of this technique is similar to SDS-PAGE, in which a denatured protein is surrounded with SDS so that the electrophoretic mobility of proteins is approximately determined by the relative molecular weight. In BN-PAGE, native protein complexes are bound by the blue dye so that the mobility of a protein complex is determined by the negative charge of the bound dye. The resolution of BN-PAGE is usually higher than that of gel-filtration. The second dimension is then a standard SDS-PAGE, which allows the identification of the proteins by their molecular weight. As was found by pull-down assays (Kageyama et al., 2006), BN-PAGE also revealed a rhythmic association pattern of the Kai proteins, with the KaiB·KaiC complex being most strongly rhythmic. This rhythmic association pattern accompanied the rhythm of KaiC phosphorylation (Mori et al., 2007). In the 2-D BN/SDS-PAGE analysis, there is a significant amount of free KaiC monomers during the KaiC dephosphorylation phase (Mori et al., 2007), which is consistent with monomer exchange, as revealed by pull-down assays (Kageyama et al., 2006) and a different kind of BN-PAGE (Clodong et al., 2007).

Small angle X-ray scattering (SAXS) analysis

Despite the fact that two-step pull-down assays, gel filtrations, and BN-PAGE indicated the repeatedly assembled and disassembled heteromolecular Kai complexes in a

circadian manner, SAXS was additionally used to study the dynamics of un-tagged proteins in real time (Akiyama et al., 2008). The forward scattering intensity, I(0), is proportional to the average molecular size of the targeted molecules. The I(0) of free KaiA, KaiB and KaiC was 460, 236, and 2200, respectively, and the I(0) measured during an *in vitro* KaiABC reaction oscillated between 2600 and 3100 with a period of 24.2 ± 1.3 hr (Akiyama et al., 2008). The SAXS results demonstrate there is a 90º phase delay between the I(0) oscillation and the phosphorylation status of KaiC (consistent with **fig.2-4E** in **Chapter II**). Binary interaction between either KaiA/KaiC or KaiB/KaiC was investigated in this paper by SAXS, and the authors speculated on the structures of the complexes based on the previously reported Kai 3-D protein structures. However, their proposal that KaiB is recruited into a KaiA·KaiC complex at the C-terminal region, resulting in either displacing KaiA or inactivating KaiA (Akiyama et al., 2008), is not consistent with what I will describe in **Chapter II**.

Native poly-Acrylmide gel electrophresis (PAGE)

Phosphorylation of S431 and T432 occurs in an ordered sequence over the cycle of the *in vitro* KaiABC oscillator (Nishiwaki et al., 2007; Rust et al., 2007). As described in detail in **Chapter II**, native-PAGE is a convenient and economical method that can be used to study the protein interactions of Kai proteins dynamically, specifically, and quantitatively.

Significance of Clock Studies from Cyanobacteria

Questions addressed in the study

In cyanobacteria, the central clock genes and the proteins they encoded (KaiA, KaiB and KaiC) are essential for the generation of circadian clocks (Ishuira et al., 1998). From more than a decade of molecular studies, from introducing the *Vibrio harveyi* luciferase gene set *luxAB* into *S. elongatus* PCC 7942, to eventually reconstituting the KaiC phosphorylation rhythm *in vitro* with the presence of ATP, it is clear that rhythmic KaiC phosphorylation is a key component of the central clockwork of cyanobacteria (Ditty et al., 2009). As reviewed above, the biochemical functional studies of the three Kai proteins and a variety of protein-protein interaction studies described how KaiC phosphorylation and the protein complexes oscillate within this system. Recently, with the discoveries of (1) a sequential phosphorylation pattern in the *in vitro* KaiABC oscillator (Nishiwaki et al, 2007; Rust et al., 2007), and (2) the configuration of KaiC's C-terminal tail (about 30 amino acids long) serving as a master switch between KaiC autokinase versus autophosphatase activities (Kim et al., 2008), the question of how the intermolecular interactions among the three Kai proteins influences the dynamics of KaiC phosphorylation needs to be addressed. For example, how might the interaction between KaiB and hyper-phosphorylated KaiC inactivate KaiA and affect the dynamics, as well as the period? And since the flexible C-terminal tail appears to be the master switch, how does the interaction among three Kai proteins affect the position of the tail? Very luckily,

I found that native-PAGE, a very convenient method, can address these questions, as described in detail in **Chapter II** (Qin et al., 2010b).

The TTFL model was thought to be a general paradigm for generating robust circadian oscillations in all organisms (Dunlap et al., 2004); however, the appearance of the robust KaiC phosphorylation rhythm without transcription & translation (Tomita et al., 2005) and the reconstitution of the rhythm *in vitro* (Nakajima et al., 2005) challenges the generality of this model. From the experimental data, we in the Johnson lab are building a mathematical model to understand how the *in vivo* global circadian rhythm, including the rhythmic fluctuations of KaiC protein abundance under constant LL conditions, is generated based on this robust post-translational oscillator. Recently, a dual KaiC-based oscillator model was proposed based on the experiment of clamping KaiC in a hyper-phosphorylated state (either by over-expression of KaiA or by S431E/T432E mutations in KaiC), which shows oscillation of the *luxAB* reporter gene expression under the control of the promoter P_{kaiBC} (Kitayama et al., 2008). This result opened the possibility that the KaiABC oscillator (PTO) was not an obligatory core oscillator in cyanobacteria. As detailed in **Chapter III**, my colleagues and I extended this type of analysis and concluded that the PTO is the core pacemaker while the TTFL is a slave oscillator that quickly damps when the PTO stops (Qin et al., 2010a).

Significance for cyanobacteria specifically

As a major photosynthetic organism, cyanobacteria are one of the most abundant

species on the planet and are responsible for a large proportion of the total photosynthesis on Earth (Partensky et al., 1999). Very recently, cyanobacteria have become one of the most promising organisms for producing natural bio-fuels (Angermayr et al., 2009). Although cyanobacteria are one of the newest model organisms for studies of circadian rhythms, they are the first organism in which the benefits of possessing a circadian clock have been rigorously demonstrated. Specifically, in the Johnson lab, this was first demonstrated with direct evidence that the circadian clock enhances fitness in *S. elongatus* (Ouyang et al., 1998). Our lab showed that cyanobacterial strains whose internal clocks have similar period to the environmental LD cycle can defeat strains with different periods in a mixed culture. Furthermore, our lab demonstrated that rhythmic strains can out-compete clock-disrupted strains in a rhythmic environment (Woelfle et al., 2004). The mechanism by which the consonance of the internal clock with the external environment enhances fitness is still an open question.

Evolutionarily, it is very interesting to ask when the circadian system evolved. The *kai* genes are ubiquitous throughout cyanobacteria, except that some species are missing the *kaiA* gene (Dvomyk et al., 2003). Is the phosphorylation rhythm of KaiC still the core circadian mechanism in those species without the positive KaiA element (or is there a different protein that performs the duties of KaiA)? If not, what is the core clockwork in those species? If so, what mechanism could these cyanobacteria be using without the stimulation of the KaiC autokinase activity from KaiA? Better understanding of the *in vitro* biochemical properties of the Kai proteins together (or individually) and

the *in vivo* regulation by the KaiABC PTO will help to address these questions. Furthermore, if in the future, cyanobacteria become a real bio-fuel reactor, will modulating global gene expression by manipulating the circadian clock increase productivity by affecting the oscillating amplitude or phase?

Significance within the clock field

There are no identified *kai* gene homologs in higher eukaryotic organisms. The KaiC protein belongs to the RecA/DnaB superfamily of bacterial proteins (Leipe et al., 2000) and KaiC shares structural similarity with F1-ATPase (Abrahams et al., 1994; Hayashi et al., 2003; Pattanayek et al. 2004). However, modification of clock proteins by phosphorylation is highly conserved among the known identified systems. In *Drosophila*, the phosphorylation of PER protein undergoes a robust circadian cycle (Edery et al., 1994). It is currently believed that the phosphorylation of eukaryotic clock proteins regulates their degradation, cellular relocation, or association with their protein partners. It is possible that the circadian clock is so fundamental that all organisms evolved their clock mechanisms convergently. The rising knowledge of the cyanobacterial circadian systems encourages the scientists working on other organisms not only to investigate their systems in more biochemical/biophysical depth, but also to start thinking about the possibility that a PTO could be the central ticking clock mechanism in eukaryotes as well (see **Discussion** in **Chapter III**).

CHAPTER II *

INTERMOLECULAR ASSOCIATIONS DETERMINE THE DYNAMICS OF THE CIRCADIAN KaiABC OSCILLATOR

Abstract

Three proteins from cyanobacteria (KaiA, KaiB, and KaiC) can reconstitute circadian oscillations *in vitro*. At least three molecular properties oscillate during this reaction, namely rhythmic phosphorylation of KaiC, ATP hydrolytic activity of KaiC, and assembly/disassembly of intermolecular complexes among KaiA, KaiB, and KaiC. We found that the intermolecular associations determine key dynamic properties of this *in vitro* oscillator. For example, mutations within KaiB that alter the rates of binding of KaiB to KaiC also predictably modulate the period of the oscillator. Moreover, we show for the first time that KaiA can bind stably to complexes of KaiB and hyper-phosphorylated KaiC. Modeling simulations indicate that the function of this binding of KaiA to the KaiB•KaiC complex is to inactivate KaiA's activity, thereby promoting the dephosphorylation phase of the reaction. Therefore, we report here dynamics of interaction of KaiA and KaiB with KaiC that determine the period and amplitude of this *in vitro* oscillator.

---

* Chapter II is directly derived from the published paper: Qin X, Byrne M, Mori T, Zou P, Williams DR, McHaourab H, Johnson CH (2010b) Intermolecular associations determine the dynamics of the circadian KaiABC oscillator. *Proc Natl Acad Sci USA* [Epub ahead of print]

Introduction

Circadian rhythms are daily cycles of metabolic activity, gene expression, sleep/waking, and other biological processes that are regulated by self-sustained intracellular oscillators. A versatile system for the study of circadian oscillators has emerged from the study of the cyanobacterium, *S. elongatus* PCC 7942 (Ditty et al., 2009). The circadian pacemaker in *S. elongatus* choreographs rhythmic patterns of global gene expression, chromosomal compaction, and the supercoiling status of DNA *in vivo* (Liu et al., 1995; Smith & Williams, 2006; Woelfe et al., 2007). Just three essential clock proteins from *S. elongatus*–KaiA, KaiB, and KaiC–can reconstitute a biochemical oscillator with circadian properties *in vitro* (Nakajima et al., 2005). This *in vitro* oscillator exhibits at least three rhythmic properties: phosphorylation status of KaiC (Nakajima et al., 2005), formation of KaiA•KaiB•KaiC complexes (Kageyama et al., 2006; Mori et al., 2007), and ATP hydrolytic activity (Terauchi et al., 2007). The relationship of the *in vitro* oscillator to the entire circadian system *in vivo* is not defined, but it is clear that the oscillator underlying the rhythm of KaiC phosphorylation is able to keep circadian time independently of transcription and translation processes *in vivo* and *in vitro* (Nakajima et al., 2005; Tomita et al., 2005), and therefore this post-translational oscillator (PTO) may be necessary and sufficient as the core pacemaker for circadian rhythmicity in cyanobacteria (Johnson et al., 2008).

The Kai proteins interact with each other to form complexes in which KaiC serves as the core component (Kageyama et al., 2006; Mori et al., 2007; Iwasaki et al., 1999;

Taniguchi et al., 2001). These complexes mediate the KaiC oscillation between hypophosphorylated and hyper-phosphorylated forms *in vivo* and *in vitro* (Nakajima et al., 2005; Mori et al., 2007; Tomita et al., 2005; Iwasaki et al., 2002; Nishiwaki et al., 2004; Xu et al., 2003). KaiC autophosphorylation is stimulated by KaiA, whereas KaiB antagonizes the effects of KaiA on KaiC autophosphorylation (Iwasaki et al., 2002; Kim et al., 2008). On the other hand, dephosphorylation of KaiC is inhibited by KaiA, and this effect of KaiA is also antagonized by KaiB (Xu et al., 2003). Therefore, KaiA both stimulates KaiC autophosphorylation *and* inhibits its dephosphorylation; KaiB antagonizes these actions of KaiA. In the *in vitro* system, Kai protein complexes assemble and disassemble dynamically over the KaiC phosphorylation cycle (Kageyama et al., 2006; Mori et al., 2007). First, KaiA associates with hypo-phosphorylated KaiC and KaiC auto-phosphorylation increases. Once KaiC is hyper-phosphorylated, KaiB binds to the KaiC and KaiC dephosphorylates within a KaiA•KaiB•KaiC complex (Mori et al., 2007). When KaiC is completely hypo-phosphorylated, KaiB dissociates from KaiC and the cycle begins anew.

The three-dimensional structures for KaiA, KaiB, and KaiC are known (Johnson et al., 2008a). The crystal structure of the KaiC hexamer elucidated KaiC inter-subunit organization and how KaiC might function as a scaffold for the formation of KaiA•KaiB•KaiC complexes (Pattanayek et al., 2004). The KaiC structure also illuminated the mechanism of rhythmic phosphorylation of KaiC by identifying three essential phosphorylation sites at threonine and serine residues in KaiC at residues T426,

S431, and T432 (Nishiwaki et al., 2004; Xu et al., 2004). Moreover, phosphorylation of S431 and T432 occurs in an ordered sequence over the cycle of the *in vitro* KaiABC oscillator (Nishiwaki et al., 2007; Rust et al., 2007). These phosphorylation events are likely to mediate conformational changes in KaiC that allow interaction with KaiB and subsequent steps in the molecular cycle (Johnson et al., 2008a).

Despite these insights, however, we do not know how the intermolecular interactions among KaiA, KaiB, and KaiC influence the dynamics of the cyanobacterial PTO. For example, given that KaiA stimulates KaiC auto-phosphorylation (Johnson et al., 2008; Iwasaki et al., 2002; Nishiwaki et al., 2004; Kim et al., 2008) and that KaiA is associated with KaiC throughout the cycle (Kageyama et al., 2006; Mori et al., 2007), then why is KaiC not clamped in a constitutively hyperphosphorylated state over time? How might the interaction of KaiB with KaiA•KaiC influence KaiC phospho-state and will this affect the dynamics of the system, including its emergent period? In this study, we found that there are two kinds of association of KaiA with KaiC; the first forms a labile phosphorylation-stimulating KaiA•KaiC complex that is present during the phosphorylation phase and the second kind of association forms a very stable KaiA•KaiB•KaiC complex during the dephosphorylation phase in which KaiA's stimulating ability is inactivated. In particular, we found that KaiB specifically forms stable complexes with hyper-phosphorylated KaiC, and then recruits and inactivates KaiA only after the KaiB•KaiC complex has formed. The labile KaiA•KaiC complex depends upon the previously described interaction of KaiA with the C-terminal "tentacles" of

KaiC, but the stable KaiA•KaiB•KaiC complex can form in the complete absence of these C-terminal tentacles. Moreover, we found that mutant KaiB variants that exhibit altered rates of association with KaiC confer predictable changes in the period of the *in vitro* oscillator.

Materials and Methods

Strains and *in vivo* rhythm measurement

Cyanobacterial strains were *S. elongatus* PCC 7942 wild type and mutants that harbored different *kaiB* variants. Cells were grown and maintained as described previously (Ishiura et al., 1998). To create strains with *kaiB* variants, the *kaiB* ORF in the pC*kaiABC* plasmid (Ishiura et al., 1998) was mutagenized by site-directed PCR to replace the arginine residues at residues 22 and 74 with cysteine. The mutated pCkaiABC was then introduced into the *kaiABC*-deficient strain as described (Ishiura et al., 1998). Luminescence rhythm measurements as a reporter of circadian gene expression *in vivo* were as described previously (Xu et al., 2003).

Protein preparation and construction of KaiB and KaiC variant mutants

Kai proteins from *S. elongatus* were expressed in *Escherichia coli* and purified as described previously (Mori et al., 2007). The mutant variants of KaiB and KaiC proteins for expression in *E. coli* were constructed by site-directed mutagenesis (Stratagene, USA)

Table 2-1 Properties of Wild-type and Mutant KaiA, KaiB, and KaiC Molecules

Version	Characteristics				Source or reference
	Period in vivo (hr)	**Period in vitro**	**Protein interactions**	**ATPase activity (molecules per day)**	
$KaiA^{WT}$	24.9 ± 0.10	Wild type	Binds KaiC and KaiBC complexes	Negligible (0.4)	this study; Dong et al., 2010
$KaiB^{WT}$	24.9 ± 0.10	Wild type	Binds to KaiC	Negligible (0.4)	this study; Dong et al., 2010
$KaiB^{R74C}$	21.7 ± 0.10	Shorten	Binds to KaiC	Data Not Available	this study
$KaiB^{R22C}$	26.2 ± 0.12	Lengthen	Binds to KaiC	Data Not Available	this study
$KaiC^{WT}$	24.9 ± 0.10	Wild type	Binds KaiB	12.6 ± 1.1; 14.5 ± 2.0	this study; Dong et al., 2010; Terauchi et al., 2007
$KaiC^{AA}$	Arhythmic	Arhythmic	Does not bind KaiB	27.1 ± 1.1; 26.8 ± 2.7	this study; Nishiwaki et al., 2007; Dong et al., 2010; Terauchi et al., 2007; Nishiwaki et al., 2004
$KaiC^{AE}$	Not determined	Not determined	Does not bind KaiB	12.6 ± 1.1	this study; Dong et al., 2010
$KaiC^{DA}$	Not determined	Not determined	Does not bind KaiB	Data Not Available	this study
$KaiC^{EE}$ *	~ 40-50	Arhythmic	Binds KaiB	16.7 ± 0.8; 10.9 ± 0.3	this study; Dong et al., 2010; Terauchi et al., 2007; Kitayama et al., 2008
$KaiC^{AT}$	Arhythmic	Arhythmic	Does not bind KaiB	Data Not Available	this study; Nishiwaki et al., 2007; Nishiwaki et al., 2004
$KaiC^{DT}$	Not determined	Arhythmic	Binds KaiB	Data Not Available	this study; Nishiwaki et al., 2007
$KaiC^{489}$ **	Not determined	Not determined	Binds KaiB	59.6 ± 4.1	this study; Dong et al., 2010

* The data of ATPase activity is from $KaiC^{DE}$
** The data of ATPase activity is from $KaiC^{487}$

of the vector plasmid pGEX-6P-1 (Amersham Biosciences, USA) harboring the appropriate *kai* gene. The KaiB mutant variants studied in this paper include $KaiB^{R22C}$ (arginine at residue 22 replaced with cysteine) and $KaiB^{R74C}$ (arginine at residue 74 replaced with cysteine). The KaiC mutant variants include $KaiC^{AA}$, $KaiC^{AE}$, $KaiC^{EE}$, $KaiC^{DA}$, $KaiC^{AT}$ and $KaiC^{DT}$, where the first superscript letter refers to the residue at site 431 (native KaiC has a serine at site 431) and the second letter refers to the residue at site 432 (native KaiC has a threonine at site 432). Therefore, native KaiC ($KaiC^{WT}$) would be labeled $KaiC^{ST}$ by this nomenclature. $KaiC^{489}$ was made by changing residue 490 to a stop codon so that the final 30 residues of the C-terminus were deleted; this mutation creates a KaiC that mimics hyperphosphorylated KaiC and can interact with KaiB alone, but cannot interact with KaiA alone because the C-terminal tentacles are missing (Kim et al., 2008). The properties of these proteins are summarized in **Table 2-1**.

Protein concentration measurement

The concentration of each protein was measured with the Bradford method (Bio-Rad Protein Assay) using a dilution series of bovine serum albumin (Bio-Rad) to generate a standard curve. The purity of each Kai protein was determined by analyzing the sample on SDS-PAGE gels.

***In vitro* KaiABC oscillation reactions and analysis of KaiC phosphoforms by SDS-PAGE**

Reactions were carried out at 30ºC in reaction buffer (RB = 150 mM NaCl, 5 mM

MgCl2, 1 mM ATP, 0.5 mM EDTA, 50 mM Tris-HCl at pH 8.0) using the following Kai protein concentrations: 50-ng/μl KaiA, 50-ng/μl KaiB and 200-ng/μl KaiC. For analysis of KaiC phosphorylation status, samples (total 1μg KaiC at each time point) were collected from the *in vitro* reactions and resolved by SDS-PAGE (16 cm × 16 cm × 1mm gels with 10% acrylamide) at a constant current of 35 mA for 4-5 h. Gels were stained with colloidal Coomassie Brilliant Blue, and the gel images were digitally captured with the Gel Doc XR system (Bio-Rad). On each lane of the SDS-PAGE gels, the uppermost band is double phosphorylated KaiC (ST-KaiC), the next band down is KaiC that is phosphorylated on T432 (T-KaiC), the third band down is KaiC that is phorphorylated on S431 (S-KaiC), and the bottommost band is non-phosphorylated KaiC (NP-KaiC). Quantity One (Bio-Rad) was used to quantify each phosphoform of KaiC from the gel images.

Analysis of protein interactions among three Kai proteins by Native-PAGE

Figure 2-1 and **Figure 2-6** illustrate the method for analyzing the interaction between KaiB and KaiC (including mutant variants). KaiB (50 ng/μl) and KaiC (200 ng/μl) were incubated together at 30ºC in RB. For interaction among all three Kai proteins, KaiA (50 ng/μl) was also added. In the experiments of **Fig. 2-3D** (and **Fig. S2-2** in **Appendix A**), formation of complexes between $KaiC^{489}$ and the three KaiB mutant variants was measured with the following concentrations: KaiB variant (500 ng/μl) and $KaiC^{489}$ (200 ng/μl). The 10X higher concentration of KaiB variants in this experiment

was used to mimic the situation at the beginning of the phosphorylation phase, when KaiC phosphorylation is just beginning and KaiB would be in excess relative to the phosphorylated KaiC. $KaiC^{489}$ was used in the native-PAGE experiments to assay the KaiC-binding kinetics of the different KaiB variants because its mobility in native-PAGE is detectably different from that of KaiB (In native polyacrylamide gels, $KaiB^{WT}$ migrates to a similar position as the KaiB•KaiC complex, and consequently high concentrations of $KaiB^{WT}$ mask the signal of the KaiB•KaiC complexes in native-PAGE).

Aliquots (16μl) of the Kai protein mixtures were collected at each treatment/time point, combined with 5X native-PAGE sample buffer (50% glycerol, 0.05% bromophenol blue, 0.312M Tris-HCl at pH 6.8), flash-frozen in liquid nitrogen, and stored at -80 ºC. Native-PAGE (10 cm × 10 cm gels of 7.5% polyacrylamide gels) was performed at 4 ºC at 5mA constant current for 5 h to resolve protein complexes. Gels were stained with colloidal Coomassie Brilliant Blue, and gel images were digitally captured by Bio-Rad Gel Doc XR system. In **Figs. 2-4A** (and **Fig.S2-4** in **Appendix A**), the protein density of the KaiC hexamer or the KaiA dimer was quantified by using Image J (NIH, USA). The initial KaiA density at time 0 was defined as 1, and the Complexes Index at each time point was calculated by subtracting the density of KaiC from the initial density of KaiC. The Complexes Index was then plotted as a function of time, and the free KaiA Index was plotted on the same graph (**Fig. 2-4**).

Fluorophore labeling and fluorescence anisotropy

The fluorophore used to label the KaiA protein was fluorescein-5-maleimide (F-150, Invitrogen USA). A solution of F-150 was prepared in dimethyl sulfoxide, and the concentration was determined by using the extinction coefficient supplied by the manufacturer. Prior to labeling, KaiA protein in DTT-containing buffer (150mM NaCl, 1mM DTT, 50mM Tris-Cl, [pH 8.0]) was desalted on a G-25 Sephadex desalting column (GE Healthcare) equilibrated with the same buffer except without DTT. The desalted KaiA was labeled with F-150 at a 10:1 molar ratio for 2 h at room temperature in the dark and then overnight at 4 ºC. Unreacted fluorophore was removed from the fluorescently labeled KaiA protein with another G-25 Sephadex desalting column.

Fluorescence anisotropy (FA) was employed to determine the equilibrium dissociation constant (K_d) between the fluorescently labeled KaiA protein and the unlabeled KaiC protein. The labeled KaiA protein was 50-60 nM and the anisotropy was measured as a function of increasing concentrations of unlabeled KaiC protein after the two proteins were incubated for 30 min in the KaiABC reaction buffer (RB, see above) at 30ºC. Anisotropy measurements were made on a Photon Technology International spectrofluorimeter (T-format fluorometer). Excitation and emission wavelengths were 490 and 515 nm, respectively. Anisotropy was measured using a time-based function for 10 s (integration time = 1 s), and the data were averaged. The binding between the KaiA dimer and KaiC hexamer proteins was assumed to be a 1:1 binding stoichiometry (Pattanayek et al., 2006; Hayashi et al., 2004). The titration curves were fit to the

following equation (Müller et al., 1991; Reid et al., 2001; Kovaleski et al., 2006):

$$\Delta A = [(Y + S + K_d) - \{(Y + S + K_d)^2 - (4YS)\}^{1/2}] \cdot (A_{max} - A_{min})/(2Y)$$

Where ΔA = (the measured A) - (A_{min}), i.e. the change of the rotation of KaiA as a function of increasing [KaiC]. A is the measured anisotropy at a particular total concentration of the unlabeled KaiC protein (S) and the labeled KaiA protein (Y), A_{min} is the minimum anisotropy, A_{max} is the final maximum anisotropy, and K_d is the dissociation constant.

Electron microscopy of KaiA•KaiB•KaiC complexes

The three KaiB variants were incubated with $KaiC^{EE}$ for 18 h at 30 degrees C. As described previously (Mori et al., 2007), samples were applied to glow discharged carbon coated EM grids and negatively stained with 0.75% uranyl formate. EM images were collected digitally on a 120KeV Tecnai12 LaB6 microscope at a 101,000x magnification using a Gatan 2kx2k US1000 camera. Individual particle images were selected and classified using ImagicV software and the EMAN software packages. The class sum images that appeared as complexes were generated from the following number of particle images for each of the KaiB variants: 2097 images for $KaiB^{WT}$, 1,517 images for $KaiB^{R22C}$, and 1,363 images for $KaiB^{R74C}$. These class sum average images are presented in **Figure 2-3E**.

Mathematical model description (See **Appendix A)**

Results

The affinity of KaiA for KaiC is dependent upon KaiC phosphorylation status

KaiA is known to bind to the C-terminal "tentacles" of KaiC (Vakonakis & LiWang, 2004; Pattanayek et al., 2006). Previous studies have suggested that a single KaiA dimer can promote the phosphorylation of a KaiC hexamer (Hayashi et al., 2004), and that the binding ratio between the KaiA dimer and the KaiC hexamer is 1:1 (Pattanayek et al., 2006). On the other hand, measurements of the concentrations of KaiA, KaiB, and KaiC *in vivo* indicate that there are approximately five times as many KaiC hexamers as KaiA dimers (Kitayama et al., 2003) and the optimized conditions for *in vitro* cycling of the KaiABC oscillator use a ratio of one KaiA dimer to 1.3 KaiC hexamers (Nakajima et al., 2005). To estimate the dissociation constant between KaiA and KaiC, we used fluorescence anisotropy with labeled KaiA and increasing concentrations of unlabeled native KaiC ("$KaiC^{WT}$"). Based on the anisotropy data (representative example shown in **Fig. 2-1A**) and the assumption of a 1:1 binding ratio, a K_d of ~8 nM could be estimated for the KaiA-$KaiC^{WT}$ association. $KaiC^{WT}$ prepared under these conditions is predominantly phosphorylated. To assess whether the phosphorylation status of KaiC influences the K_d we used mutant variants of KaiC that mimic its various phospho-states (**Table 2-1** summarizes the properties of the wildtype and mutant Kai proteins studied in this paper). For example, $KaiC^{EE}$ is a mutant of KaiC with glutamate residues at positions 431 and 432 that mimics hyperphosphorylated

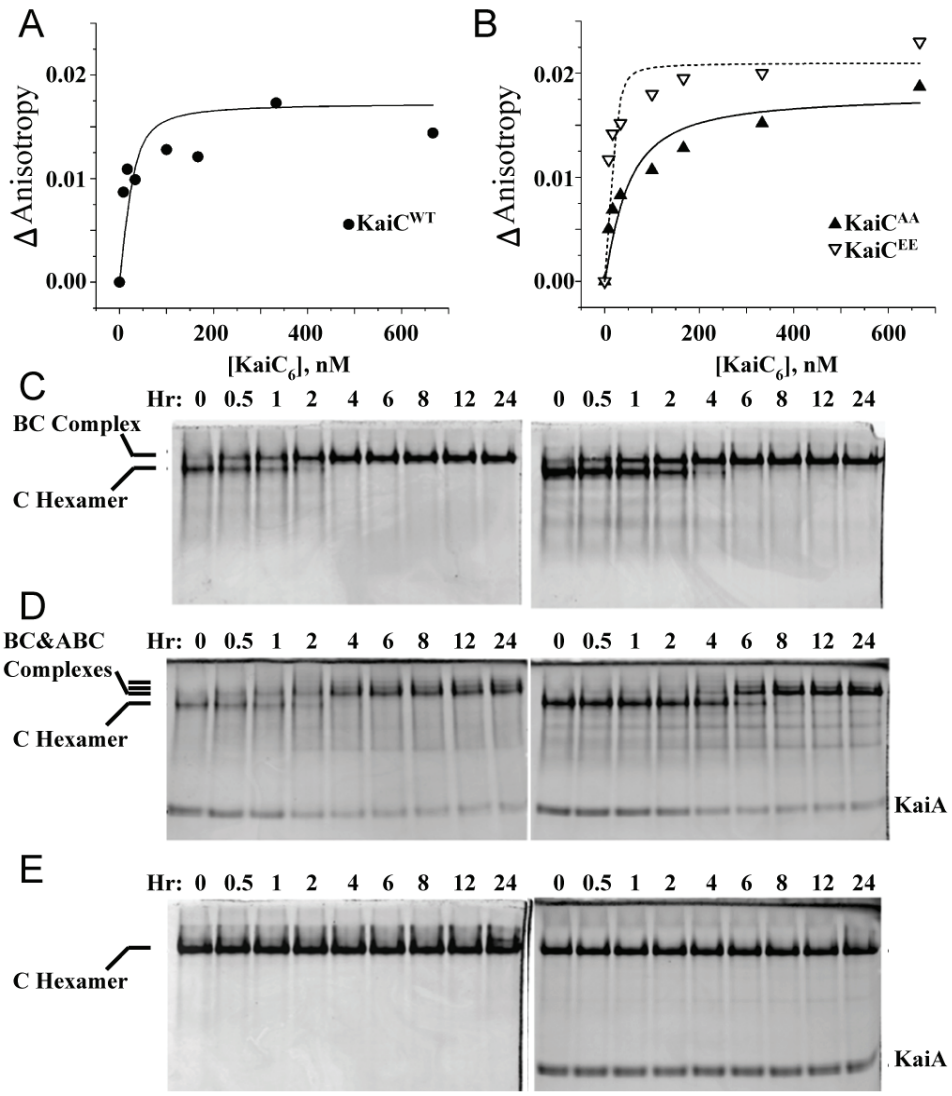

Figure 2-1. Interactions among KaiA, KaiB and KaiC. (A,B) Fluorescence anisotropy (FA) was used to calculate the binding affinity between KaiA and KaiC. Panel **A:** FA between KaiA and $KaiC^{WT}$. F150-labeled KaiA (60 nM) was mixed with increasing concentrations of unlabeled $KaiC^{WT}$ proteins, and the anisotropy was measured. The dissociation constant (K_d) was calculated by assuming a 1:1 ratio binding stoichiometry between KaiA dimers and KaiC hexamers by the equation in (Kovaleski et al., 2006), and simulated by the curves shown on the panels. Panel **B:** FA between KaiA (60 nM) and $KaiC^{AA}$ or $KaiC^{EE}$ phosphomimics. **(C-E)** Formation of stable complexes among KaiA, KaiB and KaiC was assayed by native polyacrylamide gel electrophoresis (native-PAGE). Panel **C:** Formation of stable complexes of KaiB with $KaiC^{DT}$ (left) or $KaiC^{EE}$ (right) as indicated by a reduction in the mobility of the KaiC band. Panel **D:** In the presence of KaiB, KaiA can be included in a stable KaiA•KaiB•KaiC complex as indicated by extra bands and the depletion of the free KaiA dimer band ($KaiC^{DT}$, left and $KaiC^{EE}$, right). **(E)** In the case of a KaiC variant that cannot be phosphorylated on the S431 residue ($KaiC^{AT}$), stable KaiB•$KaiC^{AT}$ (left) or KaiA•KaiB•$KaiC^{AT}$ complexes do not form.

$KaiC^{WT}$ (Kitayama et al., 2008), while $KaiC^{AA}$ is a mutant with alanine residues at positions 431 and 432 that mimics hypo-phosphorylated $KaiC^{WT}$ (Ito et al., 2007). These mutant KaiCs show significant differences in the K_d for interaction with KaiA. As depicted in **Figure 2-1B**, the K_d for the "hyper-phosphorylated" $KaiC^{EE}$ is much smaller (K_d~3 nM) than for the "hypo-phosphorylated" $KaiC^{AA}$ (K_d~32 nM). Therefore, the phosphorylation status of KaiC is likely to have a significant impact upon binding of KaiA such that KaiA has higher affinity for hyper-phosphorylated KaiC than for hypo-phosphorylated KaiC.

Formation of stable complexes of KaiC with KaiA and/or KaiB depends upon KaiC's phosphorylation status

While fluorescence anisotropy (**Figs. 2-1A&B**) can be used to assess the K_d for both labile and stable associations, we found that some complexes of KaiC with KaiB ± KaiA were so stable that they could be measured by band shifts after electrophoresis of the proteins for 5 h in native polyacrylamide gels (**Figs. 2-1C-E**). For these measurements, we used $KaiC^{WT}$ and KaiC variants that were mutated at the 431 and 432 residues to mimic the various phosphorylation states that are sequentially present over the *in vitro* oscillation (Nishiwaki et al., 2007; Rust et al., 2007). **Figure 2-2A** shows the electrophoretic patterns for the different KaiC variants by SDS-PAGE or native-PAGE. $KaiC^{WT}$, $KaiC^{AT}$, and $KaiC^{DT}$ exhibit a temperature-dependent change in the phosphorylation status as assessed by mobility shifts after SDS-PAGE. In particular, each of these variants is predominantly in a hyper-phosphorylated state after incubation at 4°C

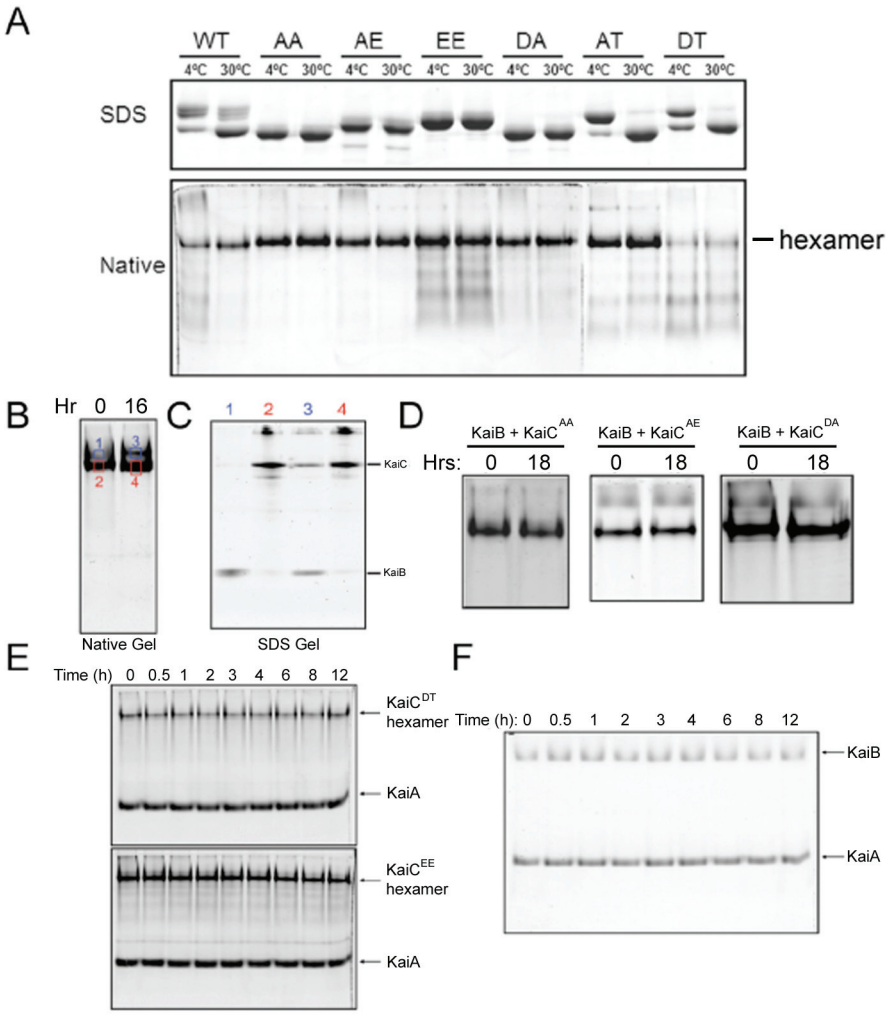

Figure 2-2. Native gel electrophoresis of different combinations of Kai protein mutants. After proteins were mixed and incubated as described in the Methods for the indicated times, they were separated by electrophoresis in either SDS or native polyacrylamide gels. **(A)** Different phospho-mimics of KaiC were incubated at either 4°C or 30°C for 24 h, then separated by either SDS-PAGE (upper panel) or native-PAGE (lower panel). **(B,C)** KaiB forms complexes with $KaiC^{WT}$ protein. To identify the components of each band in the native gel (panel B), bands from the native gel were excised and resolved independently on a subsequent SDS-PAGE gel (panel C). Band #1 (blue box) is composed of only KaiB, bands #2 & 4 (red boxes) are composed of KaiC, and band#3 (blue box) is composed of both KaiB and KaiC (note that band #3 is shifted upwards from band #1). **(D)** KaiB does not form stable complexes with $KaiC^{AA}$, $KaiC^{AE}$, or $KaiC^{DA}$, as shown by the lack of a shifted band after an 18-h incubation. **(E)** KaiA does not form stable complexes with KaiC in the absence of KaiB. When KaiA is incubated with either $KaiC^{DT}$ or $KaiC^{EE}$, there is no shift in the mobility of the KaiC hexamers and the density of the KaiA band is unchanged. **(F)** KaiB does not form a stable complex with KaiA in the absence of KaiC.

for 24 h, whereas they are predominantly hypo-phosphorylated after incubation at 30°C for 24 h. On the other hand, KaiC^{AA} and KaiC^{DA} are in a hypophosphorylated state independent of incubation temperature; conversely, KaiC^{EE} is always in a hyper-phosphorylated state and KaiC^{AE} is "halfway" phosphorylated by virtue of a glutamate at position 432 and a non-phosphorylatible alanine at position 431 (**Fig. 2-2A**). By native-PAGE, all versions of KaiC are predominantly in the hexameric configuration, but there is a significant monomer pool for both KaiC^{EE} and KaiC^{DT} (as indicated by the presence of lower MW bands in **Fig. 2-2A**).

The data of **Figure 2-1B** suggest that KaiA interacts more strongly with hyper-phosphorylated KaiC, and the same is true for interactions between KaiB and KaiC. In fact, KaiB will form a stable interaction with hyper-phosphorylated KaiC that will persist through native-PAGE electrophoresis for 5 h, and can be visualized by a mobility shift in the native-PAGE (**Fig. 2-2B**). **Figure 2-1C** shows that KaiB forms stable complexes over 1-4 hr incubation with KaiC^{DT} and KaiC^{EE}, which are both mimics of hyper-phosphorylated KaiC (at 30ºC, these KaiB•KaiC complexes are maintained for at least several days). KaiB does not form these stable complexes with mimics of different forms of hypo-phosphorylated KaiC, KaiC^{AA}, KaiC^{AE}, KaiC^{DA}, or KaiC^{AT} (left panel of **Fig. 2-1E** and **Fig. 2-2D**). Namely, while KaiA alone can form labile associations with KaiC (**Figs. 2-1A&B**), it does not form the stable complexes as assayed by native-PAGE in the absence of KaiB (**Fig. 2-2E**). On the other hand, when KaiB is present, stable complexes of KaiA & KaiB with hyper-phosphorylated KaiC mimics can be found by native-PAGE,

as seen by mobility shifts and depletion of the KaiA dimer band (**Fig. 2-1D**). These associations are dependent upon KaiC, because KaiA and KaiB do not form complexes by themselves that are stable enough to be measured by this native-PAGE method (**Fig. 2-2F**). Finally, the formation of these stable KaiA•KaiB•KaiC complexes is dependent upon the phosphorylation status of KaiC; hyper-phosphorylated KaiC ($KaiC^{DT}$ and $KaiC^{EE}$) will allow the formation of a stable complex of all three proteins (**Fig. 2-1D**), but hypo-phosphorylated $KaiC^{AT}$ will not (**Fig. 2-1E**, right). Therefore, hyper-phosphorylated KaiC will form stable complexes with KaiB into which KaiA can be incorporated to form stable KaiA•KaiB•KaiC complexes, but in the absence of KaiB, the associations of KaiA with hyperphosphorylated KaiC are not stable (**Figs. 2-1A&B** and **Fig. 2-2E**). Moreover, the time course data of the formation of these stable complexes can be used to model the dynamics of the KaiABC oscillator (see below).

Rhythmic assembly/disassembly of stable KaiABC complexes during the *in vitro* oscillation

The data of **Figures 2-1 & 2-2** used phosphomimetic mutants of KaiC to provide snapshots of the association dynamics that oscillate over the KaiC phosphorylation cycle. The rhythmic changes can also be measured directly with $KaiC^{WT}$ to confirm that the phosphomimics accurately reflect the characteristics of $KaiC^{WT}$. In this analysis, we took advantage of two mutants of KaiB that show different circadian periods *in vivo* and *in vitro*: one mutant replaces the arginine at site 22 with cysteine ($KaiB^{R22C}$) and the other replaces arginine at site 74 with cysteine ($KaiB^{R74C}$). *In vivo*, $KaiB^{WT}$ exhibits a period of

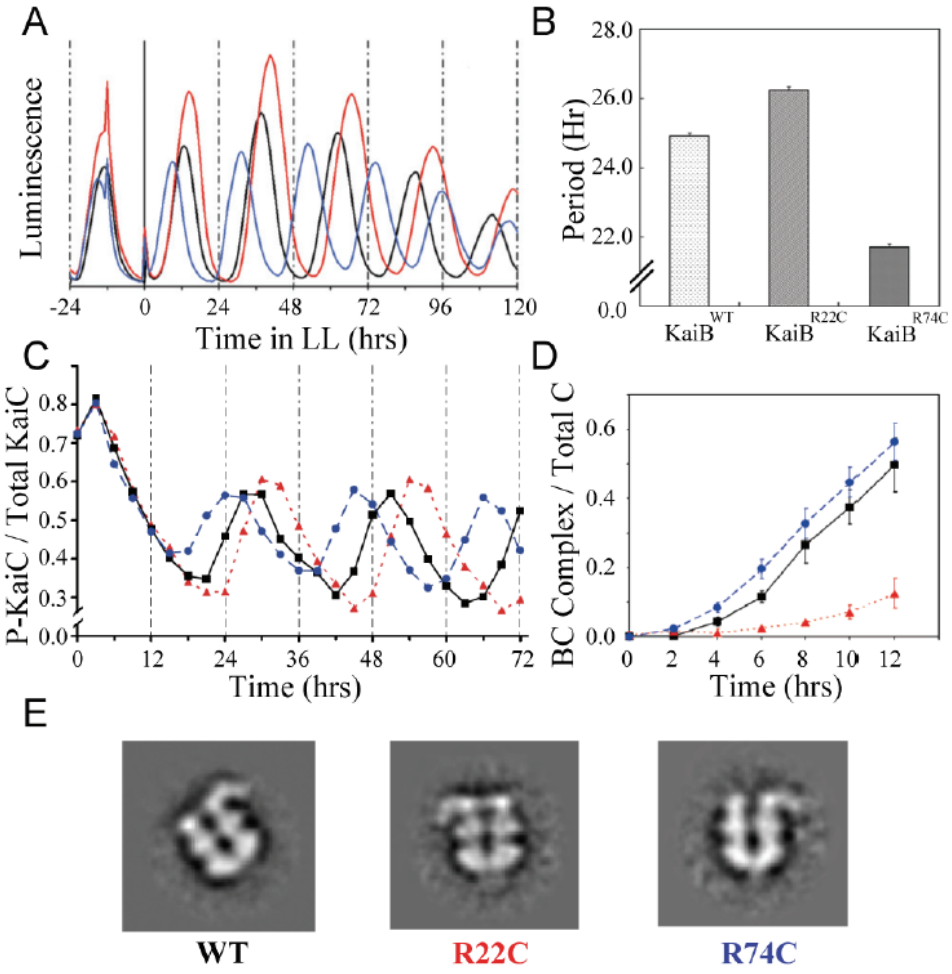

Figure 2-3. KaiB mutant variants that affect association kinetics also affect circadian period *in vivo* and *in vitro*. (**A**) Luminescence traces of cyanobacterial strains expressing different KaiB variant proteins *in vivo*; black trace = KaiB^{WT}, red trace = KaiB^{R22C} (long period), blue trace = KaiB^{R74C} (short period). **(B)** Quantitative analysis of the periods in panel A: KaiB^{WT} = 24.9 ± 0.10 h; KaiB^{R22C} = 26.2 ± 0.12 h; KaiB^{R74C} = 21.7 ± 0.10 h (mean ± S.D., n=3 for each variant). **(C)** *In vitro* rhythms with KaiA^{WT} + KaiC^{WT} and each of the three KaiB mutant variants. The mutations of KaiB show similar effects on the *in vitro* rhythm of KaiC phosphorylation as on the *in vivo* rhythm of gene expression as reported by luminescence in panel A. **(D)** Formation of complexes between KaiC^{489} and the three KaiB mutant variants (± S.D., n=3, for raw data see **Fig. S2-2**). **(E)** Electron Microscopy analysis of the stable KaiA•KaiB•KaiC complexes show similar configurations among the different KaiB variants.

24.9 ± 0.1 h, KaiB^{R74C} has a period of 21.7 ± 0.1 h, and KaiB^{R22C} has a period of 26.2 ±0.1 h (**Figs. 2-3A & B**, **Table 2-1**). *In vitro*, the same trends in period are obvious (**Fig. 2-3C**). These KaiB variants have different kinetics of formation of KaiB•KaiC complexes

(as assayed with the $KaiC^{489}$ mimic of hyperphosphorylated KaiC for technical reasons explained in **Materials and Methods**). KaiB interacts with hyperphosphorylated KaiC (± KaiA) to form stable KaiB•KaiC or KaiA•KaiB•KaiC complexes (**Figs. 2-1C & D**). At the beginning of the phosphorylation phase in the *in vitro* oscillation, the ratio of KaiB to hyperphophorylated KaiC (KaiB/KaiC-P) is high (Nishiwaki et al., 2007; Rust et al., 2007). As illustrated in **Figure 2-3D**, formation of stable KaiB•$KaiC^{489}$ complexes occurs most rapidly with the short period $KaiB^{R74C}$ mutant and most slowly with the long period $KaiB^{R22C}$ mutant (for raw data, see **Fig. S2-2** in **Appendix A**). Although these KaiB mutants affected the kinetics of KaiB•KaiC complex formation, **Figure 2-3E** shows that the appearance of the KaiA•KaiB•KaiC complexes with the KaiB mutants was indistinguishable from that of KaiA•KaiB•$KaiC^{WT}$ complexes visualized with electron microscopy by methods described previously (Mori et al., 2007).

KaiA and KaiB rhythmically interact with $KaiC^{WT}$ to assemble/disassemble stable KaiA•KaiB•KaiC complexes during the *in vitro* oscillation. As shown in **Figure 2-4A**, *in vitro* oscillations of KaiC phosphorylation status visualized by SDS-PAGE (**Fig. 2-4A**, upper panel) are paralleled by oscillations in stable KaiA•KaiB•KaiC complexes indicated by native-PAGE (**Fig. 2-4A**, lower panel) such that the peak in the abundance of complexes occurs 6-8 h after the peak in KaiC phosphorylation (**Fig. 2-4E**). The amount of stable KaiA•KaiB•KaiC complexes can be quantified as a "Complexes Index" (CI) that is plotted for *in vitro* oscillations of $KaiC^{WT}$ and KaiA with $KaiB^{WT}$ (**Fig. 2-4C**), $KaiB^{R74C}$ (**Fig. 2-4B**, raw data in **Fig. S2-3A** of **Appendix A**), and $KaiB^{R22C}$ (**Fig. 2-4D**,

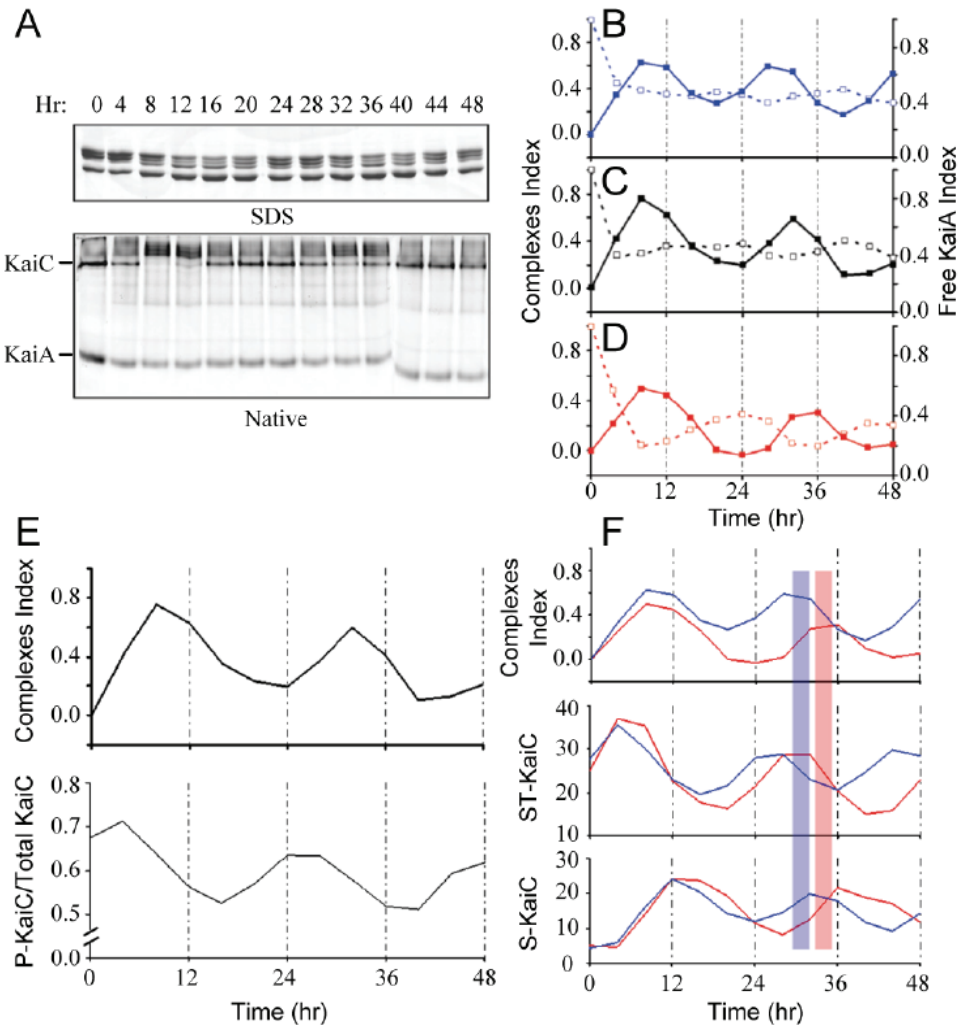

Figure 2-4. Rhythmic assembly of KaiA•KaiB•KaiC complexes quantitatively correlate with KaiC phorphostatus. (A, upper gel) Using KaiA^{WT}, KaiB^{WT}, and KaiC^{WT}, samples were collected every 4 h during the *in vitro* oscillation and analyzed by SDS-PAGE and native-PAGE. These data are quantified in the lower portion of panel **E**. **(A, lower gel)** The same samples were run on native-PAGE and low mobility KaiA•KaiB•KaiC complexes appear and disappear rhythmically in antiphase to the density of the KaiC hexamer and KaiA dimer bands. **(B)** Quantification of the formation of complexes (solid line) and free KaiA (dashed line) in the native-PAGE for KaiB^{R74C} (raw data appears in **Fig. S2-3A**). **(C)** same as for panel B except using KaiB^{WT} (raw data appears in panel **A**). **(D)** same as for panel B except using KaiB^{R22C} (raw data appears in **Fig. S2-3B**). **(E)** The formation of complexes (upper plot) is compared with the KaiC phosphorylation rhythm (lower plot) (raw data in panel **A**). Formation of KaiA•KaiB•KaiC complexes peaks in the phase of KaiC dephosphorylation. **(F)** The relationship between formation of complexes and different KaiC phosphoforms. The analysis of KaiC phosphorylation status and phosphoforms was derived from SDS-PAGE gels as shown in **Fig. S2-4**. The short period mutant KaiB^{R74C} is plotted with the long period mutant KaiB^{R22C} to show the maximum contrast (the peaks for KaiB^{WT} were intermediate between those for KaiB^{R74C} and KaiB^{R22C}, as shown in **Fig. S2-4**). The formation of KaiA•KaiB•KaiC complexes (top panel), doubly phosphorylated KaiC (S431-P and T432-P, middle panel), and singly phosphorylated

KaiC (S431-P, bottom panel) were plotted as a function of incubation time. The blue bar is a reference for the peak of KaiA•KaiB^{R74C}•KaiC complex formation, while the red bar is a reference for the peak of KaiA•KaiB^{R22C}•KaiC complex formation.

raw data in **Fig. S2-3B** of **Appendix A**). The modeling study of van Zon and coworkers (van Zon et al., 2007) predicted that KaiB•KaiC complexes would sequester KaiA rhythmically during the *in vitro* oscillation. This prediction is upheld by our data. As KaiA is incorporated into the KaiA•KaiB•KaiC complexes, it is sequestered so that free KaiA levels decrease, which leads to a depletion of the free KaiA dimer band on native-PAGE (**Fig. 2-1D**). Thus, if the prediction of van Zon and coworkers were correct (van Zon et al., 2007), then the CI should oscillate in antiphase to the level of free KaiA dimers. This antiphase oscillation is obvious for the KaiB^{R22C} data (**Fig. 2-4D**, raw data in **Fig. S2-3B** of **Appendix A**) and while less conspicuous for KaiB^{WT} or KaiB^{R74C}, there is nevertheless a significant antiphase relationship between the oscillations of free KaiA dimers and KaiA• KaiB^{WT}•KaiC or KaiA• KaiB^{R74C}•KaiC complexes (**Figs. 2-4 A,B,C** and **Fig. S2-3A** of **Appendix A**).

The oscillation in stable KaiA•KaiB•KaiC complexes occurs in a strict phase relationship to the KaiC phosphorylation status. As mentioned above for the data of **Figure 2-4A**, the oscillation of CI phase lags the oscillation of KaiC's overall level of phosphorylation by 6-8 h (**Fig. 2-4E**). **Figure 2-4F** depicts the relationships between CI and specific KaiC phosphoforms; the peak of KaiA•KaiB•KaiC formation occurs just after the peak of KaiC that is doubly phosphorylated (on both S431 and T432, i.e.,

"ST-KaiC") and just before the peak of singly phosphorylated KaiC (on S431, i.e., "S-KaiC"). The temporal relationships between these rhythms are consistent with the interpretation that doubly phosphorylated KaiC (ST-KaiC) regulates the formation of the KaiA•KaiB•KaiC complexes, and these complexes then mediate the dephosphorylation of the T432 residue to form singly phosphorylated KaiC (S-KaiC) in the sequential reaction (Nishiwaki et al., 2007; Rust et al., 2007, and **Figs. S2-1**&**S2-4** of **Appendix A**).

Modeling of PTO dynamics as a function of KaiA and KaiB associations with KaiC

In this section we briefly describe a mathematical model for the KaiABC *in vitro* oscillator based on mass action that includes monomer exchange as a mechanism of synchrony and KaiA sequestration in complexes with KaiB•KaiC during the dephosphorylation stage (see **Appendix A** for a complete list of equations and parameters used). We have previously shown in an explicit stochastic matrix model for hexamers that phase-dependent monomer exchange is sufficient to produce sustained oscillations in the KaiABC system (Mori et al., 2007). Here we construct and use a simplified ordinary differential equation (ODE) model to investigate the dynamics of KaiA sequestration and the effects of KaiB association/dissociation rates on the oscillator.

In the simplified ODE version of the full model, the series of molecular reactions in the KaiABC system are organized into the cyclic reaction sequence: $C_0 \rightarrow AC_0 \rightarrow AC_1 \ldots \rightarrow AC_N \rightarrow ABC_N \rightarrow ABC_{N-1} \rightarrow \ldots \rightarrow ABC_0 \rightarrow A+B+C_0$. We label the concentration of effective hexamer phosphorylation states by C_i ($1 < i < N$). Complexes of KaiA•KaiC with

various phosphorylation levels are indicated by AC_i; similarly various phosphorylation levels of KaiA•KaiB•KaiC complexes are labeled by ABC_i. The concentration of maximally hyperphosphorylated KaiC states is indicated by N (N_{max} is 12 to account for the two phosphorylation sites {S431 and T432} in each monomer of the hexamer). In the full model (see **Appendix A**), we (i) remove the assumption of the explicit reaction sequence accounting for auto-phosphorylation/dephosphorylation reactions, (ii) include all uncomplexed (C_i) states, and (iii) include both association and dissociation reactions for all complexes. However since KaiA rapidly binds KaiC and KaiC readily phosphorylates in these KaiA•KaiC complexes, the phosphorylation phase is well-approximated by the simple sequence $C_0 \rightarrow AC_0 \rightarrow AC_1 \ldots \rightarrow AC_N$ without considering each reaction (i.e., $C_i \leftrightarrow C_{i+1}$, $AC_i \leftrightarrow A + C_i$, $AC_i \leftrightarrow AC_{i+1}$) that is represented in the full model. Therefore, in our simplified ODE model, KaiB only binds to the hyper-phosphorylated form of KaiC ($B + AC_N \rightarrow ABC_N$), which subsequently dephosphorylates through each intermediate state that characterizes the de-phosphorylation phase, $ABC_N \rightarrow ABC_{N-1} \rightarrow \ldots \rightarrow ABC_0$. Experimentally, KaiC that is associated with KaiB appears to dephosphorylate at the same rate as free KaiC (Xu et al., 2003; Xu et al., 2009). Finally the hypo-phosphorylated complexes dissociate, releasing KaiA, KaiB and unphosphorylated KaiC: $ABC_0 \rightarrow A+B+C_0$. The cycle is then reset to its initial state.

However, by itself this cyclic reaction sequence $C_0 \rightarrow \ldots \rightarrow AC_N \rightarrow ABC_N \rightarrow ABC_{N-1} \rightarrow \ldots \rightarrow ABC_0 \rightarrow A+B+C_0$ will not produce sustained oscillations due to

desynchronization of hexamers in the population (therefore leading to damped oscillations). We use the exchange of monomers among hexamers as a mechanism for sustained oscillations (Mori et al., 2007; Ito et al., 2007) to implement "one monomer exchange" reactions $AC_i + AC_j \rightarrow AC_{i+1} + AC_{j-1}$ $(j > i)$ and $ABC_i + ABC_j \rightarrow ABC_{i+1} + ABC_{j-1}$ $(j > i)$ that increase "low" phosphorylated states (i) by taking a phosphate from a higher phosphorylated state (j). The simplified ODE model has the advantage that it is easily interpretable and contains only 6 rates: 1 effective phosphorylation rate, 1 effective dephosphorylation rate, a KaiA binding rate, a KaiB binding rate, a complex dissociation rate, and an exchange rate. A typical simulation of the net population phosphorylation with standard initial conditions of [KaiA dimer]:[KaiB tetramer]:[KaiC hexamer] = 1:1.5:1 and setting $C_0 = 1$ μM is shown in **Figure 2-5A**, which shows the well sustained nature of the oscillation. The kinetics of sequestration of KaiA in high molecular weight complexes (with KaiB and KaiC) is indicated in **Figure 2-5B** which shows the rapid formation of labile KaiA•KaiC complexes followed by sequestration into stable KaiA•KaiB•KaiC complexes. There is about an ~8 hour delay between the peak of the phosphorylation rhythm and the peak of KaiA•KaiB•KaiC complex formation, which is similar to the experimental data depicted in **Figure 2-4**. To examine the effect of KaiB binding in the model, we varied the rate by which KaiB binds to the hyper-phosphorylated form of KaiC (per μM per h). As shown in **Figure 2-5C** and **Table 2-1**, a faster binding rate (larger number) decreases the period while a slower binding rate increases the period and decreases the amplitude of the KaiC phosphorylation rhythm.

These results qualitatively match those of the experimental data of **Figs. 2-3A-C**. Therefore, based on the empirical data of KaiA and KaiB associations with KaiC, the simplified ODE model qualitatively and quantitatively predicts the period and dynamics of the KaiABC oscillator.

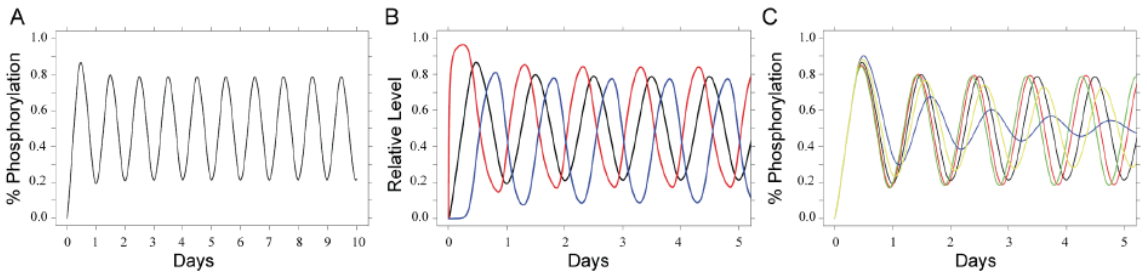

Figure 2-5. Computational model of the dynamics of KaiABC complexes. (A) A typical simulation from the simplified mathematical model of the net KaiC population phosphorylation with standard initial conditions of [KaiA dimer]:[KaiB tetramer]:[KaiC hexamer] = 1:1.5:1 and setting C_0 = 1 μM. **(B)** The kinetics of sequestration of KaiA in high molecular weight complexes (with KaiB and KaiC) shows the rapid formation of labile KaiA•KaiC complexes (red trace) followed by sequestration into stable KaiA•KaiB•KaiC complexes (blue trace). The black trace is net KaiC phosphorylation. **(C)** The simulated effect of varying the association kinetics of KaiB to hyper-phosphorylated KaiC on net KaiC phosphorylation shows a correlation between an increased rate of association (0.25 = blue, 0.5 = yellow, 1.0 = black, 2.5 = red , 5.0 = green) and a shorter circadian period.

Recruitment of KaiA to the stable KaiA•KaiB•KaiC complex occurs at a novel site on KaiC

KaiA is thought to enhance the autokinase activity of KaiC by interacting with the C-terminal tentacles of KaiC (Johnson et al., 2008b; Kim et al., 2008; Vakonakis & LiWang, 2004). However, removing the 30 amino acid tentacles from the C-terminus of KaiC (to create $KaiC^{489}$) does not prevent the formation of stable complexes with either KaiB or KaiA/KaiB. As shown by the native-PAGE analyses in **Figure 2-6**, $KaiC^{489}$ forms stable complexes with KaiB (middle panel). $KaiC^{489}$ does not form stable KaiA•

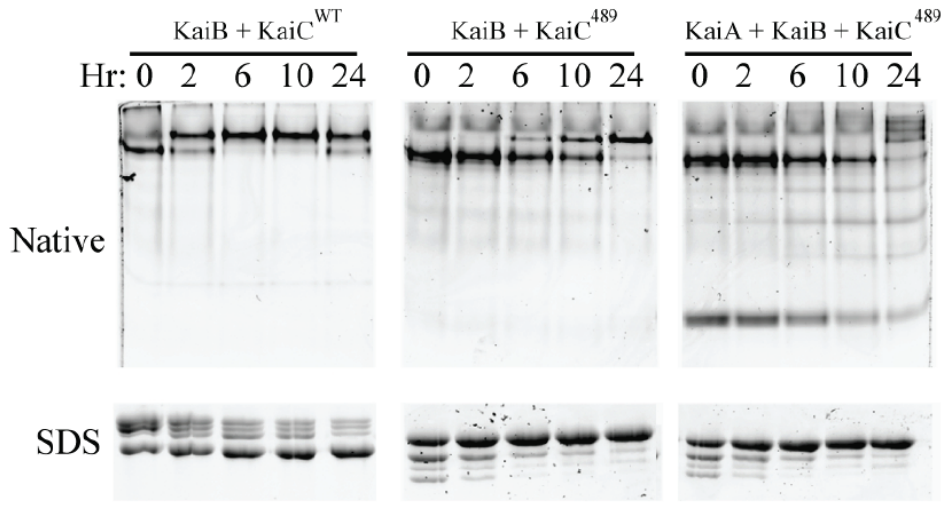

Figure 2-6. KaiC^{489} forms stable complexes with KaiB and KaiA. KaiC^{489} forms a hexamer that can assemble into a stable KaiB•KaiC complex (middle panel) as well as a stable KaiA•KaiB•KaiC complex (right panel). KaiC^{WT} also forms stable KaiB•KaiC complexes (left panel). Note from the SDS-PAGE analyses at the bottom of the figure that KaiC^{WT} dephosphorylates over time at 30ºC (left), but KaiC^{489} hyperphosphorylates over time at 30ºC (middle) independently of the presence of KaiA.

KaiC^{489} complexes, but when KaiB is present KaiC^{489} will sequester KaiA into a stable KaiA•KaiB•KaiC^{489} complex (**Fig. 2-6**, right panel). KaiC^{489} forms hexamers but has a slightly higher mobility than KaiC^{WT} in native-PAGE due to its loss of 30 residues (**Fig. 2-7A**); λ-PPase treatment confirmed that the multiple bands of KaiC^{489} observed by SDS-PAGE are a result of phosphorylation (**Fig. 2-7C**). As reported by Kim and coworkers (Kim et al., 2008), KaiC^{489} maintains its autokinase activity but has a reduced autophosphatase activity, so it hyperphosphorylates over time to reach a steady state of doubly phosphorylated S431 and T432 residues (ST-KaiC^{489}) independently of KaiA (bottom panels of **Fig. 2-6**, and **Fig. 2-7B**). Therefore, the native-PAGE data strongly support the interpretation that KaiA is sequestered into complexes with KaiB and KaiC by an interaction that is independent of KaiC's C-terminal tentacles. Possibly this novel

site on KaiC is created by the binding of KaiB to KaiC (possibly KaiB itself provides a part of the KaiA binding site), which could explain the KaiB-dependency of the formation of stable KaiA•KaiB•KaiC complexes.

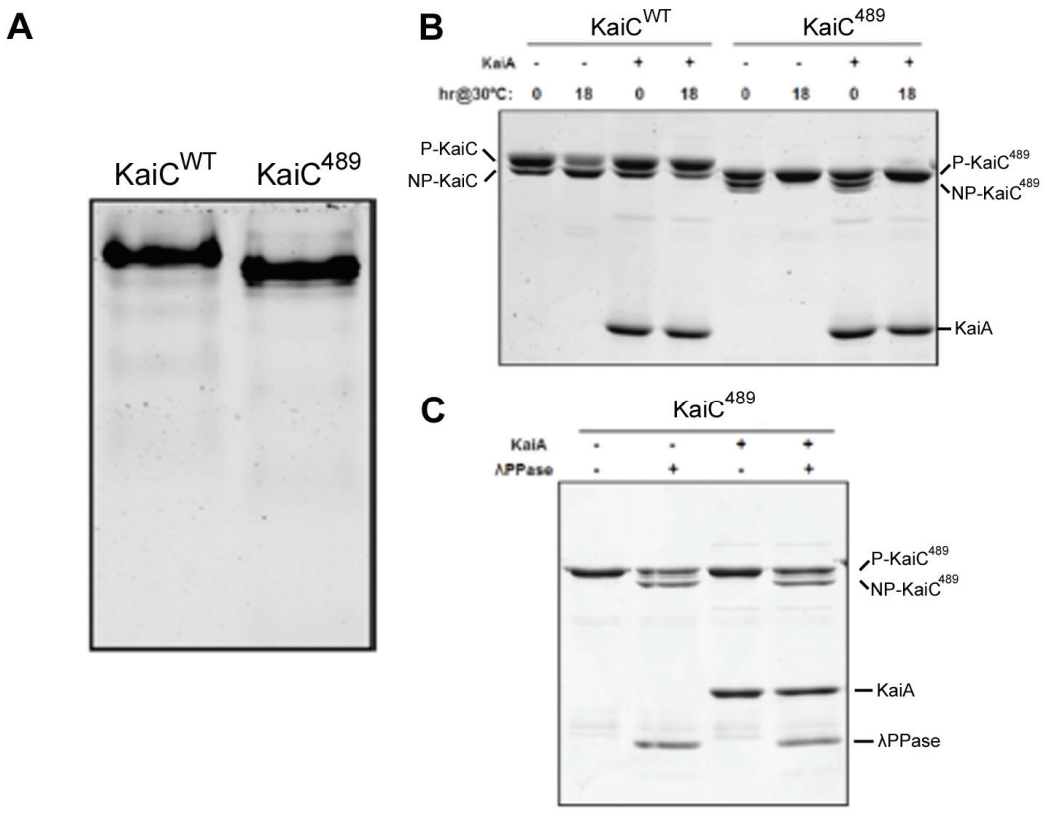

Figure 2-7. Characterization of hyperphosphorylated KaiC^{489}. (A) Native-PAGE indicates that KaiC^{489} forms hexamers as well as does KaiC^{WT}, and that its mobility is slightly higher than that of KaiC^{WT} due to the loss of the C-terminal tentacles. **(B)** KaiA enhances the auto-kinase activity of KaiC^{WT} at 30ºC. In the absence of KaiA, KaiC^{WT} becomes progressively less phosphorylated when incubated at 30ºC due to auto-phosphatase activity. However, KaiC^{489} does not auto-dephosphorylate in the absence of KaiA at 30ºC (in fact, it becomes progressively more phosphorylated), indicating that KaiC^{489} has low phosphatase activity (or at least that the auto-kinase activity can easily overbalance the auto-phosphatase activity). **(C)** Although the auto-phosphatase activity of KaiC^{489} is low, an external phosphatase (λPPase) is able to dephosphorylate KaiC^{489} in the absence or presence of KaiA.

Discussion

Terauchi and coworkers have proposed that the rhythm of KaiC ATPase activity constitutes the most fundamental reaction underlying circadian periodicity in cyanobacteria (Terauchi et al., 2007). Another possibility, however, is that the ATP hydrolysis observed by Terauchi and colleagues is a consequence of the energy released by the conformational changes of KaiC that are regulated by the associations with KaiA and KaiB. Our results support the latter interpretation. We find that the intermolecular dynamics of interaction among KaiA and KaiB with KaiC determine the period and amplitude of this *in vitro* oscillator. It is possible that the ATPase activity is a reflection of an underlying biochemical activity of KaiC that has not yet been identified. Nonetheless, our hypothesis is that (i) the basic timing loop of the KaiABC oscillator and (ii) its outputs are mediated by conformational changes of KaiC in association with KaiA and KaiB.

For example, mutations within KaiB that alter affinity to KaiC predictably alter the period of this clock *in vivo* and *in vitro* as confirmed by our mathematical modeling. Therefore, with native versions of KaiC and KaiA, mutations within KaiB that change affinity to KaiC will modulate key circadian properties, which is consistent with the hypothesis that intermolecular associations determine KaiABC oscillator dynamics. At the very least, if the ATPase activity is the basic timing loop as suggested by Terauchi and coworkers, then the intermolecular associations with KaiB must regulate the ATPase activity in a deterministic way (Terauchi et al., 2007). Our interpretation is that the

formation of Kai protein complexes is coupled with KaiC phosphorylation status; because different KaiB variants modulate the rate of KaiB•KaiC formation, they affect the period of the KaiC phosphorylation. Our modeling analysis confirms that this interpretation is consistent with the empirical data.

Another important conclusion from our study is that we found that the characteristics of KaiA's association with KaiC go through two phases–during the phosphorylation phase in which KaiA is stimulating KaiC's autophosphorylation, the association of KaiA with KaiC is labile. However, in the later dephosphorylation phase, a stable KaiB•KaiC complex recruits KaiA into a stable KaiA•KaiB•KaiC complex that facilitates KaiC's dephosphorylation because it sequesters KaiA into an inactive configuration. The stable KaiA•KaiB•KaiC^{WT} complex can be mimicked by associations of KaiA and KaiB with the hyperphosphorylated KaiC^{489} mutant. Even though KaiC^{489} is devoid of the C-terminal tentacles (and cannot therefore associate with KaiA by itself), it forms stable complexes with KaiB, and this KaiB•KaiC^{489} complex can recruit KaiA into a complex that is so stable it resists dissociation during electrophoresis through a native gel (**Figs. 2-6** and **2-8A**). In the case of the cyclic reaction with KaiC^{WT}, KaiA first repetitively interacts with the tentacles of hypophosphorylated KaiC to enhance KaiC's auto-kinase activity until KaiC is hyperphosphorylated, at which time the KaiC hexamer undergoes a conformational change that allows it to form a stable complex with KaiB (**Fig. 2-8B**) (Kageyama et al., 2006; Mori et al., 2007; Johnson et al., 2008; Iwasaki et al., 2002; Kim et al., 2008; Vakonakis & LiWang, 2004). This stable KaiB•KaiC complex

exposes a novel binding site for KaiA, which sequesters KaiA into the stable KaiA•KaiB•KaiC complex that is visualized in **Figure 2-3E**. The sequestered KaiA is unable to further stimulate KaiC's auto-kinase activity and therefore the auto-phosphatase activity dominates such that KaiC dephosphorylates to its hypophosphorylated conformation from which KaiB and KaiA dissociate and the cycle begins anew (**Fig. 2-8B**).

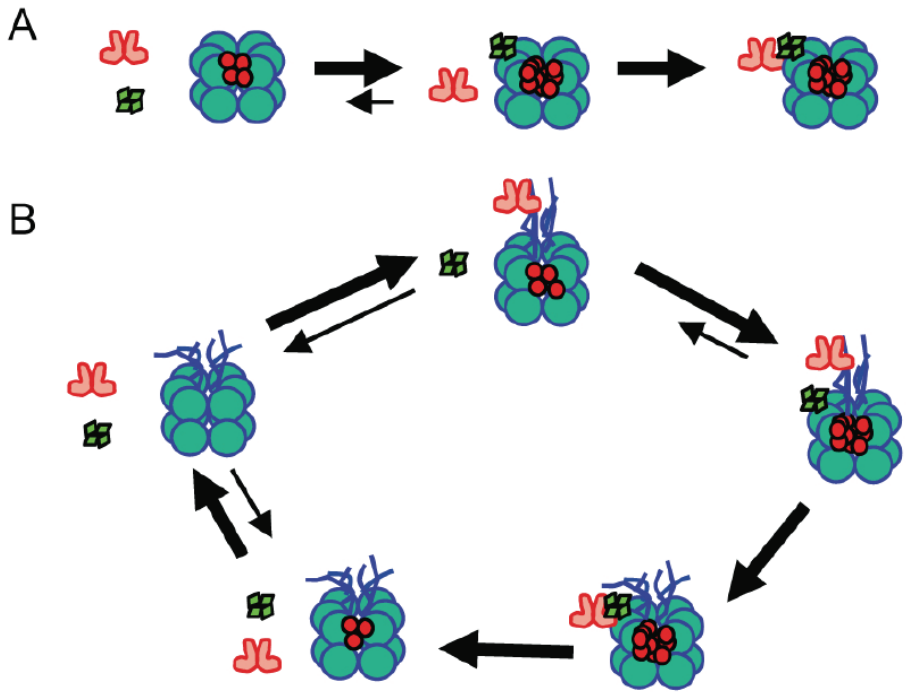

Figure 2-8. KaiB•KaiC sequesters KaiA. (A) $KaiC^{489}$ ("double-donut" hexamer) cannot associate with KaiA (red dimers) by itself, but once it has autophosphorylated, it can form stable complexes with KaiB (tetramer of green diamonds) that are then able to recruit KaiA into KaiA•KaiB•KaiC complexes. **(B)** With $KaiC^{WT}$ ("double-donut" hexamer with C-terminal "tentacles") in the cycling reaction, KaiA repeatedly and rapidly interacts with KaiC's C-terminal tentacles during the phosphorylation phase. When $KaiC^{WT}$ becomes hyperphosphorylated, it first binds KaiB stably. Then, the KaiB•KaiC complex binds KaiA, sequestering it from further interaction with KaiC's tentacles. At that point, KaiC initiates dephosphorylation. When KaiC is hypophosphorylated, it releases KaiB and KaiA, thereby launching a new cycle.

Our conclusion of a labile interaction between KaiA and KaiC during the phosphorylation phase is consistent with previous experimental studies (Kageyama et al., 2006; Kim et al., 2008; Vakonakis & LiWang, 2004). On the other hand, there are no previous empirical data supporting a stably sequestered KaiA complex. The hypothetical existence of a sequestered KaiA complex had been suggested previously in a modeling paper as a potential mechanism for maintaining synchrony within a population of KaiC hexamers (van Zon et al., 2007). However, in our model the sequestration of KaiA is used as a means by which $KaiC^{WT}$ shifts between a predominantly auto-kinase mode and a predominantly auto-phosphatase mode. Moreover, we model the primary mechanism for maintaining synchrony among KaiC hexamers as residing in the phenomenon of KaiC monomer exchange among the hexamers in the population of complexes, which is an interpretation that is strongly supported by experimental data (Mori et al., 2007; Ito, et al., 2007). Therefore, our data are the first concrete experimental support for the existence of a KaiB•KaiC complex that sequesters KaiA into a stable three-protein complex whose function is to inactivate the phosphorylation-stimulating properties of KaiA and thus initiate the dephosphorylation phase. Our empirical data are integrated with a mathematical model that demonstrates the hierarchy of these relationships.

CHAPTER III *

COUPLING OF A CORE POST-TRANSLATIONAL PACEMAKER TO A SLAVE TRANSCRIPTION/TRANSLATION FEEDBACK LOOP IN A CIRCADIAN SYSTEM

Abstract

Cyanobacteria are the only model circadian clock system in which a circadian oscillator can be reconstituted *in vitro*. The underlying circadian mechanism appears to comprise two subcomponents: a post-translational oscillator (PTO) and a transcriptional/translational feedback loop (TTFL). The PTO and TTFL have been hypothesized to operate as dual oscillator systems in cyanobacteria. However, we find that they have a definite hierarchical interdependency — the PTO is the core pacemaker while the TTFL is a slave oscillator that quickly damps when the PTO stops. By analysis of overexpression experiments and mutant clock proteins, we find that the circadian system is dependent upon the PTO and that suppression of the PTO leads to damped TTFL-based oscillations whose temperature compensation is not stable under different metabolic conditions. Mathematical modeling indicates that the experimental data are compatible with a core PTO driving the TTFL; the combined PTO/TTFL system is resilient to noise. Moreover, the modeling indicates a mechanism by which the TTFL can

* Chapter III is directly derived from the published paper: Qin X, Byrne M, Xu Y, Mori T, Johnson CH (2010a) Coupling of a core post-translational pacemaker to a slave transcription/translation feedback loop in a circadian system. *PLoS Biol* 8: e1000394. doi:10.1371/journal.pbio.1000394

feed into the PTO such that new synthesis of clock proteins can phase-shift or entrain the core PTO pacemaker. This prediction was experimentally tested and confirmed by entraining the *in vivo* circadian system with cycles of new clock protein synthesis that modulate the phosphorylation status of the clock proteins in the PTO. In cyanobacteria, the PTO is the self-sustained core pacemaker that can operate independently of the TTFL, but the TTFL damps when the phosphorylation status of the PTO is clamped. However, the TTFL can provide entraining input into the PTO. This study is the first to our knowledge to experimentally and theoretically investigate the dynamics of a circadian clock in which a PTO is coupled to a TTFL. These results have important implications for eukaryotic clock systems in that they can explain how a TTFL could appear to be a core circadian clockwork when in fact the true pacemaker is an embedded biochemical oscillator.

Introduction

The mechanism of circadian (daily) clocks in eukaryotes is generally thought to be based upon autoregulatory transcriptional/translational feedback loops (TTFLs) (Hardin et al., 1990; Dunlap et al., 2004). When the essential components of the circadian clock in the prokaryotic cyanobacterium *Synechococcus elongatus* were identified (Ishiura et al., 1998) as the proteins KaiA, KaiB, and KaiC, the initial interpretation that the core of this prokaryotic clockwork might also be a TTFL was based on the same kind of evidence that supports TTFL oscillators in eukaryotes, namely: (i) rhythms of

abundance for mRNAs and proteins encoded by "clock genes," (ii) feedback of clock proteins on their gene's transcription, and (iii) phase setting by experimental expression of clock proteins (Ishiura et al., 1998; Xu et al., 2000; Johnson et al., 2008). However, later studies found data that were inconsistent with a core TTFL oscillator in cyanobacteria; e.g., global inhibition of transcription and translation had little effect upon the circadian rhythm of KaiC phosphorylation (Tomita et al., 2005), and the promoters driving *kaiBC* gene expression could be replaced with non-specific heterologous promoters without disturbing the circadian rhythm (Xu et al., 2003; Nakahira et al., 2004). Moreover, prolonged treatments of cyanobacterial cells with the protein synthesis inhibitor chloramphenicol did not perturb the phase of the circadian system after return to normal conditions (Xu et al., 2000; Johnson et al., 2008). Then in 2005 came the amazing discovery that the phosphorylation status of KaiC *in vitro* continued to cycle when the three Kai proteins were combined in a test tube with ATP (Nakajima et al., 2005). This *in vitro* rhythm persists with a circa-24 h period for at least 10 days and is temperature compensated (Nakajima et al., 2005; Ito et al., 2007), which indicates that a circadian temperature compensation mechanism is also encoded in the characteristics of the three Kai proteins and the nature of their interactions. *In vivo*, this three-protein biochemical oscillator operates as a post-translational oscillator (PTO) (Tomita et al., 2005; Nakajima et al., 2005). Clearly, a TTFL is not necessary for the circadian rhythm of KaiC phosphorylation.

The PTO manifests itself *in vitro* as three different rhythms that are probably

interrelated. The first is the originally observed rhythm of KaiC phosphorylation (Nakajima et al., 2005). The second is a rhythm of formation of complexes among KaiA, KaiB, and KaiC (Kageyama et al., 2006; Mori et al., 2007), and the third is a rhythm of ATP hydrolysis (Terauchi et al., 2007). At this time, it is not clear which of these rhythms is the most fundamental to the PTO mechanism or whether they are all so tightly intermeshed as to be inseparable. Some or all of these rhythmic processes may also be involved in the control of outputs through interactions with other proteins such as SasA and/or RpaA (Takai et al., 2006). Moreover, while each of these three rhythms can be measured *in vitro*, only the KaiC phosphorylation rhythm can be monitored *in vivo* (as a rhythmic shift of KaiC mobility on immunoblots). Therefore, in this paper, the phosphorylation rhythm will be taken as the indicator of the PTO *in vivo*.

Since the *kaiABC* gene cluster is essential for rhythms *in vivo* and the rhythm of KaiC phosphorylation could run without a TTFL *in vitro* (Nakajima et al., 2005) and *in vivo* (Xu et al., 2000; Tomita et al., 2005), those results implied that the KaiABC oscillator was the self-sustained core pacemaker and that transcription & translation was involved only in the output (Tomita et al., 2005; Nakajima et al., 2005). More recently, however, Kitayama and coworkers suggested "that transcription- and translation-based oscillations in KaiC abundance are also important for circadian rhythm generation in cyanobacteria" (Kitayama et al., 2008). First, those authors reported that over-expression of KaiA resulting in constitutively hyper-phosphorylated KaiC (a “clamp” of KaiC phosphorylation status) allows circadian rhythms of gene expression as monitored by

promoter-driven luciferase reporters *in vivo*. Moreover, mutants of KaiC that mimicked constitutive hyperphosphorylation or hypophosphorylation allowed rhythms *in vivo*. The key phospho-regulatory sites on KaiC are S431 and T432 (Xu et al., 2004; Nishiwaki et al., 2004); Kitayama and coworkers reported that substitution of glutamate on those two residues ($KaiC^{EE}$) created a constitutively hyper-phosphorylated KaiC that "showed a dampened but clear rhythm with a period of 48 h" (Kitayama et al., 2008). Because cyanobacterial cells apparently exhibited oscillations when the KaiABC oscillator was inactivated by clamping the phosphorylation status of KaiC, these two experimental approaches led Kitayama and coworkers to conclude that "transcription-translation oscillates even in the absence of the KaiC phosphorylation cycle and that this oscillation can persist regardless of the phosphorylation state and kinase activity of KaiC" (Kitayama et al., 2008). These results therefore opened the possibility that the KaiABC oscillator (PTO) was not an obligatory core oscillator in cyanobacteria.

We have extended the experiments of Kitayama and coworkers, and our results lead us to different interpretations, namely that the TTFL is a damped slave oscillator while the PTO is the core pacemaker. Our results indicate that repression of the KaiC phosphorylation rhythm by KaiA overexpression strictly correlates with the suppression of the larger circadian system. We find that the rhythms generated by cells expressing $KaiC^{EE}$ are clearly damped and of long period. Moreover, the damped rhythms exhibited by $KaiC^{EE}$ are not compensated for metabolic activity and therefore cannot be considered as a *bona fide* circadian phenomenon. These results direct us towards a model of the

entire system that explains how the core pacemaker can be a PTO while having input from a TTFL. The implications of this organization extend beyond the cyanobacterial case and encourage a re-evaluation of the evidence for a core TTFL in eukaryotic circadian clocks.

Materials and Methods

Strains and culture conditions

The wild-type reporter strain (AMC149) of the cyanobacterium *S. elongatus* PCC 7942 harbors luciferase reporter constructs, either *psbAIp::luxAB* or *kaiBCp::luxAB*. In either reporter, the expression of the *Vibrio harveyi* luciferase gene cassette *luxAB* is driven by the *psbA1* (Kondo et al., 1993) or the *kaiBC* promoter (Xu et al., 2003). Luminescence rhythms from the *psbAIp::luxAB* or *kaiBCp::luxAB* reporters are approximately equivalent in both phase and intensity. Strain KaiA^{OX} has a *kaiBCp::luxAB* reporter (spectinomycin resistance marker in NS I) in which additional expression of wild-type *kaiA* is under the control of an IPTG-derepressible heterologous *trc* promoter, *trc*p*::kaiA* (kanamycin resistance marker in NS II) (Kutsuna et al., 2007). Strain KaiC^{OX} has a *psbAI*p*::luxAB* reporter (spectinomycin resistance marker in NS I) and *trc*p*::kaiC*^{WT} (kanamycin resistance marker in NS II) (Xu et al., 2000). KaiC^{EE} is a *kaiBC*p::*luxAB* reporter expressing the double mutant KaiC$^{S431E/T432E}$ (Xu et al., 2009). For measurement of KaiC degradation rate, strain ΔKaiC/*trc*p*::kaiC*^{WT} was used, which is a *kaiC*-null strain

with *trc*p*::kaiC*^{WT} in NS II (Xu et al., 2003). All strains were grown in modified BG-11 medium (Bustos & Golden, 1991) containing appropriate antibiotics with air bubbling of liquid cultures or on agar plates for solid cultures at 30ºC.

In vivo rhythm measurement and experimental overexpression of KaiA

For assay of *in vivo* rhythms, cells were grown in constant light (LL; cool-white fluorescence at 40-50 μE/m2s). Before release to LL for assay, 1 ~ 2 light:dark cycles (e.g. LD 12:12) were given to synchronize the cells in the population. Luminescence rhythm measurements *in vivo* were performed as described previously (Xu et al., 2000). For experimental overexpression of KaiA, KaiA^{OX} was grown in liquid BG-11 medium at 30ºC in LL until an OD_{750} of between 0.6-0.8 was reached. Then the cells were treated with two cycles of LD12:12, and IPTG was added 6 h before the beginning of the second 12 h dark interval.

Analysis of damping and bandwidth was performed with the LumiCycle data analysis program (Actimetrics, Evanston IL, courtesy of Dr. David Ferster). The program fits the data to a sine wave multiplied by an exponential decay factor. The damping rate (d) is the time constant of the following exponential fit:

$$L = A \{[\sin(2\pi f + \Phi)][\exp(-t/d)]\}$$

Where d is the damping rate, L is the luminescence (counts/min), A is the amplitude, f is the frequency of the sine wave, Φ is the phase of the oscillation, and t is time. The data are fit to a low-order polynomial to get a baseline, which is then subtracted

from the raw data. A Fourier Transform is performed to find the dominant frequency and phase. The timepoints for the peaks and troughs of the dominant sine wave are taken from the baseline-subtracted data, and the timepoints are then fitted to an exponential decay, which gives the amplitude (A) and the time constant of the damping (d). Damping rate (d) is the number of days required for the amplitude of the rhythm to decrease to 1/e (≈ 36.79 %) of the starting value.

Determination of KaiC abundance and phosphorylation levels

For the experiments of **Fig. 3-1**, *S. elongatus* cells were harvested every 4 h for the LL and LD12:12 conditions and every 1 h for the LD2:2 conditions. Total protein was extracted as previously described (Xu et al., 2000). Protein concentration was determined by the Lowry method using BSA as a standard, and equal amounts of proteins were loaded into each well for SDS-PAGE and transfer to nitrocellulose membranes. The blots were treated with anti-KaiC serum, and detected by enhanced chemiluminescence (Pierce, Rockford, USA). KaiC protein abundance was determined on 15% SDS-PAGE gels (to obtain a single KaiC band), whereas KaiC phosphorylation was determined on 10% SDS-PAGE gels (to separate the various KaiC phosphoforms). Gel size was 16 cm X 16 cm X 1 mm, with electrophoresis at 4 ºC for 4-5 h at a constant current of 35 mA per gel. Gel images were analyzed by NIH Image J software.

Phase locking by cycles of low levels of KaiC

Cultures of $KaiC^{OX}$ were inoculated onto nitrocellulose (NC) membranes placed on the surface of BG-11 agar plates containing appropriate antibiotics. After 5 d of growth in LL, these NC membrane cultures were divided into four groups with duplicates, and they were entrained with two LD12:12 cycles. There were a total of 4 different phasings of the LD12:12 cycles (Φ1, Φ2, Φ3, and Φ4) that were different from each other by 6 h (i.e., starting at laboratory clock time 06:00, 12:00, 18:00, and 00:00). After the final dark interval of the last group of plates (Φ4), the cultures were transferred back and forth between pre-warmed fresh BG-11 agar plates containing 0 or 5 μM IPTG for two cycles of: 12 h no IPTG followed by 12 h IPTG, thereby creating an experimentally controlled 12h:12h cycle of new KaiC synthesis (the parallel control cultures were transferred every 12 h between plates that had no IPTG). See **Fig. S3-9A** (in **Appendix B**) for an illustration of this protocol. We determined that a concentration of 5 μM IPTG increases KaiC abundance within cells by only ~40-50% above basal levels (**Fig. S3-9C** in **Appendix B**). After the final IPTG cycle, measurement of the luminescence rhythms in the cultures from each of these phases was performed in LL as previously described (Xu et al., 2003).

Preparation of Kai proteins and *in vitro* reactions

Kai proteins from *S. elongatus* were expressed in *Escherichia coli* and purified as described previously (Mori et al., 2007). *In vitro* reactions were carried out at 30ºC in

reaction buffer (20 mM Tris-HCl (pH 8.0), 150 mM NaCl, 5 mM $MgCl_2$, 1mM ATP, 0.5 mM EDTA) using standard Kai protein concentrations: 50 ng/µl KaiA, 50 ng/µl KaiB and 200 ng/µl KaiC. The reaction mixture was dialyzed against this reaction buffer without ATP at 30 ºC for 24 h. The reaction was initiated by addition of 1mM ATP at 30 ºC. Extra KaiA protein (2X and 4X) was added as indicated (i.e., 2X = 100 ng/µl KaiA, and 4X = 200 ng/µl KaiA). Sample collections and analysis were as described previously (Mori et al., 2007).

Results

The KaiC phosphorylation rhythm is the most consistent rhythm under different *in vivo* conditions

Compared with the rhythm of KaiC abundance that could be the result of a TTFL involving KaiC expression (Xu et al., 2000; Tomita et al., 2005), the KaiC phosphorylation rhythm is the most reproducible molecular rhythm that can be measured *in vivo* under a range of conditions in *S. elongatus*. In both LL and DD, KaiC phosphorylation is robustly rhythmic, despite the fact that KaiC abundance is rhythmic in LL but not in DD (Tomita et al., 2005). **Fig. 3-1** shows that KaiC abundance is rhythmic in LL as noted before (Xu et al., 2000) with a concomitant rhythm of KaiC phosphorylation (**Fig. 3-1A&B**; see **Fig. S3-1A&B** in **Appendix B** for representative immunoblots). However, in a light/dark cycle of 12 h light, 12 h dark (= LD 12:12), there is not a clear daily rhythm of KaiC abundance, while the KaiC phosphorylation rhythm

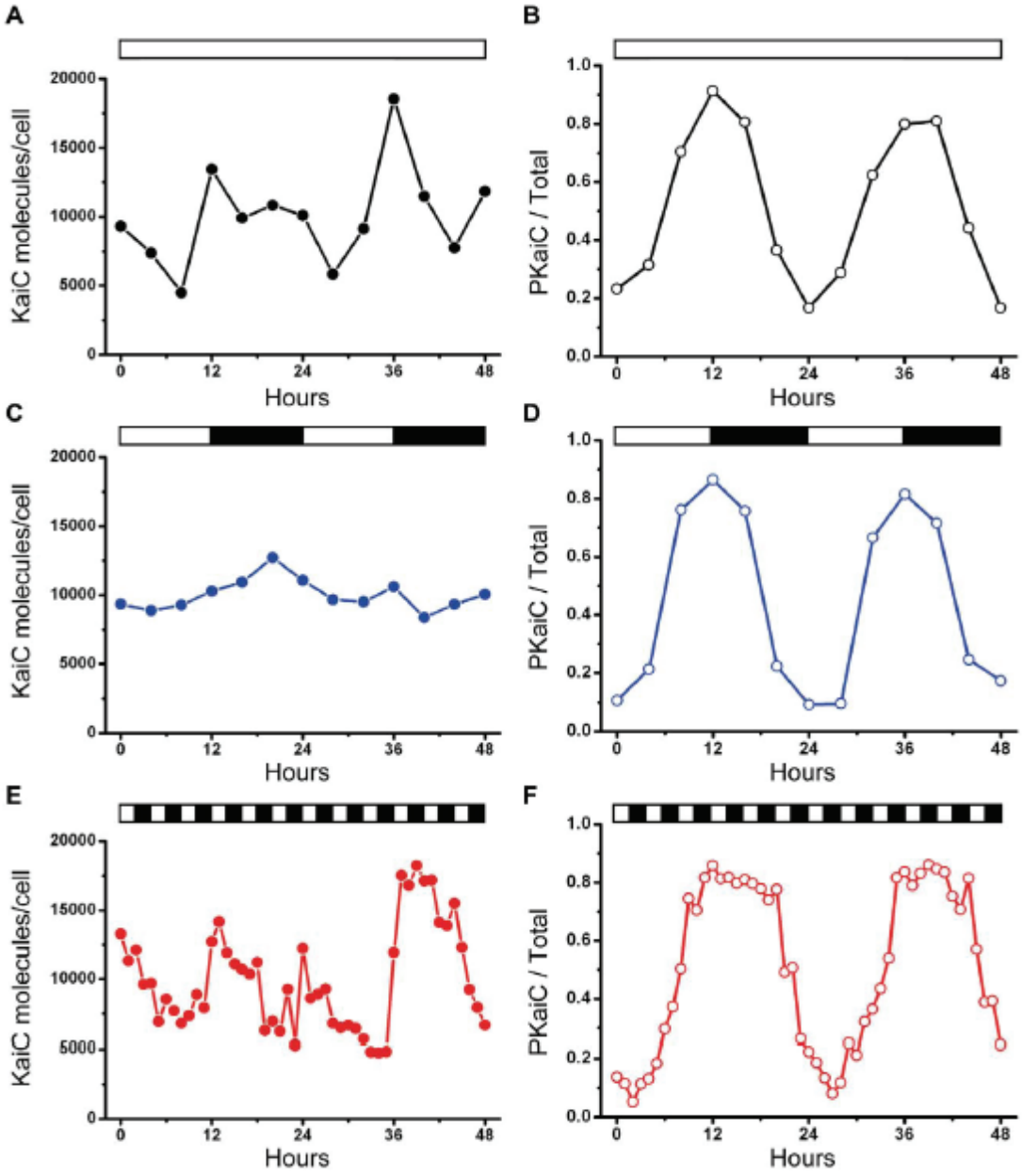

Figure 3-1. ***In vivo*** **patterns of KaiC abundance and phosphorylation under different illumination conditions.** WT cells (strain AMC149) were assayed in (**A, B**) LL (constant light; data are averages of three independent experiments), (**C, D**) LD12:12 (12 h light/12 h dark; data are averages of two independent experiments), (**E, F**) LD2:2 (2 h light/2 h dark). (**A, C, E**) KaiC abundance. Based on data of Kitayama and coworkers (Kitayama et al., 2003), the values are normalized to an average number of 10,000 KaiC molecules/cell. (**B, D, F**) KaiC phosphorylation status, expressed as a ratio of phosphorylated KaiC (P-KaiC) to total KaiC. The KaiC phosphorylation pattern is the most consistent rhythm among the three different in vivo conditions. White/black bars denote light/darkness. Raw data from representative experiments are shown in **Fig. S3-1A** (in **Appendix B**) for KaiC abundance and **Fig. S1B** (in **Appendix B**) for KaiC phosphorylation.

remains robust with a phase relationship that is similar to that in LL (**Fig. 3-1C&D**). The abundances of KaiA and KaiB are also not rhythmic in LD 12:12 (representative example shown in **Fig. S3-2** in **Appendix B**). Note that LD 12:12 is more relevant to the organism in nature than LL, and yet there is no reproducible KaiC abundance rhythm that would be expected to result from a TTFL. The result of **Fig. 3-1C** is initially inexplicable since global transcription is strongly dependent upon light in *S. elongatus* (Tomita et al., 2005), and therefore a rhythm of KaiC abundance would be expected. However, we discovered that KaiC degradation is also strongly light-dependent; in darkness, KaiC degradation is inhibited (**Fig. S3-3** in **Appendix B**). Therefore, synthesis and degradation of KaiC is counterbalanced in the light phase of LD, while KaiC is neither synthesized (Tomita et al., 2005) nor degraded (**Fig. S3-3** in **Appendix B**) in the dark phase of LD; consequently, KaiC abundance remains nearly constant in LD (**Fig. 3-1C**). On the other hand, in LL the synthesis of KaiC is rhythmic but degradation continues in the subjective night, leading to a rhythm of KaiC abundance in LL (Imai et al., 2004).

To test whether the KaiC phosphorylation rhythm was disrupted by metabolic noise, we altered the environmental conditions to LD 2:2 (2 h light followed by 2 h darkness). Because *S. elongatus* is an obligate photoautotroph that is absolutely dependent upon photosynthesis for energy, a high frequency light/dark cycle will have major effects on intracellular photosynthesis, redox status, and metabolism. The four hour cycle of LD 2:2 allowed the persistence of a circa-24 h rhythm of luminescence as a reporter of circadian gene expression (**Fig. S3-1C** in **Appendix B**). Under these

conditions, there is a noisy and possibly rhythmic pattern of KaiC abundance while there is a robust and clear rhythm of KaiC phosphorylation (**Fig. 3-1E & 3-1F**). Therefore, it is the KaiC phosphorylation rhythm (an indicator of the PTO) that is the most reproducible rhythm under a wide range of *in vivo* conditions (LL, LD 12:12, and LD 2:2), not the KaiC abundance rhythm that could be a direct consequence of a TTFL oscillator.

Constitutive hyper-phosphorylation of KaiC disrupts the normal circadian system

As described in the Introduction, Kitayama and coworkers (Kitayama et al, 2008) concluded that "transcription-translation oscillates even in the absence of the KaiC phosphorylation cycle and that this oscillation can persist regardless of the phosphorylation state and kinase activity of KaiC" (Kitayama et al, 2008). One of the main lines of evidence that they marshaled to support their conclusions was that constitutive hyper-phosphorylation of KaiC–either by over-expression of KaiA or by mutation of KaiC–allowed the *in vivo* system to operate relatively normally. In the *in vitro* system, a higher proportion of KaiA causes KaiC hyperphosphorylation and a suppression of the *in vitro* oscillation (**Fig. S3-4** in **Appendix B**), so it is reasonable to hypothesize that KaiA overexpression *in vivo* will have the same effect. However, when we express KaiA *in vivo*, we find either different results and/or interpret the data from a different perspective than the report of Kitayama et al. (Kitayama et al, 2008).

First, Kitayama and coworkers over-expressed KaiA under the control of an IPTG-inducible construct and found concentrations of IPTG that apparently suppressed

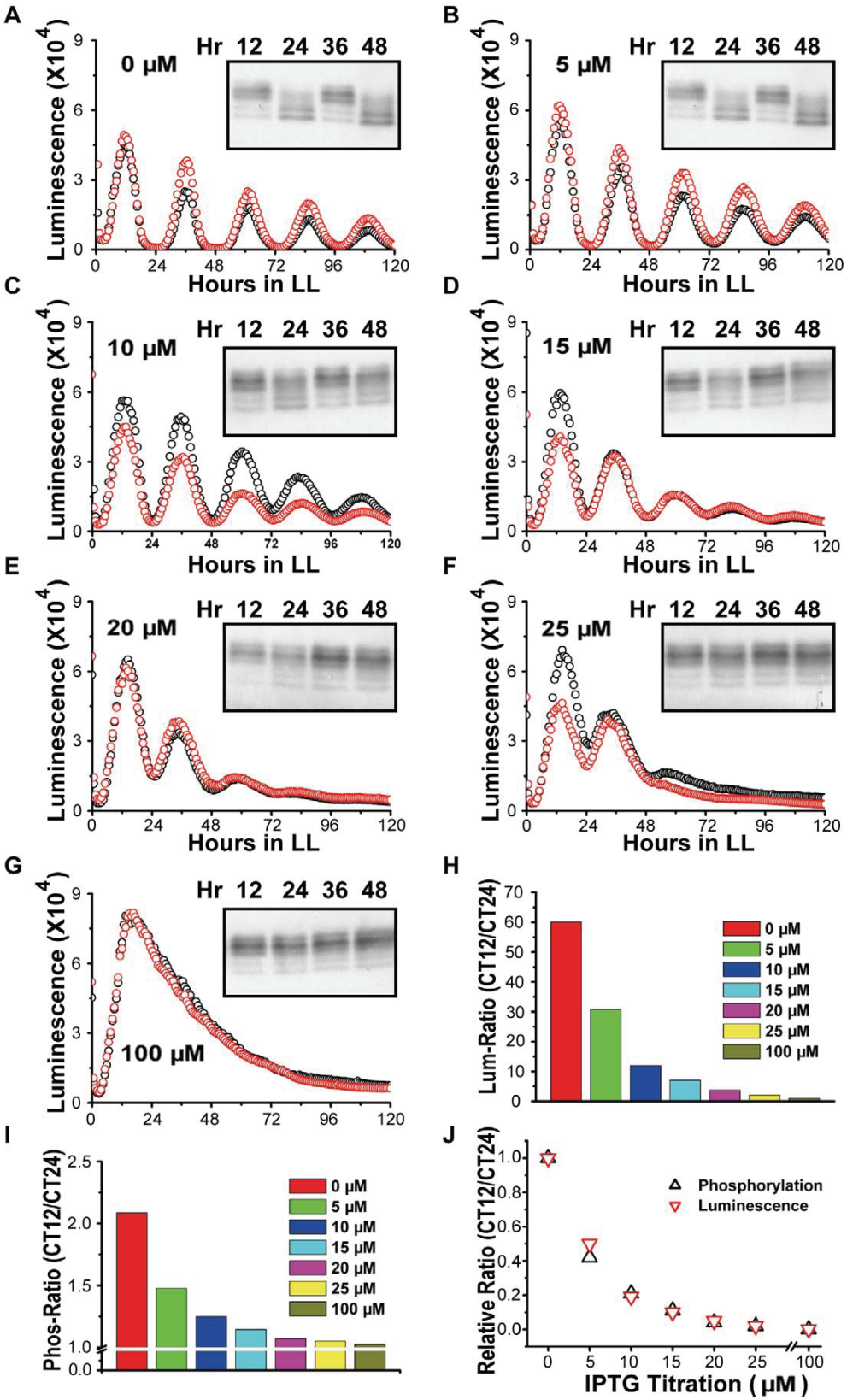

Figure 3-2. Increasing expression of KaiA suppresses the KaiC phosphorylation rhythm and the gene

expression rhythm in parallel. Gene expression was monitored by luminescence from the kaiBCp::luxAB reporter. The expression level of kaiA was under the control of an IPTGderepressible heterologous trc promoter. (**A–G**) Inducer at the concentration indicated in the upper left corner of each panel (IPTG, from 0 to 100 mM) was added 18 h before the onset of LL to express KaiA. Each panel depicts the effect of that level of KaiA expression on the luminescence rhythm (measurements for 5 d on duplicate samples—black and red circles) and the KaiC phosphorylation rhythm at peak and trough phases for the first 2 d in LL (immunoblot insets to each panel). (**H**) Amplitude of the luminescence rhythm as a function of KaiA expression level (driven by varying IPTG concentrations). The amplitude was calculated as the ratio of the first luminescence peak to the first trough using the average of the two replicates (background/trough levels were not subtracted). The data in panels A–H made use of the kaiBCp::luxAB reporter, but similar results were obtained with the psbAIp::luxAB reporter. (**I**) Amplitude of the phosphorylation rhythm as a function of KaiA expression level/IPTG. The amplitude was calculated as the ratio of the first peak to the first trough and plotted as a function of [IPTG]. Note ordinal scale break. (**J**) The ratios of the luminescence and phosphorylation rhythms at 0 mM IPTG were set to 1.0, and ratios of the same two rhythms at 100 mM IPTG were set to 0. These normalized amplitude data were then plotted as a function of IPTG concentration.

the KaiC phosphorylation rhythm but allowed the rhythm of gene expression (as monitored by a luminescence reporter) to continue (Kitayama et al, 2008). We used the same inducible construct to express KaiA and find in contrast a clear correlation between the suppression of the KaiC phosphorylation rhythm by KaiC hyperphosphorylation and the rhythm of gene expression, as depicted in **Fig. 3-2**. In response to increasing concentrations of the inducer IPTG, KaiC becomes progressively more hyper-phosphorylated (insets to panels A-G of **Fig. 3-2**), and the luminescence rhythm damps to arhythmicity. When the suppression of the phosphorylation rhythm is quantified and normalized (**Fig. 3-2I**), it correlates precisely with the suppression of the luminescence rhythm (**Fig. 3-2H**) that reflects the global rhythm of promoter activity (**Fig. 3-2J**). This precise correlation strongly supports the interpretation that repression of the PTO (as gauged by the KaiC phosphorylation rhythm) leads inevitably to the suppression of the

emergent global rhythm of gene expression (**Fig. 3-2J**). The basis of the discrepancy between our results and those of Kitayama and coworkers is not clear, but it might be explained as a population phenomenon–perhaps there are a few cells in the population with a higher resistance to the IPTG induction that continue to oscillate their KaiC phosphorylation and luminescence in the experiments of Kitayama and coworkers; this could lead to an apparent suppression of KaiC phosphorylation in the population as measured by the relatively insensitive immunoblotting technique, whereas the few rhythmic cells confer a weak, low amplitude rhythm of luminescence (which is a very sensitive gauge). Moreover, simulations with the model that we introduce below indicate that even a very low amplitude rhythm of KaiC phosphorylation in individual cells (that would be undetectable by immunoblotting) can result in a measurable oscillation of transcriptional activity (**Fig. S3-5** in **Appendix B**).

A second method by which Kitayama and coworkers achieved constitutive hyper-phosphorylation of KaiC was by mutation of the critical phospho-sites on KaiC (S431 and T432) to glutamate residues, thereby creating $KaiC^{EE}$ (i.e., S431E and T432E). $KaiC^{EE}$ is a phosphomimetic of hyper-phosphorylated KaiC that cannot have its phosphorylation status regulated further since sites 431 and 432 are now blocked by the glutamate residues (Kitayama et al, 2008). When the endogenous *kaiC* gene is replaced with a mutated gene encoding $KaiC^{EE}$, there are long-period rhythms of luminescence *in vivo* at 30°C (Kitayama et al, 2008). We can replicate the results of Kitayama and colleagues with $KaiC^{EE}$, but we interpret those results differently. Our results may be seen

most clearly in **Fig. 3-3** (and **Fig. S3-6** in **Appendix B)**, which shows that rhythms with $KaiC^{WT}$ oscillate robustly for at least 6-12 cycles in LL at 30°C with a period of ~25.4 h (there is a slight damping over time due to growth/density of cells and depletion of medium, **Fig. S3-6A** in **Appendix B**). Conversely, with $KaiC^{EE}$, not only are the periods much longer (average > 50 h) and more variable than for $KaiC^{WT}$ at 30°C, but more crucially the rhythms damp significantly over time (**Figs 3-3B**, **3-4**, and **S3-6B** in **Appendix B**). This damping is a consistent feature of the rhythms with the $KaiC^{EE}$ strain at 30°C, and it is also evident in the data of Kitayama and coworkers (Kitayama et al, 2008).

Even more interesting, temperature compensation of the $KaiC^{EE}$ strain is not stable under different metabolic conditions. In healthy cultures on agar, colonies of wild-type and $KaiC^{EE}$ strains show temperature compensated rhythms (**Fig. 3-3E, F, &I**); Q_{10} for cultures on agar was 1.08 for wild-type cells and 1.02 for $KaiC^{EE}$ cells (however, the variability of periods among $KaiC^{EE}$ strains is significantly larger than for wild-type strains, **Fig. 3-3I**). However, for healthy cultures in liquid medium ("planktonic cultures") a temperature compensation defect is obvious in the $KaiC^{EE}$ strain (**Fig. 3-3G, H, &I**). In particular, planktonic wild-type cells show practically the same period at 24°C and 30°C (**Fig. 3-3G&I**) with a $Q_{10} = 1.08$. However, planktonic $KaiC^{EE}$ cells show dramatically different periods at 24°C *versus* 30°C (**Fig. 3-3H&I**; $Q_{10} = 2.02$) that are drastically more variable at 24°C than for wild-type cells (compare **Fig. 3-3G** with **3-3H**, and S.D. error bars in **Fig. 3-3I**). Metabolic conditions for bacteria in liquid culture are different from

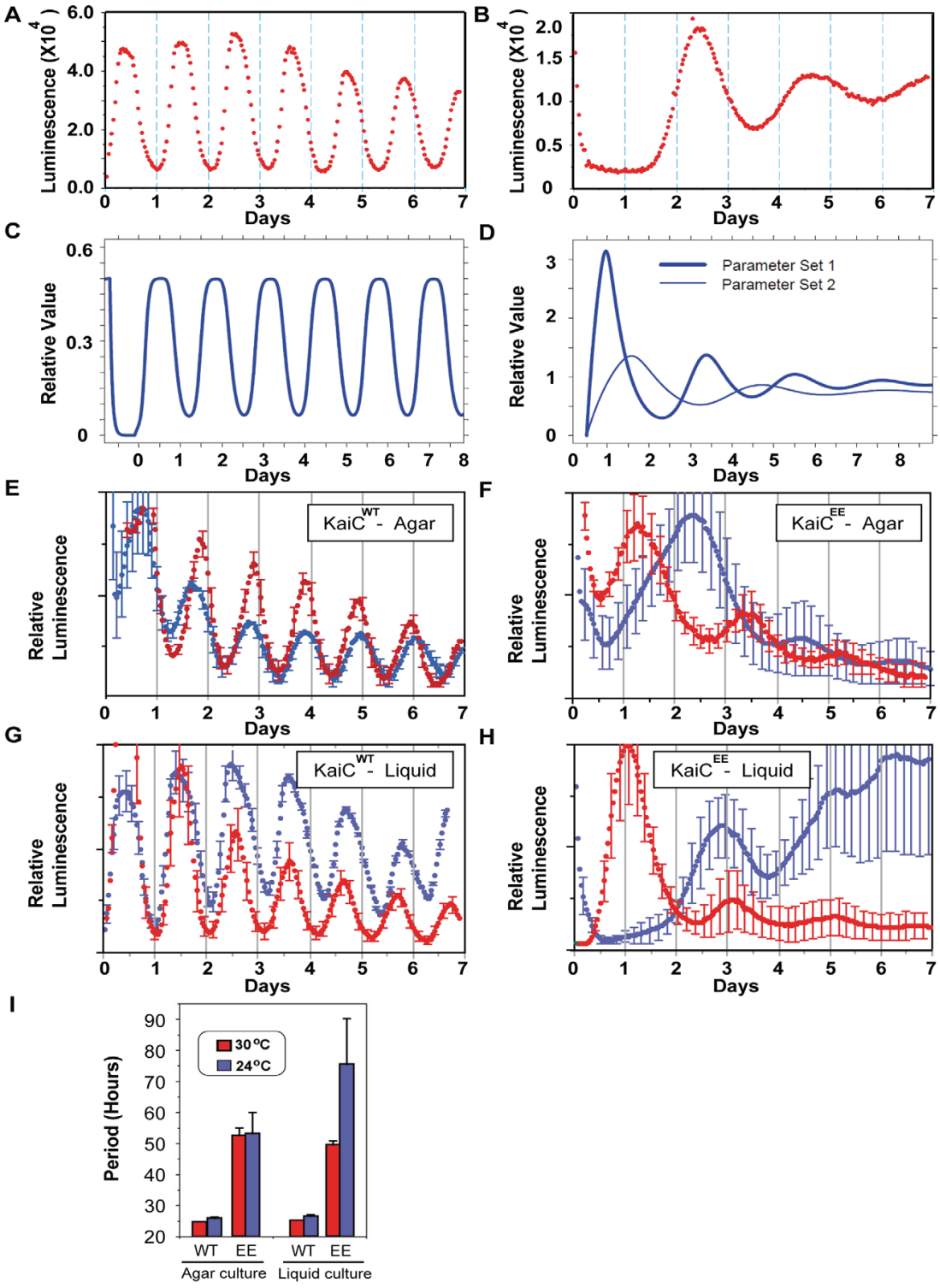

Figure 3-3. Cells expressing KaiC^{EE} exhibit damped oscillations in LL that have an abnormally long period and are not temperature compensated under different metabolic conditions. (**A**) Cells expressing KaiC^{WT} show robust circadian oscillations in LL at 30ºC with a period of ~25.4 h. (**B**) Cells expressing KaiC^{EE} (S431E/T432E) exhibit damped, long-period oscillations in LL at 30ºC (period ~58 h,

another example is shown in **Fig. S3-6** in **Appendix B**). (**C**) Simulated circadian oscillatory dynamics of KaiC mRNA abundance in the $KaiC^{WT}$-expressing strain in constant light (LL) in the combined PTO/TTFL model of the KaiABC oscillator. (**D**) Characteristic simulated oscillatory dynamics of KaiC mRNA in the $KaiC^{EE}$-expressing strain in constant light (LL) using a generic TTFL without a PTO cycle. In the simulations, KaiB·$KaiC^{EE}$ complexes suppress transcription. A constant light dependent degradation term (proportional to concentration) removes complexes; translation from mRNA creates KaiB and $KaiC^{EE}$. The output of simulations from two different parameter sets of the TTFL is shown; damped oscillations of varying period are typical for a wide range of parameters in the model. Details of the model (differential equations and parameter values) can be found in **Appendix B**. (**E–H**) Rhythms of luminescence *in vivo* at 24ºC (blue traces) versus 30ºC (red traces) under different metabolic conditions: (**E**) WT cultures on agar medium, (**F**) $KaiC^{EE}$ cultures on agar medium, (**G**) WT planktonic cultures in liquid medium, (**H**) $KaiC^{EE}$ planktonic cultures in liquid medium. (**I**) Period estimates for the data of panels E–H, where WT= $KaiC^{WT}$ and EE = $KaiC^{EE}$ strains. Error bars in panels E–I are S.D. (n values are as follows in panels E–I: 6 for WT at 24ºC, 15 for EE at 24ºC, and 5 for both WT and EE at 30ºC). Note that the number of days plotted on the abscissae is different among panels A/B, C/D, and E–H.

those on agar, and therefore temperature compensation is dependent on metabolic conditions in the $KaiC^{EE}$ strain, but not in wild-type cells. Kitayama and coworkers also showed data for a strain expressing constitutively non-phosphorylated KaiC, named K294H, but we find the rhythms of this strain to be highly unstable with respect to period, phase, and amplitude as shown in **Fig. S3-7** (in **Appendix B**) and will therefore not be considered further here.

Moreover, the number of cycles exhibited by $KaiC^{EE}$ strains before they damp out is a function of the number of environmental LD cycles experienced by the cells prior to release into LL (**Figs. 3-4,** and **S3-8** in **Appendix B**). In these experiments, we grew cells expressing either $KaiC^{WT}$ or $KaiC^{EE}$ in LL, then gave them 1-2 cycles of LD with either 12 or 24 h dark intervals, followed by a final release to LL and the monitoring of luminescence. For cultures expressing $KaiC^{WT}$, there were consistent and robust rhythms

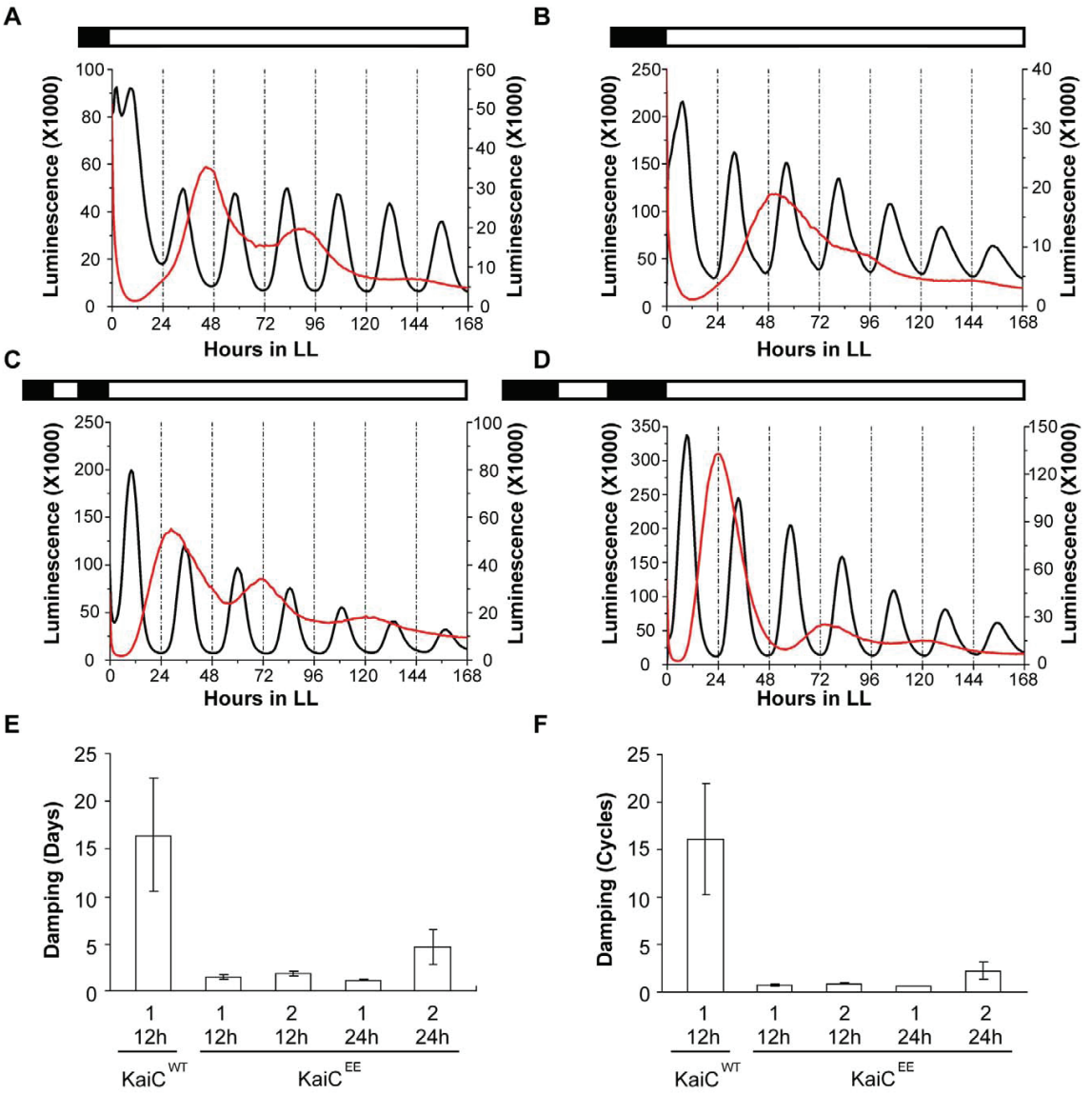

Figure 3-4. Prior entrainment conditions determine the rate of damping in cells expressing KaiC^{EE}. Cells were in LL at 30ºC before and after the following entrainment conditions: (**A**) one 12 h dark pulse, (**B**) one 24 h dark pulse, (**C**) two 12 h dark pulses separated by one 12 h light pulse (i.e., 1.5 cycles of LD12:12), and (**D**) two 24 h dark pulses separated by one 24 h light pulse (i.e., 1.5 cycles of LD24:24). In all panels, the left ordinate is the luminescence level of the WT strain and the right ordinate is the luminescence level of the KaiC^{EE} strain. In panels A–D, the black traces are the WT luminescence and the red traces are the KaiC^{EE} luminescence (these traces are the average of duplicate measurements, see **Fig. S3-8** in **Appendix B** for all raw data). (**E**) Damping analysis as the number of days required for the amplitude of the rhythm to decrease to 1/e (<36.79%) of the starting value. (**F**) Damping analysis as the number of cycles required for the amplitude of the rhythm to decrease to 1/e. In panels E and F, n = 5 for KaiC^{WT} and n=7 for each of the KaiC^{EE} sample sets; error bars are SEM.

in the final LL that damped at a slow rate (**Figs. 3-4,** and **S3-8** in **Appendix B**). On the other hand, cells expressing $KaiC^{EE}$ exhibited obvious damping that was a function of the number of prior cycles of LD–two cycles of LD promoted longer-lasting oscillations than one cycle of LD; this difference between rhythms expressed by $KaiC^{WT}$ vs. $KaiC^{EE}$ strains was most obvious with the LD 24:24 conditions (**Fig. 3-4E&F**; compare **Fig. 3-4B** vs. **3-4D,** and **Fig. S3-8F** vs. **Fig. S3-8H** in **Appendix B**). These data imply that the rhythms expressed by the $KaiC^{EE}$ strain are driven by a damped oscillator whose persistence can be cumulatively stimulated by increasing the number of cycles of driving stimuli.

Modeling damped, long-period oscillations in the $KaiC^{EE}$ strain

Building upon our previous stochastic model of the PTO (Mori et al., 2007) to simulate the larger circadian system that includes transcription and translation, we constructed a mathematical model where the core PTO oscillator is coupled to a "slave" TTFL oscillator in which the KaiB•KaiC complex nonlinearly suppresses transcription of the *kaiBC* gene (see **Appendix B** for a complete model description). This negative feedback is based on generic TTFL repression adapted from a *Drosophila* clock model (Goldbeter, 1995). To understand how a damped, long-period oscillation might persist in the $KaiC^{EE}$ strain, it is only necessary to consider the TTFL portion of the model. Briefly, starting with low quantities of KaiB•KaiC, repression of *kaiBC* transcription is low and KaiB and $KaiC^{EE}$ protein abundances increase (*kaiB* and *kaiC* genes are adjacent and

transcribed as a dicistronic mRNA, Ishiura et al., 1998). KaiB associates with $KaiC^{EE}$ and the level of KaiB•$KaiC^{EE}$ complex increases; this constitutively "hyper-phosphorylated" KaiB•$KaiC^{EE}$ complex acts non-linearly to repress further transcription of *kaiBC* mRNA. As KaiB and $KaiC^{EE}$ protein abundances reach their peak, degradation takes over the dynamics in LL such that KaiB•$KaiC^{EE}$ levels then drop, relieving the suppression of *kaiBC* and typically resulting in oscillatory dynamics. However, as the model shows, because the phosphorylation status of $KaiC^{EE}$ cannot be altered, the transcription and translation loop does not show sustained oscillations (i.e., *kaiBC* mRNA exhibits damped oscillatory dynamics in LL, **Fig. 3-3D**). On the other hand, inclusion of a PTO with the TTFL for $KaiC^{WT}$ generates robust and consistent oscillations (**Fig. 3-3C**). In addition, the period of the damped $KaiC^{EE}$ cycles are significantly longer than those of the sustained $KaiC^{WT}$ cycles (compare **Fig. 3-3C** with **3-3D**). Therefore, a generic TTFL model can accurately reproduce the damped, long-period oscillation of cells expressing $KaiC^{EE}$. We therefore conclude that the data with $KaiC^{EE}$ (**Figs. 3-3B, 3-4**, and Kitayama et al, 2008) can be faithfully interpreted in terms of a damped "slave" TTFL oscillator in which a self-sustained PTO pacemaker is embedded.

Modeling the larger PTO/TTFL system *in vivo*

We used the same TTFL repression function from the $KaiC^{EE}$ model described in the previous section to simulate the *in vivo* oscillator with $KaiC^{WT}$ consisting of a PTO and TTFL in LL, DD or LD conditions. The resulting simulations compare changes in

protein, mRNA and phosphorylation levels with experimental data. Briefly (and in simplified form), the PTO portion of the model consists of the following cycle (not including the dissociation kinetics):

$$C_0 \rightarrow A\bullet C_0 \rightarrow A\bullet C_1 ... \rightarrow A\bullet C_N \rightarrow A\bullet B\bullet C_N \rightarrow A\bullet B\bullet C_{N-1} \rightarrow ... \rightarrow A\bullet B\bullet C_0 \rightarrow A + B + C_0,$$

where "C_i" = KaiC hexamers with "i" number of phosphates, "A" = KaiA, "B" = KaiB, "$A\bullet C_0$" is the complex between KaiA and unphosphorylated KaiC, and so on. The exchange of KaiC monomers among the hexamers synchronizes the phosphorylation status within the population of KaiC molecules (Ito et al., 2007; Mori et al., 2007). In our ordinary differential equation (ODE) model, initially unphosphorylated KaiC binds KaiA and proceeds sequentially through the phosphorylation states C_1,C_2, ..C_{12}. Hyper-phosphorylated KaiC associates with KaiB, and the KaiB•KaiC complex sequesters KaiA. This sequestration nullifies the stimulatory effect of KaiA and the system dephosphorylates. Synchronization of the phosphorylation status among the KaiC hexamers in the population by KaiC monomer exchange results in sustained oscillations that do not dampen. On the other hand, in the absence of synchronization, this "cyclic" ODE system shows damped oscillations, as we had previously observed with an explicit stochastic matrix model of hexamer interactions (Mori et al., 2007). The complete ODE model that comprises the PTO and TTFL includes the association/dissociation kinetics for each state of KaiC with KaiA & KaiB, as well as KaiC auto-phosphorylation and auto-dephosphorylation kinetics. We have not included a more complicated site-dependent (S431 and T432) model of KaiC phosphorylation as experimentally

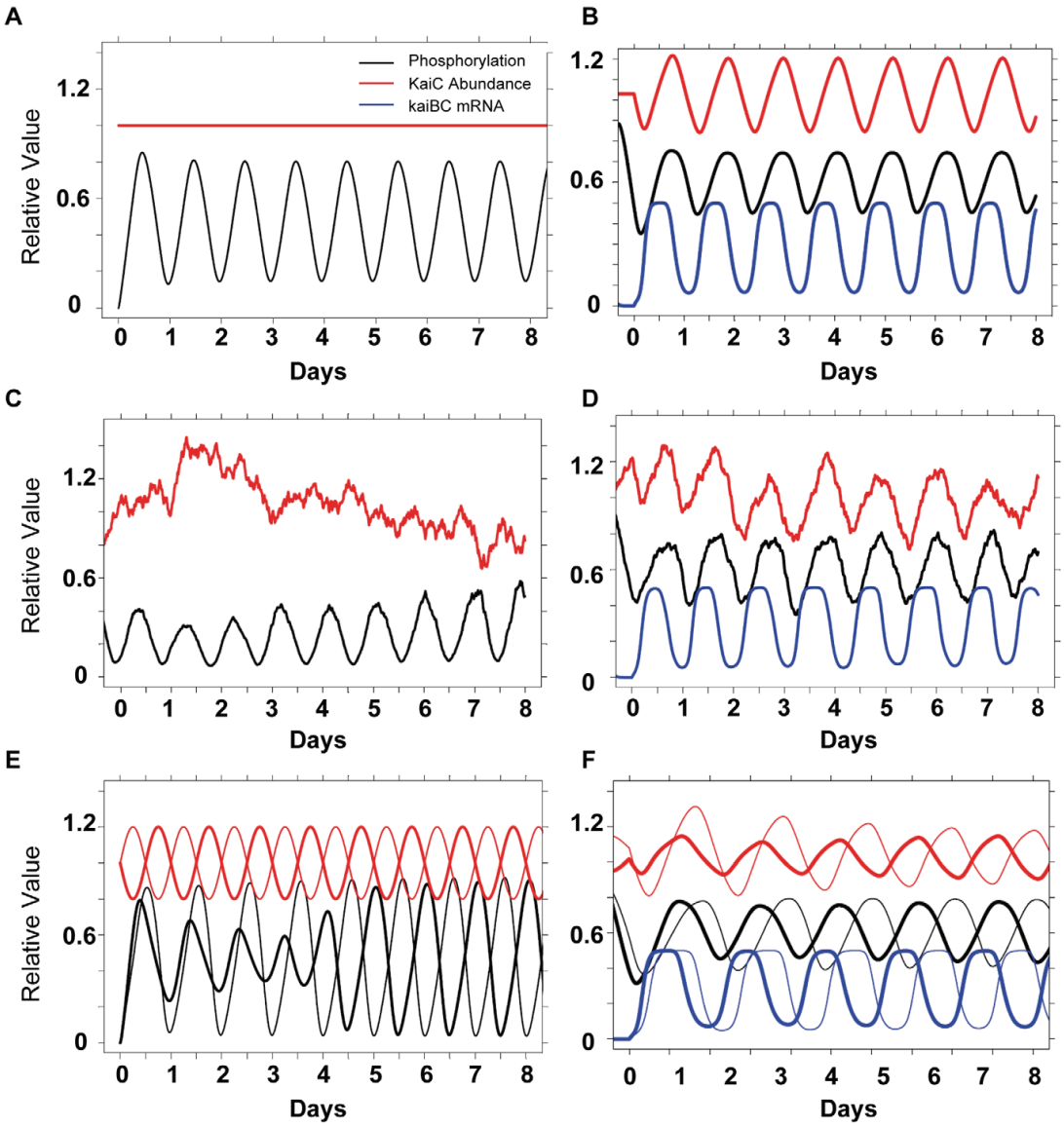

Figure 3-5. Simulations derived from the PTO/TTFL model, including resilience and phase-locking. (**A**) PTO alone: In the absence of transcription and translation (i.e., for the in vitro reaction or for cells in DD), KaiC abundance is constant (red trace) and simulation of the PTO model indicates a sustained circadian oscillation in KaiC phosphorylation (black trace). Phosphorylation is reported as a fraction of total KaiC. The initial ratios in simulations are 1:1.5:1 KaiA:KaiB:KaiC (dimer, tetramer, hexamer) with a nominal initial KaiC concentration of 1 mM (at initial conditions, KaiC is in the unphosphorylated form). (**B**) Combined PTO/TTFL: Inclusion of a simple TTFL in which hyperphosphorylated KaiB·KaiC complexes that suppress *kaiBC* transcription show sustained circadian oscillations in KaiC phosphorylation (black), KaiC abundance (red), and *kaiBC* mRNA (blue) in LL. The phase relationships are consistent with previous in vivo studies of the cyanobacterial system. Simulations are shown following two simulated LD 12:12 cycles. KaiC abundance has been scaled to a mean of 1 (max value ~3.5 $KaiC_0$). Levels of *kaiBC* mRNA are reported as a fraction of initially unphosphorylated KaiC (= $KaiC_0$). (**C**) PTO resilience as assessed by the effect of noisy unphosphorylated KaiC on the PTO. Random noise in unphosphorylated

KaiC was introduced as shown (red trace). KaiC abundance is normalized to a mean of 1.0 (initial concentration is set at 1 mM). The phosphorylation rhythm (black) remains robustly rhythmic despite significant fluctuations in KaiC abundance. (**D**) Combined PTO/TTFL resilience as assessed by the effect of noisy unphosphorylated KaiC on the PTO/TTFL system. Random noise in unphosphorylated KaiC was introduced at the same level as in Panel C. However, with the inclusion of the TTFL, the same noise fluctuations (as in panel C) result in noisy KaiC abundance oscillations (red trace; KaiC abundance is normalized to a mean of 1.0). The phosphorylation rhythm (black) remains circadian despite significant fluctuations in KaiC but is perturbed by fluctuations in abundance. The abundance of kaiBC mRNA (blue trace) is much less noisy as it reflects the effect of hyper- phosphorylated KaiBNKaiC complexes. Monomer exchange reactions in the PTO decrease the effect of noisy fluctuations in unphosphorylated KaiC fluctuations on the hyper-phosphorylated states. (**E**) Phase-locking in the PTO. External circadian sinusoidal driving of the abundance of unphosphorylated KaiC in two different phases (0 h, thick lines and 12 h, thin lines) results in the same ultimate asymptotic phase relationship between abundance (red) and phosphorylation (black). At the beginning of the simulation, the phase relationship between KaiC phosphorylation and KaiC abundance is optimal for the thin-trace case and remains so. However, for the thick-trace case, the initial conditions have a non-optimal phase between KaiC phosphorylation and KaiC abundance that resolves into the optimal relationship after about 4 d. (**F**) Phase-locking in the combined PTO/TTFL. External circadian sinusoidal driving of the abundance of unphosphorylated KaiC as in Panel E in two different phases (0 h, thick lines and 12 h, thin lines) results in the same asymptotic phase relationship between abundance (red), phosphorylation (black), and kaiBC mRNA (blue). The result is similar to that simulated in Panel E except that a final effect on mRNA levels is shown. Details of the models (differential equations and parameter values) can be found in **Appendices A&B**.

observed (Nishiwaki et al., 2007; Rust et al., 2007), resorting instead to a simpler yet effective description of net KaiC phosphorylation level within the population (this PTO model using net KaiC phosphorylation levels and complex association/dissociation kinetics implicitly includes the effects of site-dependence in a phenomenological manner).

We modeled the TTFL using a generic nonlinear repression term (as in the $KaiC^{EE}$ case described in the previous section) and a light-dependent protein degradation term (based on the data of **Fig. S3-3** in **Appendix B**). For the $KaiC^{WT}$ strain, the PTO shows robust sustained circadian oscillations in net phosphorylation level (**Fig. 3-5A**) for a

variety of parameter choices. Inclusion of a TTFL without any specific parameter "tuning" results in a circadian oscillation in KaiB/KaiC protein abundances, *kaiBC* mRNA levels, and KaiC phosphorylation status in LL (**Fig. 3-5B**). In DD when transcription/translation and protein degradation is turned off (**Fig. S3-3** in **Appendix B**, and Tomita et al., 2005), there is a circadian KaiC phosphorylation rhythm due solely to the PTO (**Fig. 3-5A**). Therefore, this model that combines a core PTO plus a damped "slave" TTFL oscillator can accurately reproduce the sustained circa-24 h rhythms of protein/mRNA abundances and KaiC phosphorylation in the $KaiC^{WT}$ strain, while the TTFL portion alone can create damped, long-period oscillations of *kaiBC* mRNA as observed in cells expressing $KaiC^{EE}$ (**Figs. 3-3C, 3-3D, 3-5A&B**).

Resilience of the PTO/TTFL model to noise

As further evidence that the PTO can function as the core circadian pacemaker in the larger system, we included noisy fluctuations in the concentration of unphosphorylated KaiC in the PTO/TTFL model. For the PTO alone, both (i) the stochastic matrix model for small molecular numbers (not shown) and (ii) the ODE model allow robust circadian oscillations in the presence of noisy fluctuations of unphosphorylated KaiC levels (**Fig. 3-5C**). When the TTFL is included, the simulated system continues to show robust circadian oscillations in the phosphorylation rhythm and circadian dynamics for the protein abundance even though the same external noise fluctuations were introduced as in the PTO simulation (**Fig. 3-5D**). These modeling data

are supported by experimental data in the LD 2:2 cycle–the 4 h light/dark cycle drives a four hour modulation of photosynthesis and metabolism, leading to a noisy KaiC abundance pattern (**Fig. 3-1E**); nevertheless, KaiC phospho-status exhibits a clean circadian rhythm (**Fig. 3-1F**) as does the luminescence indicator of transcriptional activity (**Fig. S3-1C** in **Appendix B**).

These simulations of noisy KaiC abundance examine typical fluctuations that may occur in cellular components due to intrinsic noise in transcriptional & translational processes, cell division, and external random perturbations on the clock components. We also simulated the effect of non-random perturbations of abundance on the system both for the PTO alone and including the TTFL. For example, experimental manipulation of KaiC abundance as pulsative increases in KaiC levels have been reported to reset the phase of the circadian system *in vivo* (Ishiura et al., 1998; Xu et al., 2000). To examine the effects of non-random KaiC perturbations, we first introduced a sinusoidally driven rhythm of KaiC protein abundance to determine how the PTO would respond. The PTO's phosphorylation rhythm was begun in different initial phases relative to the driving KaiC sinusoidal abundance (**Fig. 3-5E**). After a few "sorting out" cycles, the PTO system shows "phase locking" to the abundance rhythm in a specific phase relationship. The intuitive reason for this effect is that the KaiC phosphorylation rhythm is optimal only when synthesis of unphosphorylated KaiC occurs in phases near the trough of the phosphorylation rhythm (see below). When the TTFL is included, the effect of driving the KaiC abundance externally results in an analogous phase-locking effect (**Figs. 3-5F,**

3-6A).

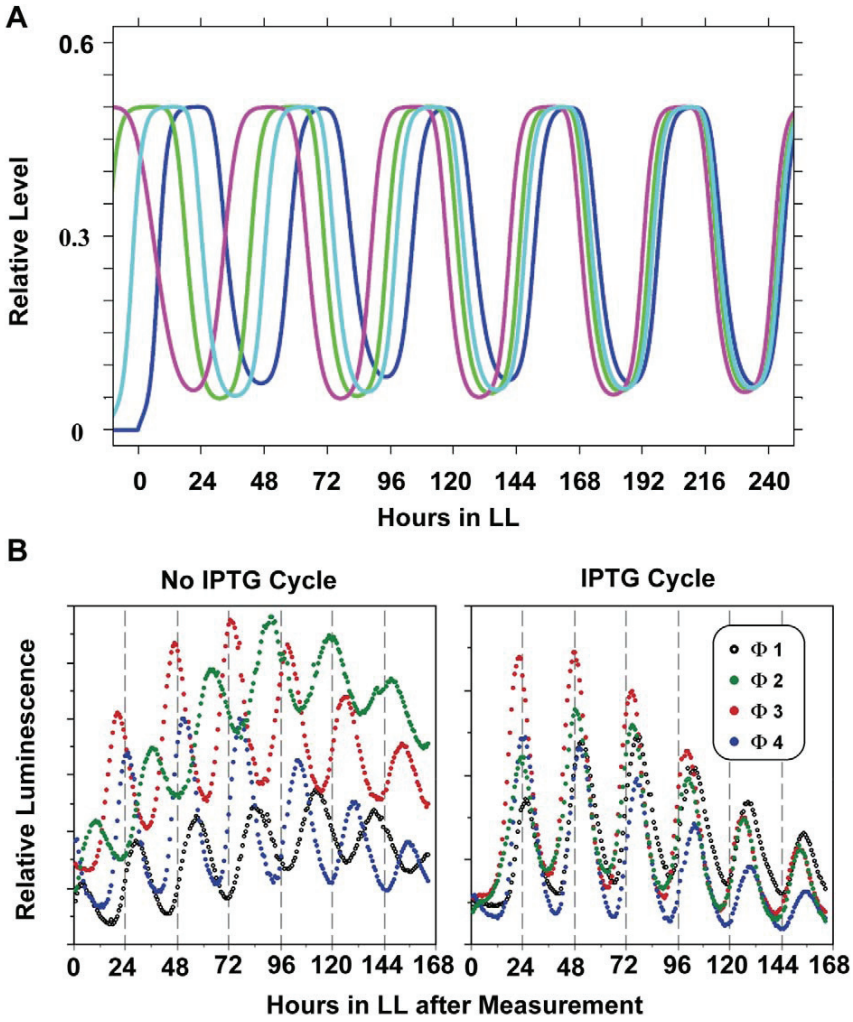

Figure 3-6. Experimental test of phase locking and entrainment. (**A**) Model predictions: simulated phase-locking of *kaiBC* mRNA rhythms in the combined PTO/TTFL model for four different starting initial phases of mRNA abundance rhythms. Sinusoidal external driving (of unphosphorylated KaiC protein) is implemented as in **Figs. 5E&F**. The four phases preferentially lock into a single phase set by the external driving rhythm. The blue trace illustrates the case of initial conditions that are already in the optimal phase relationship to the driving rhythm. (**B**) Experimental confirmation: cycles of induction of new KaiC synthesis cause phase-locking. Entrainment to four different LD12:12 cycles in which the phase was set to times 0, 6, 12, 18 (i.e., at 6 h intervals) prior to LL release generates four separate populations of cells that are roughly different in phase by 6 h. Cells in four separately phased populations were then treated with two cycles of 0: 0 mM IPTG (i.e. no IPTG cycle, left panel) or 0: 5 mM IPTG (i.e. IPTG cycle: 12 h IPTG, 12 h no IPTG, 12 h IPTG, right panel), and released to free-run in LL. See **Fig. S3-9A** (in **Appendix B**) for an illustration of the experimental protocol.

Experimental tests of model's prediction for phase locking

One experimental test of the model's prediction can be provided by *kaiBC* transcription & translation under the control of an oppositely phased promoter–the *purF* promoter (Ditty et al., 2005). The cyanobacterial clock system under directed anti-phase expression of the *kai* genes was reported to have phase relationships that are practically the same as wild-type (Ditty et al., 2005), and we have confirmed those results. Those results support the model's prediction of "locking in" to the preferred phase relationship between the KaiC phosphorylation rhythm and synthesis of unphosphorylated KaiC.

Another experimental test of the model's prediction is to experimentally create a cycle of new KaiC synthesis (of necessarily unphosphorylated KaiC) *in vivo* that begins in different initial phase relationships to the rhythm of KaiC phosphorylation. As shown in **Fig. 3-6A** (and **Fig. 3-5F**), these varying phase relationships should resolve after a few cycles into a single steady-state phase relationship between new KaiC synthesis and the KaiC phosphorylation rhythm. Using a strain with additional KaiC expression driven by an IPTG-inducible promoter (*trc*p) at an ectopic site in the chromosome, we experimentally created a 24 h cycle (12:12) of new KaiC synthesis within a physiological [KaiC] range by administering two cycles of 5 μM IPTG (12 h IPTG, 12 h no-IPTG, 12 h IPTG, then a free-run without IPTG; **Fig. S3-9A** in **Appendix B**). This concentration of IPTG will increase KaiC levels by 40-50% over basal values and it concomitantly decreases the phosphorylation status of KaiC (**Fig. S3-9B-D** in **Appendix B**). Four cultures that had been phased into four distinct phases (0, 6, 12, and 18 h apart) were

treated with this IPTG:no-IPTG cycle. As shown in Fig. 6B, we obtained the clear result that two cycles of new KaiC synthesis caused a locking of the four cultures to a single synchronous phase. Of particular significance is that the phase relationship of these synchronized luminescence rhythms to the cycle of new KaiC synthesis was as predicted by the model. Therefore, the core biochemical PTO is not totally insensitive to changes in levels of unphosphorylated KaiC, but it can be entrained by cycles of KaiC that result from the damped TTFL.

Discussion

A PTO pacemaker embedded within a TTFL slave oscillator

This investigation is the first to our knowledge to investigate the dynamics of a circadian clock in which a PTO is coupled to a TTFL. Our data strongly support the interpretation that when the cyanobacterial PTO is suppressed, the emergent circadian rhythms, including the TTFL and global gene expression, are concomitantly suppressed. Moreover, when the PTO is suppressed–either by KaiA-overexpression or by mutation of KaiC–the remaining TTFL shows clear characteristics of a damped oscillator that is effectively a "slave" of the self-sustained PTO. As shown in **Fig. 3-7**, our model proposes that the PTO is embedded within a TTFL with the KaiB•KaiC complex repressing transcriptional activity through control of chromosomal topology (Woelfle et al., 2007) and/or transcriptional factors such as RpaA (Takai et al., 2006). This pervasive

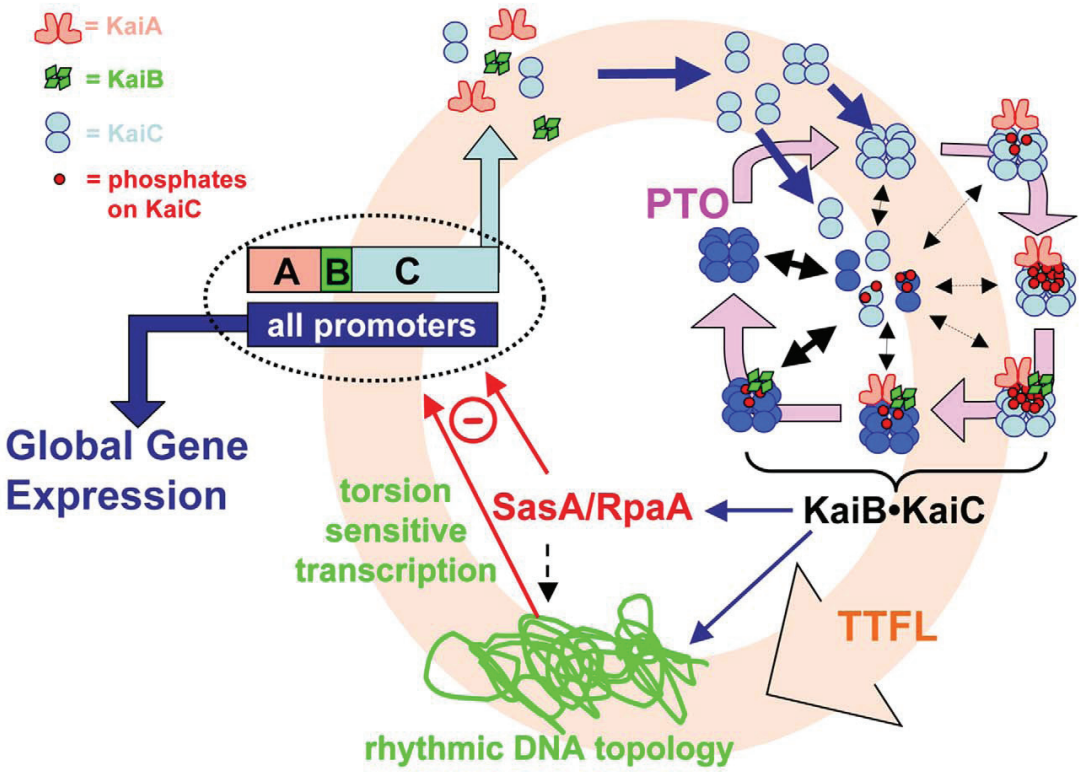

Figure 3-7. The core PTO is embedded in a larger TTFL. The PTO is linked to the damped TTFL (indicated by the pink background circle) by transcription and translation of the kaiABC cluster. Global gene expression is mediated by rhythmic modulation of the activity of all promoters, including those driving the expression of the central clock gene cluster, *kaiABC* (= ABC in figure). Rhythmic DNA torsion and/or transcriptional factor activity (e.g., RpaA/SasA) modulate global promoter activities. Cyclic changes in the phosphorylation status of KaiC that mediate the formation of the Kai·KaiC complex regulate DNA topology/transcriptional factors. The PTO (cycle connected by lavender arrows in upper right quadrant) is determined by KaiC phosphorylation as regulated by interactions with KaiA and KaiB. Robustness is maintained by synchronization of KaiC hexameric status via monomer exchange. Monomer exchange is depicted in the figure by "dumbbell" KaiC monomers exchanging with KaiC hexamers in the middle of the PTO cycle; phase-dependent rate of monomer exchange is indicated by the thickness of the double-headed black arrows. The shade of KaiC hexamers (dark versus light blue) denotes conformational changes that roughly equate to kinase versus phosphatase forms. New synthesis of KaiC feeds into the KaiABC oscillator as non-phosphorylated hexamers or as monomers that exchange into pre-existing hexamers. If the new synthesis of KaiC occurs at a phase when hexamers are predominantly hypo-phosphorylated, the oscillation of KaiC phosphorylation is reinforced (enhanced amplitude). If on the other hand, new synthesis of unphosphorylated KaiC happens at a phase when hexamers are predominantly hyper-phosphorylated, this leads to an overall decrease in the KaiC phosphorylation status, thereby altering the phase of the KaiABC oscillator (phase shift) and/or reducing its amplitude.

transcriptional activity regulates global gene expression but also rhythmically regulates new synthesis of KaiA, KaiB, and KaiC, thus completing a transcription & translation loop (**Fig. 3-7**).

Despite the fact that the PTO can oscillate independently of the TTFL *in vitro* and *in vivo* (Tomita et al., 2005; Nakajima et al., 2005), the PTO is not totally independent from the TTFL *in vivo*. The data and simulations depicted in **Fig. 3-5C&D** imply that stochastic changes in KaiC abundance will not eliminate the circadian dynamics for physiological perturbations. However, experimental manipulations of KaiC abundance as pulsative increases in KaiC levels have been reported to reset the phase of the circadian system *in vivo* (Ishiura et al., 1998; Xu et al., 2000). How can these disparate conclusions be reconciled? A likely answer is that because the newly synthesized KaiC monomers/hexamers are necessarily unphosphorylated, the phase at which they are added into the PTO is critical. If they are added at a phase when most of the KaiC hexamers are phosphorylated, then the newly synthesized proteins will monomer-exchange into the existing population of KaiC hexamers (Ito et al., 2007; Kageyama et al., 2006; Mori et al., 2007) and alter the phospho-status of the KaiC population, potentially disrupting the PTO. On the other hand, if the newly synthesized and unphosphorylated KaiC proteins are added at a phase when the KaiC population is largely unphosphorylated, then the PTO will not be disrupted and will even be potentially reinforced. Therefore, regular cycles of new KaiC synthesis can entrain. On the other hand, if the KaiC abundance fluctuates randomly, the system is resilient and its circadian nature dominates. This interpretation is

supported by both the experimental data and by the modeling simulations. When KaiC abundance is constant, its phosphorylation status oscillates with a circadian period (experimental data in Tomita et al., 2005; simulations: **Fig. 3-5A**). When KaiC abundance is allowed (or forced) to oscillate, then the PTO locks into a preferred phase relationship to the KaiC synthesis rhythm (resulting from the TTFL) such that newly synthesized KaiC is introduced at phases of the PTO when KaiC is relatively hypo-phosphorylated (experimental data: **Fig. 3-6B**; simulations: **Figs. 3-5E&F**, and **3-6A**). When the synthesis of KaiC is driven at an unusual phase by an antiphase promoter, the PTO and TTFL nevertheless lock-in at the preferred phase relationship (experimental data in Ditty et al., 2005 and our unpublished results; simulations: **Fig. 3-5F**).

What about entrainment to the environmental cycles? Because transcription and translation proceed in the daytime but are turned off in darkness in photoautrophic *S. elongatus* cells (Tomita et al., 2005), there is a daily rhythm of synthesis of the Kai proteins in LD (for the case in LL, see: Imai et al., 2004). Therefore, it is reasonable to suppose that daily rhythms of total Kai protein abundance could be an entraining stimulus. However, we did not find a reproducible rhythm of total KaiC abundance in LD 12:12 (**Fig. 3-1C**). At the same time, we found that degradation of KaiC is minimal in darkness (**Fig. S3-3** in **Appendix B**), leading to the interpretation that KaiC synthesis and degradation proceed during the illuminated day phase but essentially counterbalance each other so that there is not a major change in the net KaiC abundance during the day. Then at night, KaiC's degradation is minimal (**Fig. S3-3** in **Appendix B**) and its transcription

& translation is turned off (Tomita et al., 2005), resulting in a practically constant level of KaiC abundance over the LD 12:12 cycle (**Fig. 3-1C**). Therefore, it seems unlikely that changes in Kai protein abundance *per se* in an LD cycle could provide an entrainment mechanism. However, even though total KaiC abundance does not oscillate in LD 12:12, new synthesis of KaiC does oscillate in LD (on in the day, off at night). Because new synthesis of KaiC provides unphosphorylated protein and could thereby affect the ratio of hyper- to hypo-phosphorylated KaiC (**Fig. S3-9D** in **Appendix B**), this stimulus could contribute to the transduction pathway for entrainment. As shown in **Figs. 3-5E&F**, and **3-6A**, simulations predict such a phasing effect, and our experimental test of this prediction by providing a low amplitude rhythm of new KaiC synthesis supports this hypothesis (**Fig. 3-6B**). In this sense, the TTFL could play a role in both input and output pathways of the PTO pacemaker, as has been suggested for the mammalian clock (Merrow & Roenneberg, 2007).

Implications of a PTO embedded within a larger TTFL: Robustness

A system composed of a mass-action biochemical pacemaker embedded within a damped transcription/translation loop has important implications. Biochemical reactions that involve small numbers of molecules are intrinsically noisy, being dominated by large concentration fluctuations (Gillespie, 1977; McAdams & Arkin, 1999). In general, the number of transcription factor molecules in a prokaryotic cell is small and this could lead to a high intrinsic noise (Ozbudak et al., 2002). On the other hand, a PTO that is rooted in

the phosphorylation status of thousands of molecules would be expected to be robust in the face of noise. In the case of KaiC, the current estimate is that there are approximately 10,000 KaiC monomers per cell (Kitayama et al., 2003). The model of the PTO supports the hypothesis that the KaiABC PTO is resilient to noise. **Fig. 3-5C** shows a simulation of noise in the PTO model by introducing fluctuations in the abundance of KaiC in a population of hexamers, and **Fig. 3-5D** shows the same influence to the combined PTO/TTFL model. Despite the noisy KaiC abundance fluctuations, the circadian rhythm of KaiC phospho-status oscillates consistently, whether the PTO is considered separately (**Fig. 3-5C**) or within the larger TTFL system (**Fig. 3-5D**). These modeling data are supported by experimental data in the LD 2:2 cycle–the 4 h LD cycle drives an ultradian modulation of metabolism, leading to a noisy KaiC abundance pattern (**Fig. 3-1E**); nevertheless, KaiC phospho-status exhibits a clean circadian rhythm (**Fig. 3-1F**).

Not only is the circadian system resilient within the cell, but it is robust among a population of cells. The experimental observation of reproducible rhythms among non-communicating cyanobacterial cells in populations (Mihalcescu et al., 2004) imply that the ODE model is applicable to modeling the mean population behavior of cells, with the noise reflecting population variance in LD (**Fig. 3-5D**). Resilience of the daily timekeeper is particularly important for cells that must keep accurate track of time in the face of cell division, when a TTFL might become perturbed because the ratio of DNA to transcriptional factors can change during replication and when DNA can become less accessible during chromosomal condensation in preparation for division. In bacterial

oscillators that were synthetically designed to be strict TTFLs, cell division clearly disrupts the phasing and/or period of these synthetic clocks (Elowitz & Leibler, 2000). Cell division or chromosomal events should not, however, perturb a strictly biochemical oscillator, as observed in *S. elongatus* (Mihalcescu et al., 2004; Mori et al., 1996). Therefore, evolution appears to have selected in cyanobacteria a core biochemical pacemaker that regulates a TTFL that in turn regulates global DNA topology and gene expression.

Implications of a PTO embedded within a larger TTFL for eukaryotic circadian clocks

Early evidence for a TTFL as the core pacemaker in the cyanobacterial system came from numerous studies that showed the same phenomena which has been used to support a TTFL model in eukaryotes, namely: (1) "clock genes" deemed to be essential based on knockout studies (Ishiura et al., 1998); (2) rhythmic abundances of mRNAs and proteins encoded by clock genes (Ishiura et al., 1998; Xu et al., 2000; Tomita et al., 2005); (3) autoregulatory negative feedback of clock proteins on their gene's transcription (Ishiura et al., 1998; Xu et al., 2003); and (4) phase setting by pulsatile expression of clock genes (Ishiura et al., 1998; Xu et al., 2000). Eukaryotic circadian genes have no detectable homology to *kaiABC* sequences, so if there is an evolutionary relationship between the bacterial and eukaryotic systems, it is so diverged as to be undetectable by genetic sequence comparisons. But, how about the possibility of convergent evolution to a fundamentally similar biochemical mechanism? Could self-sustained biochemical core

oscillators underlie eukaryotic clocks? It might seem implausible that independent origins for clocks would converge upon an essentially similar core post-translational oscillator made more robust by an overlying TTFL. However, the advantages that accrue to the cyanobacterial system by having a post-translational mechanism at its core are also relevant to eukaryotic clocks (Johnson et al., 2008). For example, individual mammalian fibroblasts express cell-autonomous, self-sustained circadian oscillations of gene expression that are largely unperturbed by cell division (Nagoshi et al., 2004; Welsh et al., 2004) in a fashion reminiscent of cyanobacteria (Mihalcescu et al., 2004; Mori et al., 1996). In contrast, synthetic TTFL oscillators constructed in mammalian cells (CHO cells) only display reproducible oscillations when the cells are arrested in G1 phase of the cell cycle by cultivating the cells at 30° C (Tigges et al., 2009; Tigges et al., 2010).

Could the imperturbability of circadian clocks even when buffeted by the gusts of metabolic changes provoked by cell division provide an evolutionary driving force for clock mechanisms in disparate organisms to converge on a relatively similar core mechanism? Perhaps. Recent results from the mammalian circadian clock do not easily fit into the original TTFL formulation. For example, mammalian clocks are surprisingly resilient to large changes in transcriptional rate (Dibner et al., 2009), but tight regulation of transcriptional rate would be expected to be necessary if it is a state parameter in a TTFL clock. Also, the mammalian clock is resilient to clamping the level of some of the mammalian clock proteins whose cycling had been thought to be essential (Merrow & Roenneberg, 2007; Fan et al., 2007). Moreover, recent results have led to a greater

appreciation of the role of small signaling molecules in the mammalian clock (Hastings et al., 2008). Finally, classical experiments in eukaryotic algae have shown that persisting circadian rhythms are possible in enucleated cells (in *Acetabularia*, Sweeney & Haxo, 1961; Woolum 1991) or under translational control in the absence of transcription (in *Gonyaulax,* Hastings 2001). Are *Acetabularia* and *Gonyaulax* anomalous cases, or are they relevant indicators of the underlying capabilities of the eukaryotic clockwork? Our growing appreciation of the cyanobacterial system combined with results from eukaryotic clocks that are inconsistent with a TTFL pacemaker embolden such speculations (Merrow & Roenneberg, 2007; Hastings et al., 2008; Lakin-Thomas 2006). At the least, the studies on prokaryotic cyanobacteria lead to more rigorous criteria for distinguishing whether a TTFL is at the core of eukaryotic clocks.

CHAPTER IV

MONOMER EXCHANGE AMONG KaiC HEXAMERS INITIATE THE ASSOCIATION WITH KaiB

Introduction

Previous chapters have discussed the dynamic interactions among the three Kai proteins in the *in vitro* KaiABC oscillator system and the proposed hierarchical relationship between the TTFL and the PTO in the cyanobacteria. In this chapter, I will show more data about the biochemical properties of the KaiC protein that are important for the generation of robust circadian oscillations. I have used FRET (fluorescence resonance energy transfer) to reveal the monomer exchange among KaiC hexamers and we proposed that this monomer exchange allows individual KaiC hexamers to remain synchronized in populations of KaiC hexamers (Mori et al., 2007). Monomer exchange is dependent on the phosphorylation status of KaiC hexamers, i.e. only hyper-phosphorylated KaiC is capable of exchanging monomers (Ito et al., 2007). In my studies of the *in vitro* system, I found a hyper-phosphorylated (almost 100%) KaiC mutant, $KaiC^{489}$, that shows a faster migration than $KaiC^{WT}$ in native polyacrylamide gels, which raised the idea of using native-PAGE to study monomer exchange between a test KaiC population and a $KaiC^{489}$ population. However, so far the resolution has not been good enough to use this method reliably, and I will discuss this issue in the **Discussion**.

Monomer exchange occurs during the dephosphorylation phase of the *in vitro*

KaiABC system (Kageyama et al., 2006; Mori et al., 2006; Ito et al., 2007). In **Chapter II**, I discussed the binding between KaiB and hyper-phosphorylated KaiC during the dephosphorylation phase (**Fig. 2-4**). This coincidence stimulates an interesting question. Are monomer exchange and KaiB-KaiC interaction mechanistically interrelated? Clearly, monomer exchange is KaiC's own characteristic, independent from the other components (e.g., it occurs in the absence of KaiA or KaiB). Therefore, we can ask the interesting question, "Is monomer exchange a prerequisite for KaiC to associate with KaiB?" Dr. Yao Xu in our lab recently had some interesting results from a series of *in vivo* co-expression assays. Briefly, Dr. Xu co-expressed some of the *kaiC* mutant genes in a WT background strain so that $KaiC^{WT}$ was co-expressed with mutant KaiCs, and found some of the co-expression combinations lengthened the period of the clock *in vivo*, and some disrupted the period. Among his results, a very interesting pair was *kaiC*-aST and *kaiC*-nST (the last three letters represent the residue at the putative phosphorylation sites, T426, S431, and T432, reported in Xu et al., 2004). When the main phosphorylation sites S431 and T432 are wild type (Xu et al., 2004; Nishiwaki et al., 2004), mutations at T426 to alanine (aST) or asparagine (nST) have different effects on the circadian rhythms. In particular, when $KaiC^{aST}$ is coexpressed with $KaiC^{WT}$ in vivo, the rhythm is abolished, whereas when $KaiC^{nST}$ is coexpressed, the rhythm continues, but with a longer period (Xu et al., 2009). The proteins $KaiC^{aST}$ and $KaiC^{nST}$ were tested *in vitro* for their ability to exchange monomers and associate with the KaiB protein. The results of testing on monomer exchange and KaiB-KaiC associations indicate strong correlations. Other KaiC

mutants that Dr. Xu has tested in his co-expression experiments were purified and prepared for testing *in vitro* for their ability of accomplishing monomer exchange (data not shown here).

Although I have discussed in detail about the interactions among the Kai proteins both in **Chapter I** and **Chapter II**, the exact molecular mechanism is still unknown. For example: 1. Do individual KaiC subunits behave the same within a hexamer? 2. Where is the interface between KaiB and KaiC in the KaiB·KaiC complex? 3. What binding site does the KaiB·KaiC complex create for the stable sequestration of KaiA? 4. What triggers the dissociation of the KaiB·KaiC complexes? 5. And other questions! High resolution structures of the complexes by crystallography would be helpful, but they are not available at this time. The currently available crystal structures of each Kai protein and the convenient native-PAGE assay of testing the interactions give the opportunity for mapping the interaction interface between KaiB and KaiC from mutagenesis studies. A PCR-based random mutagenesis library for the *kaiB* locus has been reported, but the library has not been released yet (Hitomi et al., 2005). Our current information about mutations in *kaiB* that affect the circadian clock can be extracted from several published studies and unpublished data (**Table 4-1** lists the known KaiB mutants of *S. elongatus*).

KaiB is rich in charged residues on its surface, and forms a tetramer plate (**Fig. 1-6B**). The structural studies of the KaiB protein have identified a remarkable feature of the surface potential: two parallel ridges of highly concentrated negative charge surrounding a positively charged cleft on one surface of the tetramer plate but not on the

other (Iwase et al., 2005, modified here as **Fig. 4-1**). On the same side as the cleft, there is another positive area at the boundary between two subunits (Iwase et al., 2005). I purified some of the KaiB mutant proteins (see **Table 4-1**, and **Fig. 4-1**) and tested the hypothesis that the mutants disrupt the clock by interfering with the association of KaiB with KaiC. However, the result that I ultimately found was that these mutants fail to recruit KaiA into the KaiA·KaiB·KaiC complex.

Table 4-1. The phenotypes of selected *S. elongatus* KaiB mutants *in vivo*

Residue	Electrostatics	Mutation	Phenotype *in vivo*	Reference
K5 *	Positively charged	K5A	period slightly shortened	Iwase et al., 2005
K10 *	Positively charged	K10A	rhythm disrupted	Iwase et al., 2005
L11	Neutral	L11F	period shortened about 4 hr	Ishiura et al., 1998
R22	Positively charged	R22C	period lengthened ~ 1.5 hr	Chapter II
K25	Positively charged	K25C	period slightly shortened	unpublished data
K42 *	Positively charged	K42A	rhythm disrupted	Iwase et al., 2005
K57 *	Positively charged	K57A	rhythm disrupted	Iwase et al., 2005
K66 *	Positively charged	K66A	rhythm disrupted	Iwase et al., 2005
R74	Positively charged	R74C	period shortened ~ 3.3 hr	Chapter II
		R74W	period shortened ~ 3 hr	Ishiura et al., 1998
D90	Negatively charged	D90G	severely impaired rhythm (19 h), damped to arythmicity in 3 days	Hitomi et al., 2005
E95	Negatively charged	E95Q	period shortened ~ 3 hr	Iwase et al., 2005
D98	Negatively charged	D98N	period shortened ~ 3 hr	Iwase et al., 2005
D100	Negatively charged	D100N	barely affected	Iwase et al., 2005
D101	Negatively charged	D101N	barely affected	Iwase et al., 2005
GELQDSDDF 94-102 C-terminal	Highly negatively charged	1-100	period slightly lengthened	Iwase et al., 2005
		1-99	period slightly lengthened	Iwase et al., 2005
		1-98	period slightly lengthened	Iwase et al., 2005
		1-97	period slightly lengthened	Iwase et al., 2005
		1-96	period lengthened ~ 5 hr	Iwase et al., 2005
		1-95	period slightly lengthened	Iwase et al., 2005
		1-94	rhythm disrupted	Iwase et al., 2005

* These KaiB protein mutants were purified and tested for binding with KaiC in this chapter

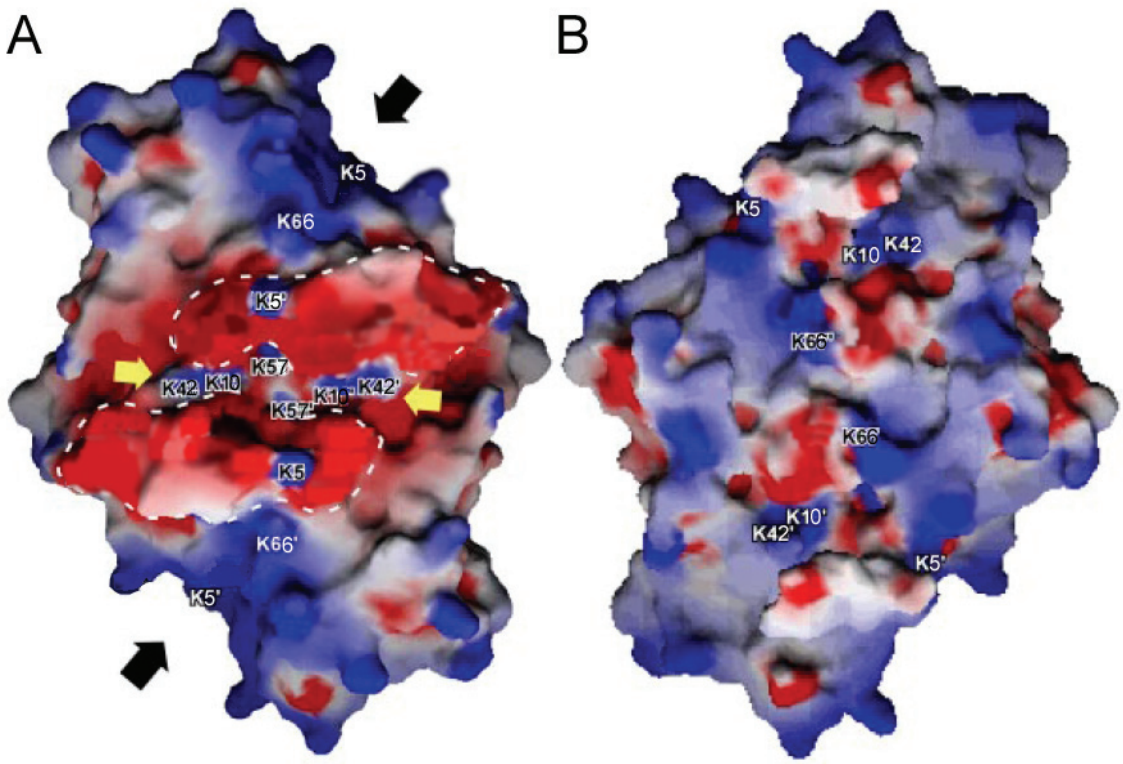

Figure 4-1. Surface potential of the KaiB tetramer and the five conserved positively charged lysine residues. (A) On one side of the tetramer, highly concentrated negative charge surrounding positively charged clefts (yellow arrows) and positively charged hollows between two subunits (black arrows). **(B)** The other side of the KaiB tetramer (PDB-ID **1VGL**). Color code: blue, positie; red, negative. (Modified from Iwase et al., 2005)

Materials and Methods

Fluorophore labeling of KaiC and measurement of FRET

The fluorophores used to label the KaiC protein were IAEDANS (Ex 336/Em 470 nm) and MTSF (Ex 490/Em 515 nm). 1,5-IAEDANS was purchased from Molecular Probes (catalog # I14; Eugene, Oregon, US). MTSF was purchased from Toronto Research Chemicals (catalog # F510000; North York, Ontario, Canada). KaiC in DTT-containing buffer (150 mM NaCl, 1 mM DTT, 1 mM ATP, 50 mM Tris-Cl, 5 mM

MgCl2, [pH 8.0]) was desalted on a G-25 Sephadex desalting column (GE Healthcare) equilibrated with the same buffer except without DTT. After desalting, KaiC was incubated with a 10-fold molar excess of either IAEDANS or MTSF in the dark. The reactions were allowed to proceed for 2 h at room temperature and then overnight at 4 ºC. Unreacted fluorophores were separated from the fluorescently labeled KaiC proteins with another G-25 Sephadex desalting column. FRET was employed to determine the monomer exchange between KaiC hexamers. The exchange reaction was initiated by mixing equal volumes of IAEDANS-labeled KaiC with MTSF-labeled KaiC in the same buffer that was used for desalting, and then placed in a stoppered cuvette at 30 ºC (final concentration of each labeled KaiC was 0.1 μg/μl for a final total KaiC concentration of 0.2μg/μl). At time points of 0, 10, 30, 60, 120, 240, 360, and 480 m, the emission spectrum of the sample that was excited at 336 nm was recorded using a spectrofluorometer (QuantaMaster-7/2005 SE; PTI, Birmingham, New Jersey, US). The decay of the emission at 470 nm (emission peak for the donor IAEDANS) was calculated and plotted as a function of time.

Protein preparation and the *in vitro* Kai protein reaction

Kai proteins used in this chapter were constructed and purified as described in **Chapter II**. The KaiC protein molecules specifically used in this chapter are $KaiC^{AA}$, $KaiC^{EE}$, $KaiC^{489}$, $KaiC^{aST}$, and $KaiC^{nST}$. The first three KaiC mutants are the same as those described in **Chapter II**. The three letters in the superscript of the $KaiC^{aST}$ and

KaiC^{nST} mutants represent the putative KaiC phosphorylation sites, T426, S431 and T432 (Xu et al., 2004), and the mutated residue is shown in lower case. The KaiB proteins in this chapter are KaiB^{K5A}, KaiB^{K10A}, KaiB^{K42A}, KaiB^{K57A}, and KaiB^{K66A}, where the superscript represents the mutated residue.

For all the *in vitro* Kai protein reactions in this chapter, either binary or ternary mixtures were prepared as described in **Chapter II**.

Analysis of monomer exchange of KaiC mutant proteins by Native-PAGE

KaiC^{489} migrates faster in native polyacrylamide gels than full-length KaiC due to the loss of the 30 amino acid-long C-terminal tail. KaiC^{489} (100 ng/μl) and the KaiC protein to be tested (100 ng/μl) were incubated together at 30ºC in reaction buffer (RB = 150 mM NaCl, 5 mM MgCl2, 1 mM ATP, 0.5 mM EDTA, 50 mM Tris-HCl at pH 8.0). Aliquots (16μl) of the KaiC protein mixtures were collected at each treatment/time point, combined with 5X native-PAGE sample buffer (50% glycerol, 0.05% bromophenol blue, 0.312M Tris-HCl at pH 6.8), flash-frozen in liquid nitrogen, and stored at -80 ºC. Native-PAGE (10 cm × 10 cm gels of 7.5% polyacrylamide gels) was performed at 4 ºC with 5mA constant current for 5 h to resolve the hexamers of (1) pure KaiC^{489}, (2) pure test KaiC, and (3) mixed hexamers of KaiC^{489}/test KaiC. Gels were stained with colloidal Coomassie Brilliant Blue, and gel images were digitally captured with the Bio-Rad Gel Doc XR system.

Results

Confirmation of monomer exchange with FRET

It has been reported that KaiC monomers appear to exchange, or ‘‘shuffle,’’ among KaiC hexamers (Kageyama et al., 2006). Those studies were performed by the method of pull-down assays. However, pull-down assays of FLAG-tagged KaiC proteins may suffer from differential cross reactivity and aggregation. Therefore, we decided to avoid the use of peptide-tagged proteins by employing a completely different technique to confirm KaiC monomer exchange, namely FRET (Clegg 1995; Bova et al., 2002). KaiC has three intrinsic cysteine residues (at residues 274, 306, and 348) that can be used for labeling with fluorophores. We used IAEDANS and MTSF, which are well-characterized FRET fluorophore partners to label these cysteine residues. Therefore, one group of KaiC hexamers was labeled with IAEDANS and the other with MTSF. These groups were then mixed and incubated while monitoring the time-dependent change in quenching of IAEDANS fluorescence (indicative of FRET) in response to excitation at 336 nm (the excitation maximum for IAEDANS). As shown in **Fig. 4-2A**, during the incubation of the two populations of KaiC, the emission at 470 nm (emission peak for IAEDANS) decreases progressively. This result indicates that monomer exchange among the two groups of KaiC has occurred so that resonance energy is transferred from IAEDANS to MTSF, thereby quenching IAEDANS’ emission at 470 nm. A change in the FRET ratio is obvious even after only 10 min, indicating that monomer exchange is a

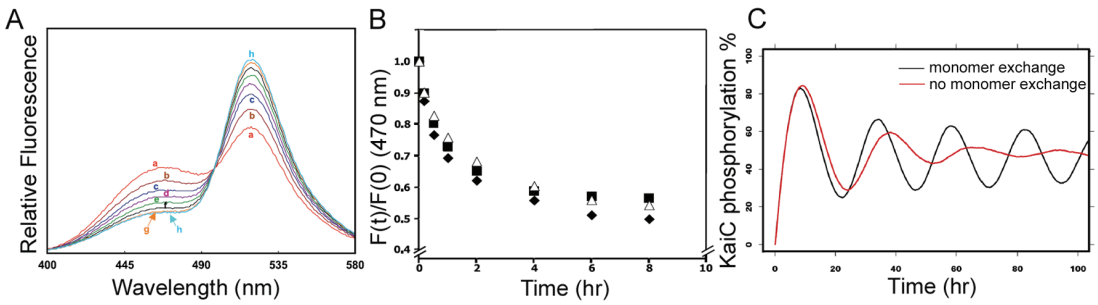

Figure 4-2. KaiC monomer exchange revealed by changes in FRET signal. (A) One sample of KaiC was labeled with IAEDANS, and another sample of KaiC was labeled with MTSF. The emission spectra of KaiC excited at 336 nm was recorded at the following times: (a) 0, (b) 0.16, (c) 0.5, (d) 1, (e) 2, (f) 4, (g) 6, (h) 8 h after mixing equal amounts of IAEDANS-labeled and MTSF-labeled KaiC at 30 ºC. The decrease in fluorescence intensity at 470 nm of IAEDANS-labeled KaiC is indicative of energy transfer due to monomer exchange between the two labeled KaiC populations. **(B)** Effect of KaiA and KaiB on monomer exchange. Measurement of monomer exchange between IAEDANS-labeled and MTSF-labeled KaiC when KaiA or KaiB was added the mixture of KaiC. The decrease in fluorescence intensity at 470 nm was plotted as a function of time. Symbols are KaiC alone (filled diamonds), KaiC + KaiA (filled squares), KaiC + KaiB (open triangles). **(C)** Model prediction of the in vitro KaiABC oscillation in the presence (black line) or absence (red line) of monomer exchange. (Modified from Mori et al., 2007 doi: 10.1371/journal.pbio.0050093)

rapid event among KaiC hexamers. After 8 h of incubation, the quenching of IAEDANS fluorescence decreased by approximately 50% of the initial intensity. The FRET ratio does not change in KaiC preparations that were labeled with only MTSF. Unlike the results obtained with the previously reported pull-down assay (Kageyama et al., 2006), our FRET analysis indicates that neither KaiA nor KaiB significantly inhibits monomer exchange (**Fig. 4-2B**).

In the paper we published in 2007 (Mori et al.), our model indicated that phase-dependent monomer exchange could be important for sustaining the high amplitude and the synchrony of the KaiABC oscillator. As shown in **Fig. 4-2C**, if phase-dependent monomer exchange among hexamers is not allowed during the

simulation, then the oscillation in KaiC phosphorylation dampens out. Alternatively, if the monomeric exchange between all states of hexamers is modeled with equivalent rates or if there is no phase dependency, then the oscillations will also dampen out. The idea of this simulation is that sustained, high amplitude oscillations in the *in vitro* rhythm are only possible if the individual KaiC hexamers in the population remain synchronized in terms of their phosphorylation status. This synchronization is possible if monomer exchange among hexamers is allowed at a defined phase of the *in vitro* oscillation.

Investigation of monomer exchange by using Native-PAGE

FRET is accurate and sensitive, but to label protein with fluorophores and to remove the extra fluorophores are time-consuming. Therefore, I searched for a label-free method to apply for many to-be-tested KaiC mutants. When I studied how the interactions among three Kai proteins could affect the dynamics of the KaiABC system, I constructed and purified the C-terminal 30 amino acid tail truncated KaiC, $KaiC^{489}$ (**Chapter II**). As shown in **Fig. 4-3A**, $KaiC^{489}$ forms a well organized hexamer and migrates faster than $KaiC^{WT}$ in native polyacrylamide gels due to the loss of the 30 residues. In **Chapter II,** I discussed that $KaiC^{489}$ is highly phosphorylated (similarly to the $KaiC^{487}$ mutant in Kim et al., 2008). The hypo- and hyper- phosphostatus mutants of KaiC, namely $KaiC^{AA}$ and $KaiC^{DE}$, have different abilities to exchange monomers (Ito et al., 2007). Since the hyper-phosphorylation mimic $KaiC^{DE}$ is able to exchange monomers with $KaiC^{WT}$ (Ito et al., 2007), it is reasonable to predict that $KaiC^{489}$ can exchange

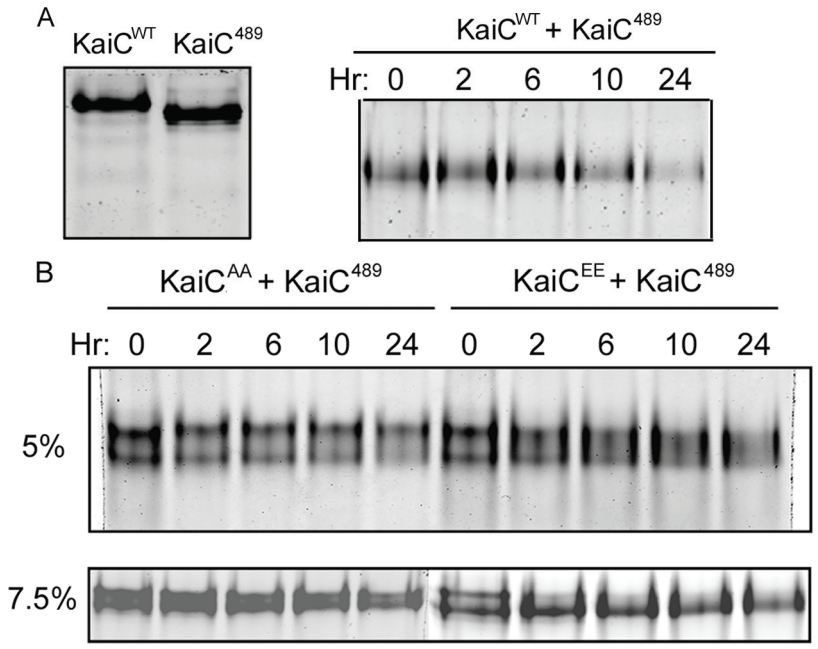

Figure 4-3. KaiC monomer exchange revealed by mixing full-length KaiC with truncated KaiC^{489}. (A) KaiC^{489} has faster migration than KaiC^{WT} in native polyacrylamide ges (7.5% in this panel). Both KaiC proteins are well hexamerized. KaiC^{WT} and KaiC^{489} are exchanging monomers as indicated from the right panel. **(B)** Hypo-phosphoform KaiC^{AA} and hyper-phosphoform KaiC^{EE} are mixed with KaiC^{489} respectively. Samples were collected at the designated time points and resolved in either 5% (upper image) or 7.5% (lower image) native polyacrylamide gels. KaiC^{AA} + KaiC^{489} show two-band pattern after 1 day incubation, but KaiC^{EE} + KaiC^{489} show a smeared band after 1 day.

monomers. Considering that KaiC^{WT} and KaiC^{489} have different mobility in native polyacrylamide gels, if they do not exchange monomers between each other, then mixtures of KaiC^{WT} and KaiC^{489} should show two distinct bands in native-PAGE. On the other hand, if KaiC^{WT} and KaiC^{489} hexamers do exchange monomers, then we might see a single intermediate molecular-weight band, but in any case, we would not see a clear two-band-pattern in the gels after incubating the two proteins together. I clearly see the latter result in the right panel of **Fig. 4-3A**. In **Fig. 4-3B**, I incubated KaiC^{489} with KaiC^{AA} and KaiC^{EE} respectively. KaiC^{AA} is known not to exchange monomers (Ito et al.,

2007), and $KaiC^{EE}$ is expected to behave similarly to $KaiC^{DE}$. In both 5% and 7.5% polyacrylamide gels, at incubation time 0, two clear bands are resolved. 24 hours later, two bands are resolved for the mixture of $KaiC^{489}$ and $KaiC^{AA}$, but not for $KaiC^{489}$ and $KaiC^{EE}$. Therefore, this native-PAGE assay implies that $KaiC^{489}$ can exchange monomers with $KaiC^{EE}$, but not with $KaiC^{AA}$.

Correlation of monomer exchange and KaiB-KaiC interaction

During the dephosphorylation phase, $KaiC^{WT}$ exchanges monomers (Kageyama et al., 2006; Ito et al., 2007) and binds KaiB (Kageyama et al., 2006; Mori et al., 2007; Nishiwaki et al., 2007; Rust et al., 2007; **Chapter II**). **Fig. 4-3** demonstrates that $KaiC^{EE}$ exchanges monomers, and we know this mutant tightly binds KaiB (see **Chapter II**). These observations support a correlation between monomer exchange and KaiB-KaiC interaction.

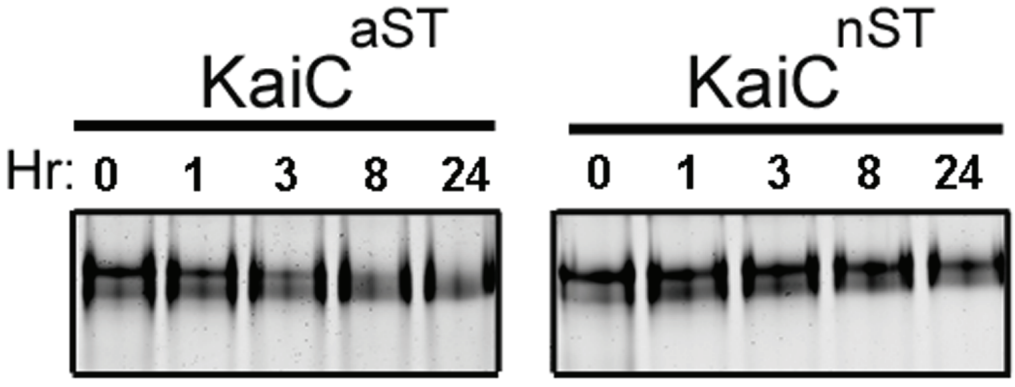

Figure 4-4. A pair of KaiC mutant proteins show opposite capabilities of monomer exchange. $KaiC^{aST}$ can exchange monomers, but $KaiC^{nST}$ cannot.

Fig. 4-4 shows that KaiC^{aST} behaves differently from KaiC^{nST} when they are mixed with KaiC^{489}. Mixtures with KaiC^{aST} are in a smeared single band after 24 hr incubation, but mixtures with KaiC^{nST} maintain two sharp bands (the native-PAGE data are still not very convincing at this moment. I will discuss this issue later in the chapter). In the *in vivo* co-expression experiments, KaiC^{aST} significantly disrupts the clock when co-expressed with KaiC^{WT} (phenotype is essentially arhythmic), while KaiC^{nST} only lengthens the period when co-expressed with KaiC^{WT}; both KaiC^{aST} and KaiC^{nST} are arhythmic when they are the only KaiC expressed *in vivo* (Xu et al., 2009). The results of **Fig. 4-4** lead to the prediction that KaiC^{nST} would not exchange monomers with KaiC^{WT} when co-expressed *in vivo*.

Native-PAGE was performed to study the protein interactions between KaiB and KaiC^{aST} or KaiC^{nST} (Xu et al., 2009). The figure from Xu et al. (2009) is re-produced here as **Fig. 4-5**. **Figs. 4-5A&B** indicates that the mutation of T426 to asparagine severely restricts the dephosphorylation ability of KaiC proteins, which might be the reason that the asparagine at the residue 426 stabilizes KaiC in the hyper-phosphorylated state at the residue S431 (Xu et al., 2004; Pattanayek et al., 2009). **Fig. 4-5C** clearly shows the association between KaiB and KaiC^{aST}, but not with KaiC^{nST}, when the proteins are incubated up to 8 hours. Combined with the data from KaiC^{AA}, KaiC^{EE} and KaiC^{489} (**Chapter II**), the results show a definite correlation between monomer exchange and KaiB-KaiC interactions. KaiC^{nST} is not able to associate with KaiB (right panel in **Fig. 4-5C**), and it is also not able to sequester and inactivate KaiA when three proteins are incubated (right panel in **Fig. 4-5D**). This results in a hyper-phosphorylated status for KaiC^{nST}, as shown in **Fig. 4-5A**.

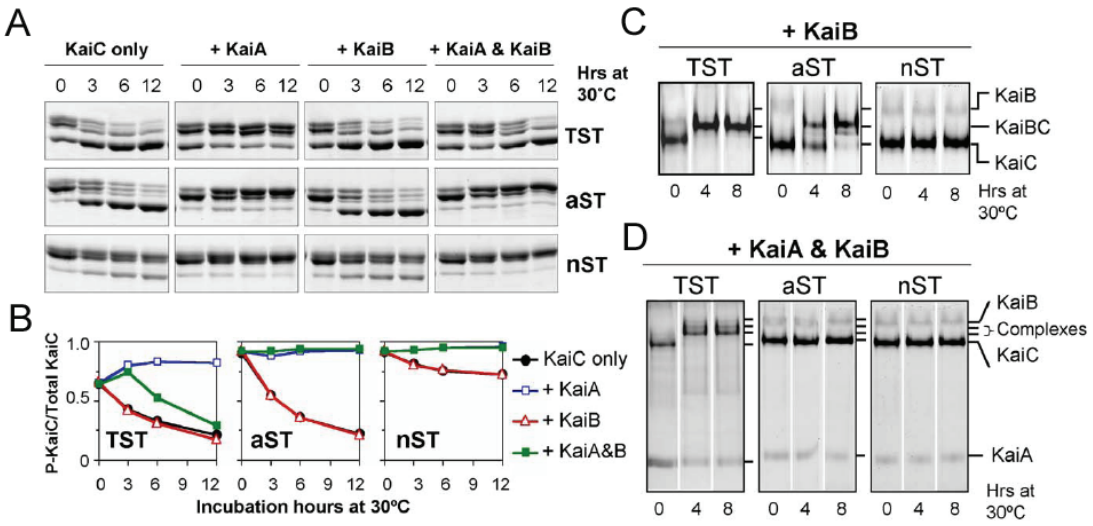

Figure 4-5. T426 mutations affect the rate of KaiC dephosphorylation and the formation of Kai complexes *in vitro*. (A) Dephosphorylation rate of wild-type KaiC ($KaiC^{TST}$) and T426 mutant KaiCs ($KaiC^{aST}$ and $KaiC^{nST}$). Purified KaiC proteins in the hyper-phosphorylated state were incubated at 30 ºC with or without KaiA and/or KaiB for up to 12 h. Samples were loaded onto 10% SDS gels. **(B)** Densitometry of the KaiC phosphorylation/dephosphorylation profiles from panel A. **(C)** & **(D)** Detection of Kai complexes. Purified $KaiC^{TST}$, $KaiC^{aST}$ or $KaiC^{nST}$ were incubated with KaiB (panel C) or KaiA & KaiB (panel D) at 30 ºC for 8 h. The formation of KaiBC complex (panel C) and/or KaiBC/ABC complexes (panel D) were then identified by native gel analyses. Positions of KaiA, KaiB, KaiC and KaiBC/ABC complexes on native gel are noted. (From Xu et al., 2009)

KaiA inhibits the binding of KaiB to KaiC

Interestingly, $KaiC^{aST}$ is also hyper-phosphorylated when it is incubated with KaiA and KaiB proteins (**Fig. 4-5A**). KaiB·$KaiC^{WT}$ complexes will sequester KaiA to inactivate the KaiA protein (left panel in **Fig. 4-5D**; and **Chapter II**), but KaiB·$KaiC^{aST}$ can not sequester KaiA when the three proteins are incubated together (middle panel in **Fig. 4-5D**). Moreover, when KaiA is present, the KaiB·$KaiC^{aST}$ complex (**Fig. 4-5C**) does not form (**Fig. 4-5D**). This leads us to conclude that KaiA either prevents the association between KaiB and $KaiC^{aST}$, or activates the dissociation of the KaiB·$KaiC^{aST}$ complex. To

Figure 4-6. KaiA inhibits the interaction between KaiB and KaiC^{aST} (Ordered B·C + A Assay). (A) The protocol to test why no complexes are detected in **Fig. 4-4D** (middle) for KaiC^{aST} with the presence of KaiA. In this protocol, KaiA is added after the formation of stable KaiB·KaiC^{aST} (~24 hr incubation of KaiB and KaiC^{aST}). Before the addition of KaiA, sample was collected as indicated by the big arrow. **(B)** Duplicate samples collected as noted in panel A (gray arrows) were assayed by native gels. Rapid formation of high-molecule complexes indicates KaiA is not triggering the dissociation of the KaiB and KaiC proteins. Note: Hr 0 is not actually time zero, because the loading process on the Native-PAGEs requires ~ 10 min.

verify which possibility is most likely, I designed the assay as illustrated in **Fig. 4-6A**. Instead of mixing three Kai proteins together at the beginning, KaiC^{aST} and KaiB were mixed first in the regular reaction buffer and KaiA was added after the stable KaiB·KaiC^{aST} complex formed. The result is shown in **Fig. 4-6B**. Unlike the case in **Fig. 4-5D** (middle panel), the KaiB·KaiC^{aST} complex recruited KaiA quickly without dissociating the complex. The interaction pattern indicates that KaiA prevents the binding of KaiB to KaiC^{aST} when all three Kai proteins are mixed together from the start, but after

KaiB and KaiC^{aST} have formed stable complexes, the KaiB·KaiC^{aST} complex will sequester KaiA without dissociating. The inhibition of the formation of KaiB·KaiC complexes also occurs for other KaiB interacting KaiC mutants, namely KaiC^{DT} and KaiC^{EE} (see the decay of KaiC hexamers with or without KaiA in the native gels in **Figs. 2-1C&D**). However, for these two KaiC mutants, the KaiB·KaiC complex formation is not completely blocked but is delayed.

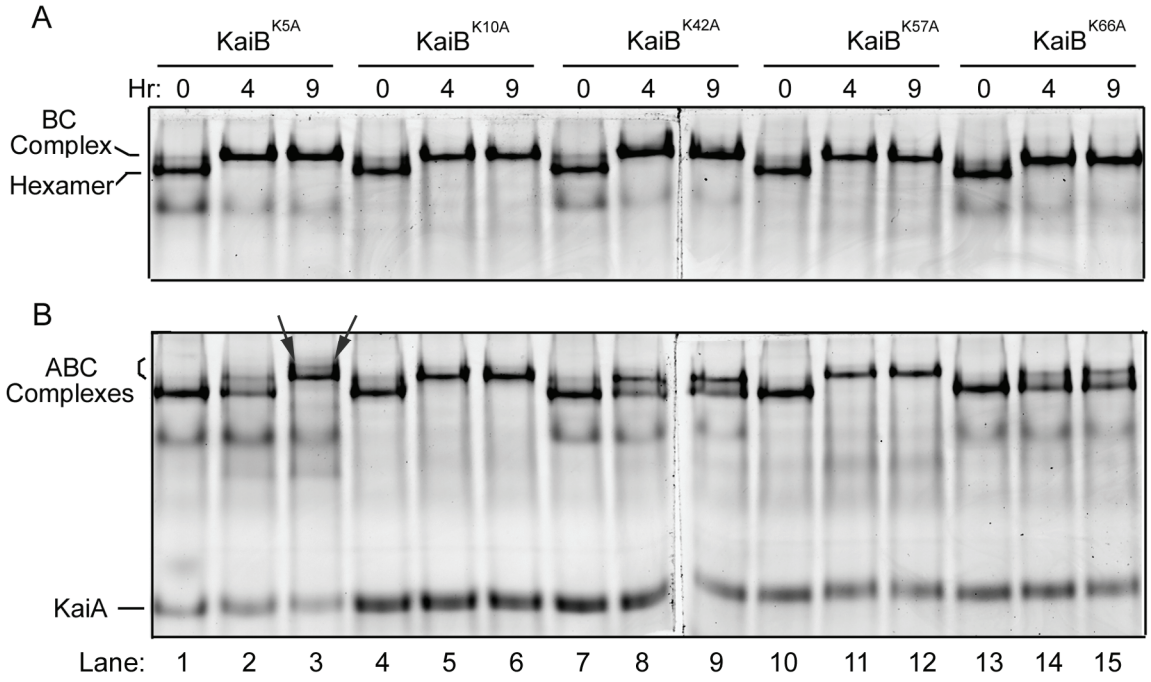

Figure 4-7. Preliminary mapping the binding interface on KaiB. Five known KaiB mutant proteins were purified and tested for the interaction with KaiC^{EE} **(A)** or with KaiA and KaiC^{EE} together **(B)**. The high-molecular weight KaiA·KaiB·KaiC^{EE} complexes in lane 3 is indicated by two arrows.

Preliminary mapping of the interactions of KaiB with KaiC

In this preliminary study, five conserved positively charged residues from KaiB that have been studied *in vivo* (Iwase et al., 2005) were selected to investigate if

electrostatics plays a role in KaiB's association with KaiC. When the five conserved positively charged residues, K5, K10, K42, K57 and K66, were mutated into alanines, K5A has little effect on the clock, but the rest disrupt the clock *in vivo* (Iwase et al., 2005). Since the phenotype of K5A is essentially the same as WT, K5A will be considered as a control for testing binding of the other KaiB proteins. As shown in **Fig. 4-7A**, all five purified KaiB mutants bind tightly with the hyper-phosphorylated KaiC mutant, $KaiC^{EE}$. Therefore the abolishment of rhythms *in vivo* is probably not because of reduced or disrupted KaiB-KaiC interactions. As mentioned before, the binding of KaiB to KaiC might provide a novel site for the sequestration of KaiA (**Chapter II**). Are the KaiB mutants unable to recruit KaiA? When KaiA is incubated with the KaiB mutants and $KaiC^{EE}$, only $KaiB^{K5A}$ is able to form the high-molecular weight complexes (lane 3 in **Fig. 4-7B**). The association between $KaiB^{K42A}$ and $KaiB^{K66A}$ with the $KaiC^{EE}$ protein is reduced in the presence of KaiA, whereas the association between $KaiB^{K10A}$ and $KaiB^{K57A}$ with the $KaiC^{EE}$ protein is not affected (**Fig. 4-7B**). These observations indicate that the electrostatics of these four positively charged residues (K10, K42, K57, and K66) are necessary for the sequestration of KaiA into KaiB·KaiC complexes. This failure of KaiA sequestration results in arrhythmic bioluminescence rhythms *in vivo* (Iwase et al., 2005).

Discussion

In this chapter, I have shown a strong correlation between monomer exchange and KaiB-KaiC interaction by using two pairs of KaiC mutant proteins, $KaiC^{AA}$-$KaiC^{EE}$, and $KaiC^{aST}$-$KaiC^{nST}$. Both pull-down results (Ito et al., 2007) and native-PAGE (this study)

indicate that $KaiC^{AA}$ and $KaiC^{nST}$ are neither exchanging monomers nor binding with KaiB, but $KaiC^{EE}$ and $KaiC^{aST}$ are doing both. Dr. Dewight Williams (the Stewart lab, Department of Molecular Physiology and Biophysics) has shown by EM that $KaiC^{EE}$ alone is not well hexamerized and appears to be prone to falling apart (unpublished data). Falling apart opens the chance for $KaiC^{EE}$ to exchange its subunits with other population of KaiC hexamers. This would further support the observation that $KaiC^{EE}$ is able to exchange monomers (**Fig. 4-3B**). Nonetheless, $KaiC^{AA}$ and $KaiC^{nST}$ are completely different with respect to phosphorylation. $KaiC^{AA}$ is the mimic form of non-phosphorylated KaiC, but $KaiC^{nST}$ contains intact phosphorylation sites and can be highly phosphorylated (**Fig. 4-5A**). Since monomer exchange among KaiC hexamers occurs in the absence of KaiA and KaiB, but KaiB cannot bind to KaiC mutants that cannot exchange monomers (e.g. $KaiC^{AA}$ and $KaiC^{nST}$), I propose that the exchange is a prerequisite for KaiB-KaiC interaction.

My colleagues and I used to think monomer exchange might facilitate dephosphorylation of KaiC subunits, since the monomer exchange could expose the phosphorylation sites to the water molecules. I showed here the evidence that $KaiC^{489}$ (similar phenotype to $KaiC^{487}$, Kim et al., 2008) maintains a highly phosphorylated state and has the ability to exchange monomers between KaiC hexamers. Therefore, monomer exchange does not necessarily result in dephosphorylation. As described in **Chapter II**, $KaiC^{489}$ forms stable complexes with the KaiB protein. These observations support my hypothesis that monomer exchange is a prerequisite for KaiB-KaiC interaction. (To take a brief excursion, I want to discuss the issue of my native-PAGE to assay monomer exchange between KaiC hexamers. Resolution of $KaiC^{489}$ and full-length KaiC in native

polyacrylamide gels is not good enough at this time to provide completely persuasive data on monomer exchange. Therefore, and I am thinking about increasing the percentage of bis-acrylamide in the gel to enhance resolution. Acrylamide gels are polymerized mainly by acrylamide, that is cross-linked with bis-acrylamide. The concentration of bis-acrylamide determines the pore size of a gel for any given concentration of total acrylamide.)

Nishiwaki and coworkers proposed that in the *in vitro* KaiABC oscillator cycles, the achievement of doubly phosphorylated KaiC (especially phosphorylation at S431) switches the KaiC from overall kinase to overall phosphatase activities (Nishiwaki et al., 2007). Furthermore, Kim et al. showed that the C-terminal truncated KaiC ($KaiC^{487}$) stays 100% phosphorylated at S431 and T432, and proposed a model that the position of the C-terminal tail is the switch between overall kinase and phosphatase activities (Kim et al., 2008). The data with my mutant $KaiC^{489}$ agrees with the hypothesis of Kim & coworkers. During the phosphorylation phase, KaiA is transiently interacting with the tail of KaiC and stabilizes the "exposure state" of the tail, resulting in overall autokinase activity; doubly phosphorylated KaiC hexamers begin to fall apart and expose a binding site for KaiB. At the transition, binding of KaiB to doubly phosphorylated KaiC recruits KaiA to a novel stable site, which inactivates KaiA's stimulation activity (**Chapter II**). Then KaiA is recruited into the high-molecular weight complexes and the tail is released back to the "most buried state," resulting in overall autophosphatase activity.

I speculate that during the phosphorylation phase, the transient KaiA-KaiC interaction is not only stimulating the autokinase activity of KaiC, but also preventing KaiB from binding with KaiC. A special mutant, $KaiC^{aST}$, is the only one that has

comparable dephosphorylation characteristics with $KaiC^{WT}$ and when incubated with KaiB, it binds tightly to KaiB (**Fig. 4-5A&C**). But when $KaiC^{aST}$ is incubated with KaiA and KaiB together, it no longer forms stable complexes with KaiB (**Fig. 4-5D**). The ordered KaiB·$KaiC^{aST}$ plus KaiA assay (ordered B·C + A assay) showed that the KaiB·$KaiC^{aST}$ complex recruits KaiA instead of dissociating (**Fig. 4-6**), which not only supports the observations that KaiB·KaiC complex sequesters KaiA in **Chapter II**, but strongly supports that KaiA inhibits the binding between KaiB and KaiC when all three Kai proteins are mixed together at the same time (compare middle panel of **Fig.4-5C** and **Fig.4-5D**). Kageyama et al. have shown that KaiA inhibits monomer exchange by using pull-down assays (Kageyama et al., 2006). This result could be compatible with my hypothesis that monomer exchange precedes KaiB binding, especially since it could explain that the absence of the KaiB·$KaiC^{aST}$ complex in the presence of KaiA is because $KaiC^{aST}$ is unable to exchange monomers when it is associated with KaiA. However, the mechanism by which KaiA inhibits KaiB-KaiC associations is still unclear. Two new KaiC mutants, $KaiC^{aST-489}$ and $KaiC^{nST-489}$, could give hints to understand the prevention effect of KaiA on KaiB-KaiC interactions. Based on my current hypothesis, I predict that both proteins would be highly doubly phosphorylated because of the truncated tail, and $KaiC^{aST-489}$ would bind KaiB with or without the presence of KaiA, but $KaiC^{nST-489}$ would not bind KaiB under either circumstance. This prediction - that $KaiC^{aST}$ does not form stable complexes with KaiB in the presence of KaiA – is based on the ideas that KaiA inhibits monomer exchange by interacting with the C-terminal tail of KaiC (which $KaiC^{aST-489}$ lacks) and that monomer exchange leads to KaiB binding. In the KaiABC oscillation cycles, the binding of KaiB may introduce a conformational change that

exposes a new binding site for KaiA, leading to the stable association of KaiA and KaiB with KaiC. However, the transient KaiA-KaiC interactions during the phosphorylation phase inhibit the binding of KaiB to the KaiC proteins. Right now, the two tail-truncated KaiC mutants, $KaiC^{aST-489}$ and $KaiC^{nST-489}$, have been made but are waiting for purification and functional tests.

In addition, a preliminary test was performed to identify the interaction interface of KaiB with the KaiC protein. The shape of KaiB is thought to be a tetrameric plate (Hitomi et al., 2005; Iwase et al., 2005). In the KaiB protein from *S. elongatus*, positively charged residues occur over two surface areas, forming a hollow and a cleft (Iwase et al., 2005, and **Fig. 4-1**). Five KaiB mutant proteins (**Table 4-1**, and **Fig. 4-1**) with single alanine mutations (K5A, K10A, K42A, K57A, and K66A) were purified and tested for binding. My preliminary conclusion from **Fig. 4-7** is that KaiB's electrostatics might be more important for the recruitment of KaiA than for the interaction between KaiB and KaiC. This could be the case if the four lysines (10, 42, 57, and 66) are important for the formation of the novel binding site that helps to form the stable KaiA·KaiB·KaiC complex.

CHAPTER V

SUMMARY

In Mother Nature, fluctuation and noise is everywhere. Biological rhythms are often reproducible, oscillating fluctuations that happen endogenously in complex biological systems. The period of these biological oscillations ranges from milliseconds to a year. One category of biological rhythms is the circadian clock, which reproducibly oscillates with a period close to 24 hours in constant conditions. It had been thought for a long time that the circadian clock only exists in eukaryotes. However, pioneering work done by Drs. Johnson, Kondo, Golden and their colleagues has had a large impact on the field of chronobiology. Not only has the mechanism of the circadian clock been elucidated in one of the most abundant prokaryotic organisms, cyanobacteria, but molecular studies from the organism have revealed a very interesting post translational oscillator, that can be reconstituted in test tubes (Nakajima et al., 2005). There have been many fascinating discoveries concerning cyanobacteria clocks: global transcriptional regulation (Liu et al., 1995), the *kaiABC* cluster (Ishiura et al., 1998), KaiC circadian phosphorylation *in vivo* (Iwasaki et al., 2002), the X-ray crystal structure of KaiC (Pattanayek et al., 2004), the KaiC phosphorylation rhythm *in vivo* that is independent of transcription & translation (Tomita et al., 2005), and the reconstituted clock *in vitro* with three Kai proteins (Nakajima et al., 2005). My goals as a graduate student have been to understand the core clock in this organism both *in vitro* and *in vivo*.

Biochemical functions of the KaiC protein itself

From sequence analyses, KaiC was suggested to be a member of the RecA/DnaB superfamily (Leipe et al., 2000), although it does not contain a DNA-binding motif. Our lab has reported that KaiC binds forked DNA substrates (Mori et al., 2002), but the function of this DNA-binding is not known. There are three main enzymatic activities known about KaiC: autokinase, autophosphatase, and ATPase. The mechanism underlying these activities is not fully understood, but the autophosphatase activity dominates when the purified KaiC protein is incubated at 30 ºC, while the autokinase activity dominates at 4 ºC (or in the presence of KaiA). Interestingly, Kim and coworkers have shown that the autokinase activity dominates in the C-terminal tail truncated KaiC ($KaiC^{487}$, Kim et al., 2008). And at about the same time, I constructed and purified $KaiC^{489}$, which is ~ 100% doubly phosphorylated at 30 ºC. This discovery strongly supports the hypothesis that the position of the C-terminal tail switches the activity of KaiC between autokinase and autophosphatase. The position of the C-terminal tail is probably directly influenced by the binding of KaiA (Kim et al., 2008). KaiC itself is able to exchange monomers among hexamers, which is proposed to be a mechanism to synchronize the KaiC population (Mori et al., 2007; Ito et al., 2007) and/or to be a prerequisite for KaiC's associating with KaiB (**Chapter IV**). It was also reported that one KaiC molecule consumes about 15 ATP molecules per day (Terauchi et al., 2007). Very recently, $KaiC^{487}$ was reported to consume ~60 ATP/day, 4-fold higher than $KaiC^{WT}$, but the kinetics of the ATP consumption by $KaiC^{487}$ from this very recent study (Dong et al., 2010) are not clear.

KaiA-KaiC & KaiB-KaiC interactions

Kai protein interactions were qualitatively studied by several methods before I started my thesis. Therefore at the beginning of my thesis study, I attempted to focus on quantitatively studying the interactions between KaiA and KaiC, KaiB and KaiC respectively. First, label-free systems were tested. BIRC (Backscattering Interferometry in Rectangular Channels, Markov et al., 2004) was the first system we tried, but it did not succeed. ITC (Isothermal Titration Calorimetry, Isin & Guengerich 2006) was also applied to measure the interactions. However, it did not succeed either. Then I turned to using fluorescent methods.

Cysteine-free proteins were constructed for KaiA and KaiC to provide a basis for labeling Kai proteins with fluorophores. KaiA from *S. elongatus* has 6 intrinsic cysteines: C8, C20, C34, C53, C71, and C273; KaiC has 3 intrinsic cysteines: C274, C306, and C348. The KaiB protein from *S. elongatus* does not have intrinsic cysteines. Three single-cysteine mutants were constructed for KaiB: R22C, K25C, and R74C. The bioluminescence traces of the cyanobacterial strains carrying these Kai mutations are shown in the **Appendix C**. The results are summarized here: Cysteine-null KaiA is insoluble when expressed in *E. coli*, and a cyanobacterial strain carrying the cysteine-null *kaiA* gene shows arhythmic bioluminescence traces; Cysteine-null KaiC is insoluble in *E.coli*, but a cyanobacterial strain carrying the cysteine-null *kaiC* gene is rhythmic with dramatic period changes. Single-cysteine KaiB is soluble in *E.coli*, and is rhythmic in cyanobacteria. Single-cysteine mutant KaiB proteins have been purified and successfully labeled with fluorophores. The attempts to use labeled KaiB mutants to measure the interactions between KaiB and KaiC by FA or EPR (electron paramagnetic resonance)

have not been successful to date.

KaiC shows a significant band shift in native gels when the protein is incubated with KaiB (Pattanayek et al., 2008). The interactions reach a steady state in several hours (**Fig. 2-1**). With KaiC that has been altered to mimic hyper-/hypo- phosphorylation, I started to use native-PAGE assays to investigate the interactions. The results of the interactions are described in **Chapter II** and **Chapter IV**, and will not be discussed here in detail. Briefly, however, the interactions between KaiB and KaiC are associated with hyper-phosphorylated KaiC, which has the ability to exchange monomers; the KaiB·KaiC complex recruits KaiA to a novel site to inactivate KaiA's function. A remaining question is what conformational change of KaiC facilitates KaiB-KaiC interactions. Structural studies indicate that KaiB interacts with the surface of the CII domain of KaiC (Pattanayek, et al., 2008), and that there are only subtle conformational changes in the region of the phosphorylation sites (buried in the interface of the CII domain, Xu et al., 2004) among different phospho-forms (Pattanayek, et al., 2009). Where is the binding site and how does a phosphorylated KaiC expose the binding site? KaiC from *S. elongatus* forms a stable hexamer ring and will precipitate at the absence of ATP (Mori et al., 2002). However, KaiC from the thermophilic cyanobacterium *T. elongatus* BP-1 is stable in monomeric form in the absence of ATP (Hayashi et al., 2003). To test the possibility that a monomeric KaiC molecule is able to form a complex with KaiB, KaiC from *T. elongatus* would be a good candidate for both biochemical and structural studies.

The oscillating KaiABC system *in vitro*

The KaiABC system *in vitro* shows three different rhythms. The first is the robust

rhythm of KaiC phosphorylation (Nakajima et al., 2005). The second is the rhythm of formation of complexes (Kageyama et al., 2006; Mori et al., 2007; **Chapter II**), and the third is the rhythm of ATP hydrolysis by the KaiC protein (Terauchi et al., 2007). Obviously, KaiC's phosphorylation status results from a balance between autokinase and autophosphatase activities. KaiC phosphorylation and formation of complexes are interlocked to regulate each other as discussed in previous chapters. During the phosphorylation phase of the *in vitro* cycle, KaiA associates with the C-terminal tail of KaiC to stabilize the "exposed state" of the tail, resulting in a dominating autokinase activity (Kim et al., 2008). Phosphorylated KaiC will form KaiB·KaiC complexes, which recruits KaiA into hetero-molecular complexes to inactivate KaiA. KaiA is sequestered at a novel site (**Chapter II**) and as a result the tail returns to the "flexible state," resulting in a dominating autophosphatase activity. Then the overall KaiC population dephosphorylates. How phosphorylation and formation of complexes are affected mutually is relatively clearer than the relation between phosphorylation/complexes and ATP hydrolysis. In the absence of KaiA or KaiB, KaiC molecule consumes about 15 ATP molecules per day. During the phosphorylation phase, KaiC consumes ATP almost linearly with a rate that is close to that when KaiC is incubated with KaiA (~30 ATP/day), but the consumption is repressed during the dephosphorylation phase (Terauchi et al., 2007). It is still not clear whether the KaiC based complexes or the KaiC conformational change affects the ATPase activity, since $KaiC^{AA}$ (hypo-phosphorylation mimic) increases the ATPase activity to ~30 ATP/day but $KaiC^{DE}$ (hyper-phosphorylation mimic) decreases to ~10 ATP/day (Terauchi et al., 2007). I speculate that the KaiC conformational change, along with monomer exchange, affects the ATPase activity.

Studying the behavior of single protein molecules rather than populations of molecules remains challenging for both biochemists and biophysicists. And an important question for the oscillating KaiABC system is whether individual KaiC hexamers, or even individual KaiC monomers, are equivalent during all the phases. All methods discussed previously were of populations of Kai proteins, and the activities of autokinase, autophosphatase and ATPase were measured from KaiC populations. One line of evidence that not all monomers within a KaiC hexamer are equivalent is that the KaiC subunits are not phosphorylated in parallel within a hexamer from the crystal structural studies (Pattanayek et al., 2004). However, crystals are formed under significantly different conditions from the physiological environment, and therefore, this evidence may be irrelevant. Biophysical methods, especially single-molecule techniques developed recently (Walter et al., 2008), should be applied on this system to address the above questions.

The TTFL is a slave oscillator in cyanobacteria

All of the promoters in cyanobacteria are regulated in a circadian pattern globally, including the *kaiBC* protmoter (Liu et al., 1995). Over-expression of KaiC protein not only represses its own promoter (the *kaiBC* promoter), but it also represses all rhythmically expressed promoters (Ishiura et al., 1998; Nakahira et al., 2004). And it has been reported that the chromosome of cyanobacteria rhythmically changes its topology (Smith & Williams, 2006; Woelfle et al., 2007; Vijayan et al., 2009). As described in detail in **Chapter III**, it is clear that when the KaiC phosphorylation is suppressed, global gene expression is repressed (promoters P_{kaiBC} and P_{psbAI} were tested). We proposed in the

model (**Fig. 2-7)** that the KaiB·KaiC complex represses transcriptional activity through the control of chromosomal topology, but the exact mechanism is still unknown.

To my knowledge, *S. elongatus* is the only organism whose core circadian clock can be reconstituted in a test tube. Single-cell study in cyanobacteria demonstrates that the daughter cells inherit precisely the same circadian phase from the mother cells (Mihalcescu et al., 2004). The issues of (1) how the KaiABC oscillator is embedded with a larger TTFL, (2) how this system generates robustness, and (3) the possibility that higher organisms could also have a robust biochemical PTO are discussed in **Chapter III**. The TTFL in cyanobacteria shares some similarities with that in mammals, which are: (1) knock-out studies have shown that clock genes are essential; (2) rhythmic abundances of mRNAs and proteins encoded by clock genes; (3) negative feedback of clock proteins on the transcription of their own genes; and (4) phase setting by pulsatile expression of clock genes. However, with regard to detailed comparisons, there are important distinctions, which are: (1) clock genes from cyanobacteria vs. mammals have no similar homologs; (2) regulated entry of clock proteins into the nucleus seems to play an important role in the timing mechanism in mammals, while cyanobacteria do not have nuclei; (3) the TTFL works directly in mammals through the E-box containing promoters, while the process is not very clear in cyanobacteria. Here, I would like to discuss the possibility that there is a PTO in mammals.

First of all, what protein(s) or other molecule(s) could serve as the core of a mammalian PTO? Among the clock proteins, the PER proteins could be good candidates, since it was reported that the *Drosophila* PER undergoes a circadian phosphorylation cycle (Edery et al., 1994). In addition, recent results have led to a greater appreciation of

the role of small signaling molecules in the mammalian clock (Hastings et al., 2008). Secondly, where is the subcellular location for the possible PTO: the nucleus or cytoplasm or both? The protein synthetic machinery and most enzymes are located in the cytoplasm. If it is similar to the case in cyanobacteria that protein-protein interactions are important for generating the PTO, then the cytoplasm might be a better location for this hypothetical PTO. And finally, what would be the mechanism underlying the rhythmic transcription regulation? The TTFL in mammals proposes that the BMAL/CLOCK complex binds to E-box in relevant promoters to activate transcription. How the KaiC phosphorylation oscillation regulates the global genomic transcription is not clear, but if there were a PTO in mammals, it would have to communicate with the transcriptional activator BMAL/CLOCK complex directly or indirectly. A protein-based PTO would be expected to have physical interactions with the BMAL/CLOCK complex, while a small molecule-based PTO linked with cellular redox state might be expected to regulate the enzymatic activity of the complex allosterically.

Signaling pathways downstream from the KaiABC oscillator

A circadian clock system can be divided into three major parts: the input pathways, the core pacemaker, and the output pathways. In cyanobacteria, the mechanism by which clock signals are passed from the core KaiABC oscillator to the global transcriptional machinery remains elusive. A two-component system was proposed to mediate the signal from the KaiABC oscillator to drive global transcription (Takai et al., 2006). SasA (*Synechococcus* adaptive sensor) was first identified as a KaiC-interacting histidine kinase through two-hybrid screening analyses (Iwasaki et al., 2000). SasA

contains a KaiB-like domain, which appears to be sufficient for interaction with KaiC. And manipulation of the expression of *sasA* severely affects the rhythm (Iwasaki et al., 2000). The same group performed a screening for the response regulator genes of *sasA*, and identified RpaA as SasA's partner (Takai et al., 2006). SasA's autophosphorylation is enhanced by KaiC, and SasA-RpaA phosphor-transfer activity is strongly dependent on the phase of the KaiABC oscillator *in vitro* (Takai et al., 2006). However, a residual transcription rhythm remains in *sasA*-null or *rpaA*-null mutant strains, which indicates the existence of another output pathway (Takai et al., 2006). After screening ~20,000 colonies, again, they identified *labA* (low-amplitude and bright), which is a novel gene required for the negative feedback regulation (Taniguchi et al., 2007). Since over-expression of KaiC (KaiC-OX) strongly represses the circadian rhythms of all the promoters in *S. elongatus* (Nakahira et al., 2004), the Kondo group searched for randomly mutagenized genes whose mutants were defective in the KaiC-OX repression (Taniguchi et al., 2007). LabA was proposed as a negative regulator that through RpaA suppresses the global transcriptional machinery (Taniguchi et al., 2007). Further investigations from the Kondo lab have suggested that CikA (circadian input kinase), which had been thought to be only involved in the input pathways (Schmitz et al., 2000), accounts for a third output pathway downstream of the KaiABC oscillator (Taniguchi et al., 2010).

Metabolism and the circadian clock

Cyanobacteria are autotrophic photosynthetic organisms and originally evolved chlorophyll. The organism uses the circadian clock to regulate its daily activities. It is

reasonable to speculate that ATP, the cellular energy unit, could oscillate in a circadian manner, coordinately regulating physiological activities, such as topological changes of the chromosome. However, by using a firefly luciferase luminescence assay kit (Promega, US) to quantify ATP, I could not identify a clear oscillation of ATP from cyanobacterial extracts in LL, although there is a robust oscillation in LD (data not shown).

Light is the most important environmental signal for the entrainment of biological clocks. To date, it is still not clear how cyanobacteria are entrained by light/dark cycles. CikA, a bacteriophytochrome, was identified as a key factor for entraining the clock in cyanobacteria (Schmitz et al., 2000). But unlike classical photoreceptors in other organisms, CikA senses not light but rather the redox state of the quinone pool in cytoplast (Ivleva et al., 2006). Quinone not only directly binds to CikA, but also affects the stability of the protein (Ivleva et al., 2006). Very recently, it was reported that the core clock protein, KaiA, also has the ability to bind quinone (Wood et al., 2010). The binding with quinone causes instability of KaiA protein, and blocks KaiA stimulation of KaiC phosphorylation (Wood et al., 2010). It was reported in *E. coli* that the membrane-bound sensor kinase ArcB, which passes phosphate to its downstream partner ArcA, a global regulator of gene expression, senses the cellular redox signal as represented by the redox state of quinone pool (Malpica et al., 2004; Green and Paget, 2004). Not many publications have attempted to connect quinone pools with circadian clocks in cyanobateria (or any other organism).

Considering the global regulation of gene transcription and the global chromosome compactions in cyanobacteria, the crosstalk between the core KaiABC oscillator and the cellular metabolism remains challenging and fascinating.

APPENDIX A

SUPPORTING INFORMATION TO CHAPTER II [#]

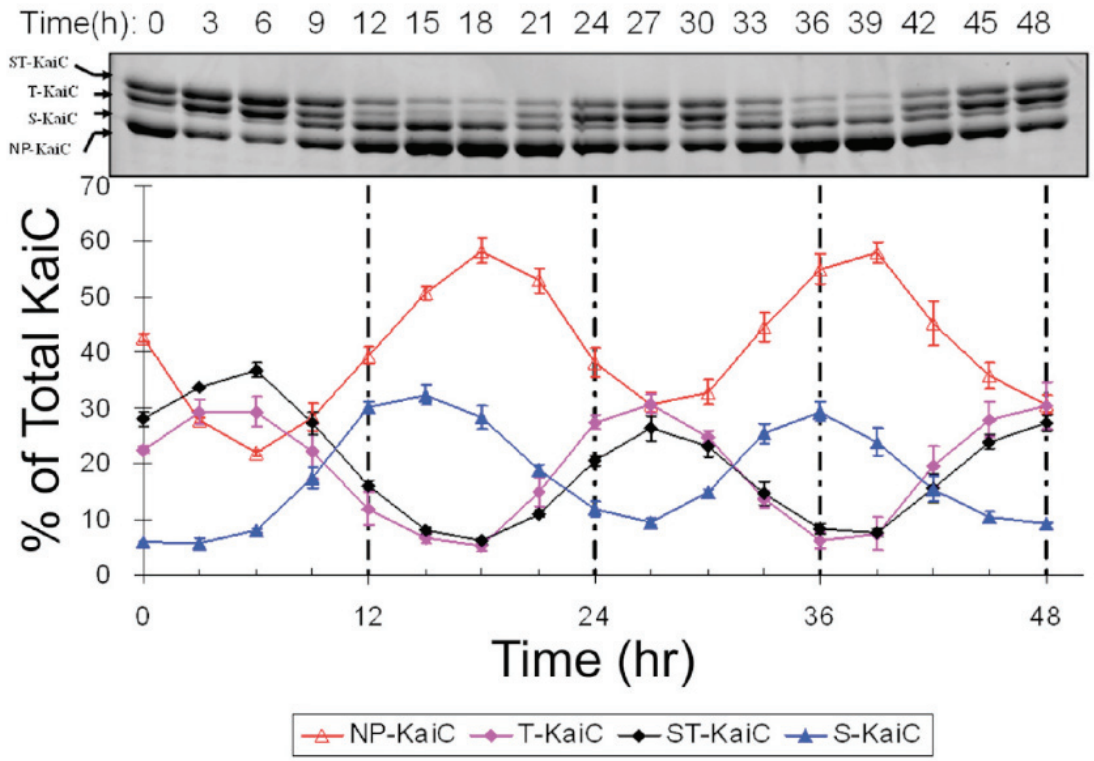

Figure S2-1. Sequential phosphorylation events during the *in vitro* KaiABC oscillation. KaiC is sequentially phosphorylated during the *in vitro* cycle, first at T432 ("T-KaiC"), then at S431 ("ST-KaiC"), then T432 is de-phosphorylated ("S-KaiC"), followed by de-phosphorylation at S431 which returns KaiC to the hypophosphorylated state (nonphosphorylated KaiC, "NP-KaiC"). The upper panel is a 10% SDS gel that depicts a representative KaiABC reaction for two days *in vitro*. The bottom panel is the densitometric analysis of each phosphoform of KaiC as a function of time from the beginning of the reaction (error bars are ± S.D. for three separate experiments). The sequential phosphorylation of KaiC is reproduced with the following order: NP-KaiC (Red), T-KaiC (Pink), ST-KaiC (Black), and S-KaiC (Blue).

[#] Chapter II is directly derived from the published paper: Qin X, Byrne M, Mori T, Zou P, Williams DR, McHaourab H, Johnson CH (2010) Intermolecular associations determine the dynamics of the circadian KaiABC oscillator. *Proc Natl Acad Sci USA* [Epub ahead of print]. **Appendix A** is the published supporting information to the paper.

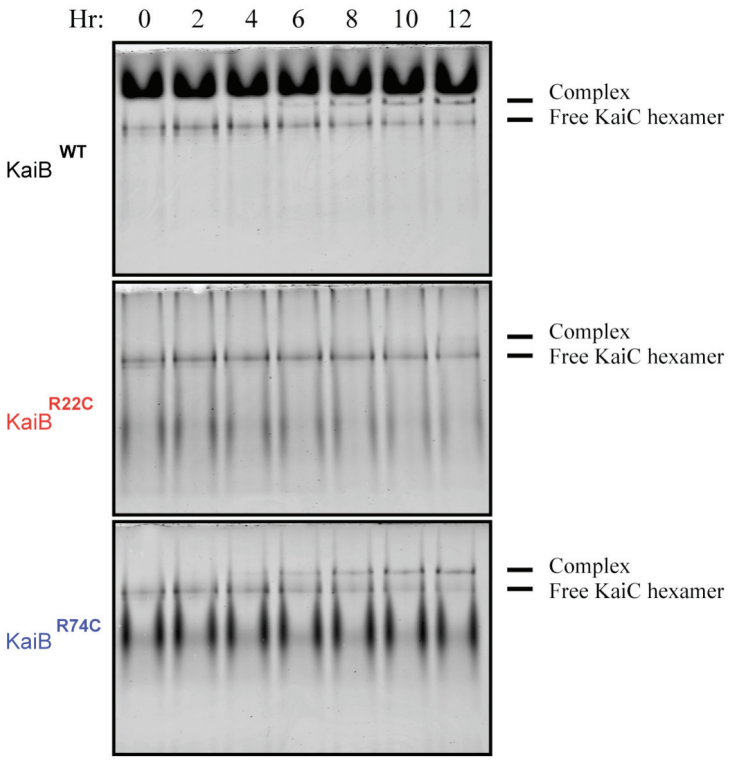

Figure S2-2. Formation of stable complexes between KaiC489 and the KaiB Variants. Native-PAGE analyses of timedependent interactions between KaiC489 and KaiB^{R74C} (bottom panel), KaiB^{WT} (upper panel), and KaiB^{R22C} (middle panel). Incubations performed at 30ºC. These are the raw data of the plots in **Figure 2-3D**.

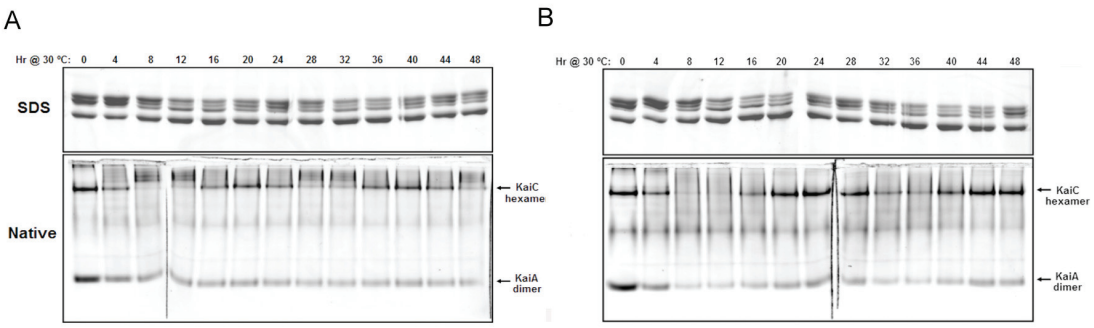

Figure S2-3. KaiA•KaiB•KaiC complexes rhythmically assemble and disassemble during the *in vitro* KaiABC oscillation with the KaiB^{R74C} and KaiB^{R22C} mutants. This supplementary figure is the raw data for **Figure 2-4** (panels B and D) and the procedure is the same as for **Figure 2-4A** except for the use of the KaiB mutants as follows: **(A)** KaiB^{R74C} (short period), **(B)** KaiB^{R22C} (long period).

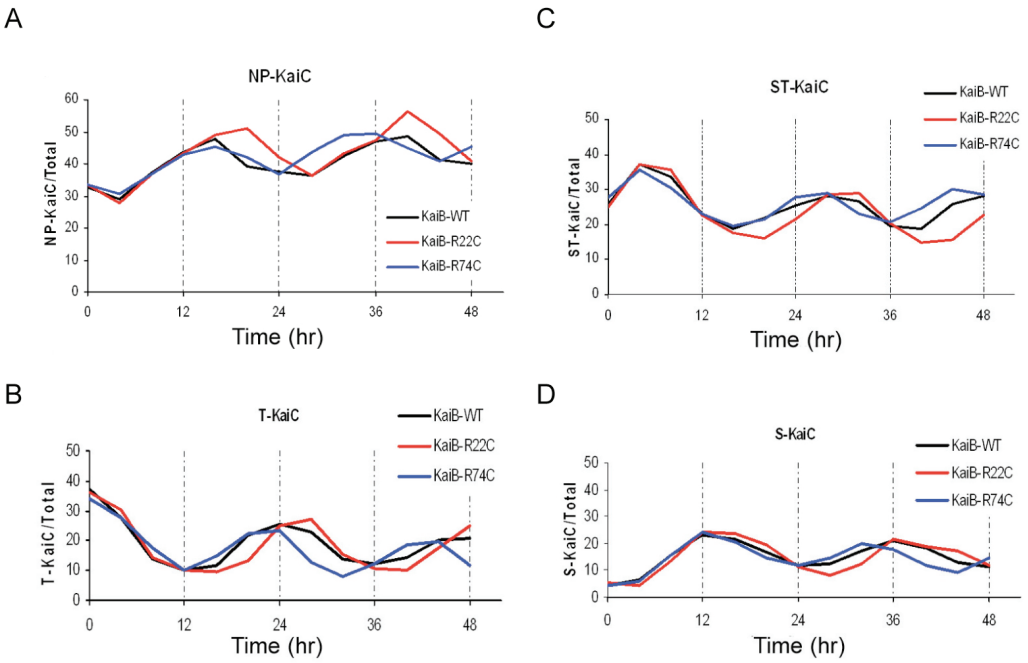

Figure S2-4. SDS-PAGE analyses of each KaiC phosphoform for all three KaiB mutant variants. Detailed analysis of each KaiC phosphoform as in **Figure S2-1** shows that the KaiB mutant variants change the period of the rhythms of : (**A**) hypophosphorylated KaiC (NP-KaiC), **(B)** KaiC phosphorylated on T432 (T-KaiC), **(C)** doubly-phosphorylated KaiC on both S431 and T432 (ST-KaiC), and **(D)** KaiC phosphorylated on S431 alone (S-KaiC).

Mathematical Model Description

KaiC hexamer concentrations are labeled by net population phosphorylation levels, C_i, where i = 0, N. We neglect specific site-dependent modeling (S431 and T432) and treat the system phenomenologically. The model reactions are as follows:

Phosphorylation and de-phosphorylation:

Auto-phosphorylation/dephosphorylation : $C_i \leftrightarrow C_{i+1}$

KaiA•KaiC phosphorylation//dephosphorylation: $A \bullet C_i \leftrightarrow A \bullet C_{i+1}$

KaiB•KaiC, KaiA•KaiB•KaiC phosphorylation/dephosphorylation: $B \bullet C_{i+1} \leftrightarrow B \bullet C_i$,

$A \bullet B \bullet C_{i+1} \leftrightarrow A \bullet B \bullet C_i$

Hexamer Reactions:

KaiA association (and dissociation): $A + C_i \leftrightarrow A\bullet C_i$

$A + B\bullet C_i \leftrightarrow A\bullet B\bullet C_i$

KaiB association above threshold phosphorylation: $B + C_i \leftrightarrow B\bullet C_i \quad (i > N)$

Dissociation of KaiA•KaiB•KaiC complexes: $B\bullet A\bullet C_0 \rightarrow B + A + C_0$

$B\bullet C_0 \rightarrow B + C_0$

Monomer Exchange (i + j = k+m): $C_i + C_j \leftrightarrow C_k + C_m$

$A\bullet C_i + A\bullet C_j \leftrightarrow A\bullet C_k + A\bullet C_m$

$A\bullet B\bullet C_i + A\bullet B\bullet C_j \leftrightarrow A\bullet B\bullet C_k + A\bullet B\bullet C_m$

PTO Differential Equations: (i =1,N-1)

<u>KaiC hexamers alone ($k_2 >> k_1$)</u>

1.1 $dC_0/dt = -k_1 C_0 + k_2 C_1 - k_A A^*C_0 + k_{-A} (AC_0) + k_d (ABC_0) + k_d (BC_0)$

1.2 $dC_i/dt = k_1 (C_{i-1} - C_i) + k_2 (C_{i+1} - C_i) - k_A A^*C_i + k_{-A} (AC_i)$

1.3 $dC_N/dt = k_1 C_{N-1} - k_2 C_N - k_B B^*C_N + k_{-B} (BC_N) - k_A A^*C_N + k_{-A} (AC_N)$

<u>KaiA-KaiC hexamers ($k_3 >> k_4$)</u>

1.4 $d(AC_0)/dt = -k_3 (AC_0) + k_4 (AC_1) + k_A A^*C_0 - k_{-A} (AC_0)$

1.5 $d(AC_i)/dt = k_3 ((AC_{i-1}) - (AC_i)) + k_4 ((AC_{i+1}) - (AC_i)) + k_A A^*C_i - k_{-A} (AC_i)$

1.6 $d(AC_N)/dt = k_3 (AC_{N-1}) - k_4 (AC_N) + k_A A^*C_N - k_{-A} (AC_N)$

KaiB-KaiC ($k_2 >> k_1$)

1.7 $d(BC_N)/dt = k_B B^*C_N - k_{-B} (BC_N) - k_2 (BC_N) + k_1 (BC_{N-1}) - k_A A^*(BC_N)$

1.8 $d(BC_i)/dt = k_1 ((BC_{i-1}) - (BC_i)) + k_2 ((BC_{i+1}) - (BC_i)) - k_A A^*(BC_i)$

1.9 $d(BC_0)/dt = -k_1 (BC_0) + k_2 (BC_1) - k_d (BC_0) - k_A A^*(BC_0)$

KaiA-KaiB-KaiC ($k_2 >> k_1$)

1.10 $d(ABC_N)/dt = k_A A^*(BC_N) - k_2 (ABC_N) + k_1 (ABC_{N-1})$

1.11 $d(ABC_i)/dt = k_1 ((ABC_{i-1}) - (ABC_i)) + k_2 ((ABC_{i+1}) - (ABC_i)) + k_A A^*(BC_i)$

1.12 $d(ABC_0)/dt = -k_1 (ABC_0) + k_2 (ABC_1) - k_d (ABC_0) + k_A A^*(BC_0)$

KaiA ($k_A >> k_{-A}$)

1.13 $dA/dt = - k_A A^*(\Sigma C_i) - k_A A^*(\Sigma (BC_i)) + k_{-A} \Sigma (AC_i) + k_d (ABC_0)$

KaiB ($k_B >> k_{-B}$)

1.14 $dB/dt = -k_B B^*C_N + k_{-B} (BC_N) + k_d ((ABC_0) + (BC_0))$

Monomer Exchange

Monomer exchange is approximated phenomenologically by the reaction $C_i + C_j \rightarrow C_{i+1} + C_{j-1}$ ($j > i$) that acts to equalize the population concentration levels of phosphorylation by transfer of phosphates from hexamers with more phosphates (j) to hexamers with lower numbers of phosphates (i), $j > i$. Letting $x_k = C_k$, (AC_k), (BC_k), or (ABC_k):

1.15 $dx_i/dt = dx_i/dt - k_e x_i^* x_j \quad (j = i+1, N)$

$dx_j/dt = dx_j/dt - k_e x_i^* x_j$

$$dx_{i+1}/dt = dx_{i+1}/dt + k_e\, x_i * x_j$$

$$dx_{j-1}/dt = dx_{j-1}/dt + k_e\, x_i * x_j$$

PTO Initial Conditions and rates

All the differential equations are scaled to the initial KaiC concentration, C_0 (t=0) so that the fraction of each is followed with respect to time.

Simplified KaiA Sequesteration Model with Monomer exchange. The simplified model neglects the auto-phosphorylation/dephosphorylation reactions of KaiC (1.1 -1.3) and corresponding KaiB•KaiC complex formation reactions (1.7-1.9) and instead considers the approximate complex formation and cyclic phosphorylation reaction sequence:

1.16 $C_0 \rightarrow AC_0 \rightarrow AC_1 ... \rightarrow AC_N \rightarrow ABC_N \rightarrow ABC_{N-1} \rightarrow ... \rightarrow ABC_0 \rightarrow A+B+C_0.$

Monomer exchange occurs among A•C complexes (phosphorylation phase) and among A•B•C complexes (dephosphorylation phase) but not between A•C complexes and A•B•C complexes. The dynamics of this model are very similar to the full model in most simulations and provide a simpler interpretation of the resulting dynamics. However, the full model is required to adequately represent the time dependence of complex abundances reported previously (Kageyama et al., 2006; Mori et al., 2007). For the text figures we have used the simplified model.

*Parameters for **Figure 2-5***

	phosphorylation (hr^{-1})	dephosphorylation(hr^{-1})
+ KaiA	$k_3 = 0.6$	$k_4 = 0.0$
+ KaiB	$k_1 = 0.0$	$k_2 = 0.6$

KaiA Association $k_A = 5.0$ (μM^{-1} hr^{-1})
KaiA Dissociation $k_{-A} = 0.0$ (hr^{-1})

KaiB Threshold N = 6

KaiB Association $k_B = 1.0$ (μM^{-1} hr^{-1})
KaiB Dissociation $k_{-B} = 1.0$ (hr^{-1})

KaiA-KaiB-KaiC Dissociation: $k_d = 1.0$ (hr^{-1})

	phosphorylation phase	dephosphorylation phase
Monomer Exchange (hr^{-1})	k_{e1} =2.5	k_{e2} = 5.0

***Figure 2-5C**:* As above except k_{-B}/k_d =1.0; k_{+B} = 0.25, 0.5, 1.0, 2.5, 5.0 (different traces).

Simulations

Code for implementing the model was written in Fortran (G77, Free Software Foundation) using a 4th Order Runge-Kutta algorithm for ODE solutions.

APPENDIX B

SUPPORTING INFORMATION TO CHAPTER III [#]

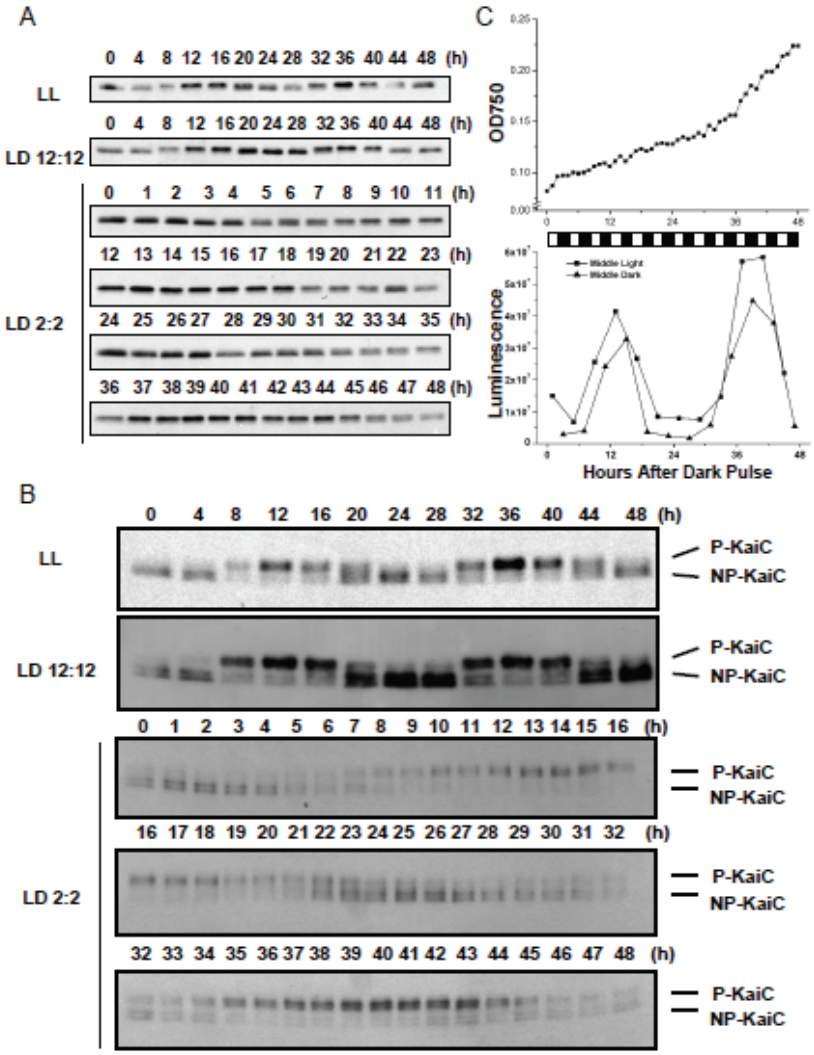

Figure S3-1. Representative immunoblots for KaiC abundance (A) and KaiC phosphorylation (B) in LL, LD12:12, and LD2:2. Densitometry of these blots is shown in **Figure 3-1**. **C**. Persistence of 24-hr

[#] Chapter III is directly derived from the published paper: Qin X, Byrne M, Xu Y, Mori T, Johnson CH (2010) Coupling of a core post-translational pacemaker to a slave transcription/translation feedback loop in a circadian system. *PLoS Biol* 8: e1000394. doi:10.1371/journal.pbio.1000394. **Appendix B** is the published supporting information.

circadian rhythm of luminescence in LD2:2 conditions. Upper panel, growth curve for cells in LD2:2. Lower panel, samples taken from the middle of the light interval or the middle of the dark interval in LD2:2 show robust luminescence rhythms. Before release into LD2:2 conditions, cells were given two LD12:12 cycles. To measure the luminescence of cultures from the batch flasks under LD2:2 conditions, 1 ml of cell culture was manually removed in either the middle of the light portion of LD2:2 or the middle of the dark portion of LD2:2 and transferred to a 20-ml vial with a tube containing *n*-decanal to measure the luciferase activity using a luminometer (Femtomaster FB12, Zylux Corporation, Knoxville, USA). The maximum luminescence level at each timepoint was plotted for both the middle light (solid square) and the middle dark (solid triangle) collection times.

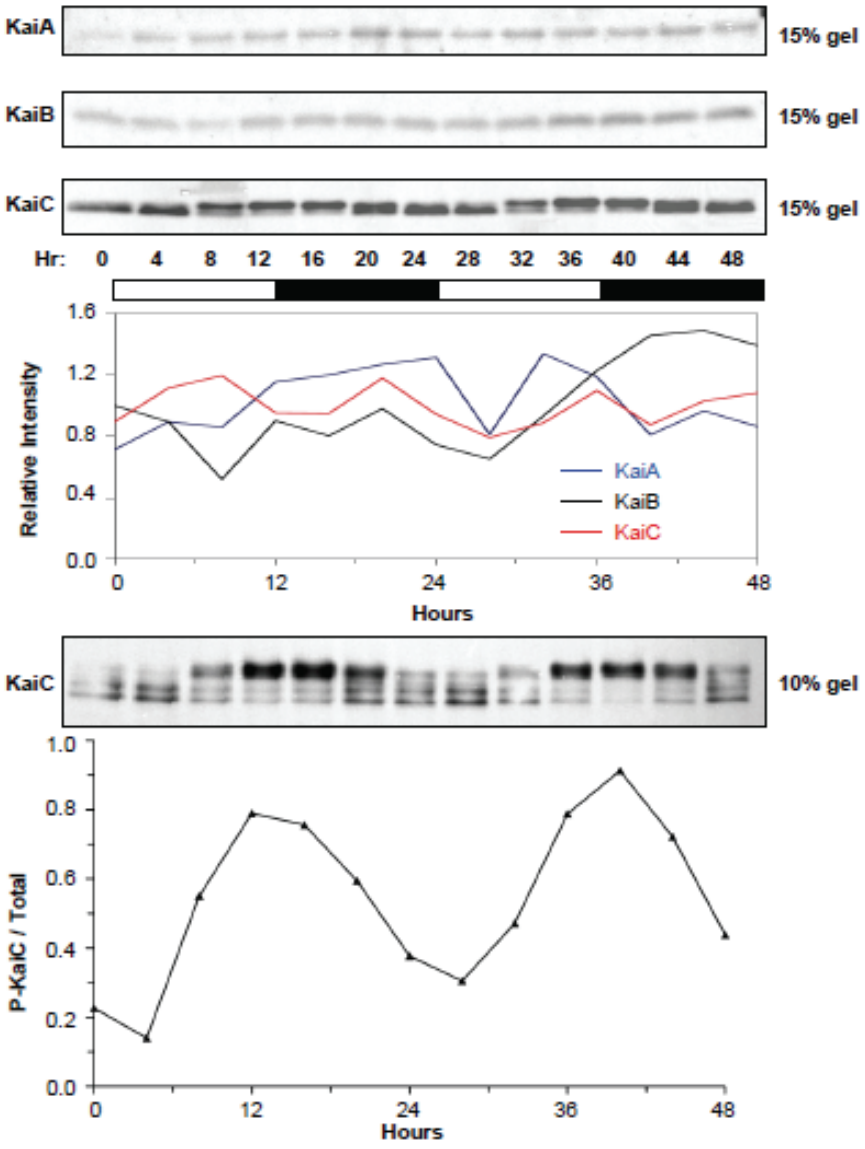

Figure S3-2. Absence of clear rhythmicity of abundances of KaiA, KaiB, and KaiC in the presence of

a robust KaiC phosphorylation rhythm. A representative example is shown of an experiment where the phosphorylation rhythm was robust, while the abundances of the Kai proteins were not clearly rhythmic. Abundance data was collected from immunoblots run on 15% SDS-PAGE gels (to obtain a single protein band), whereas KaiC phosphorylation was determined on 10% SDS-PAGE gels (to separate the various KaiC phosphoforms)

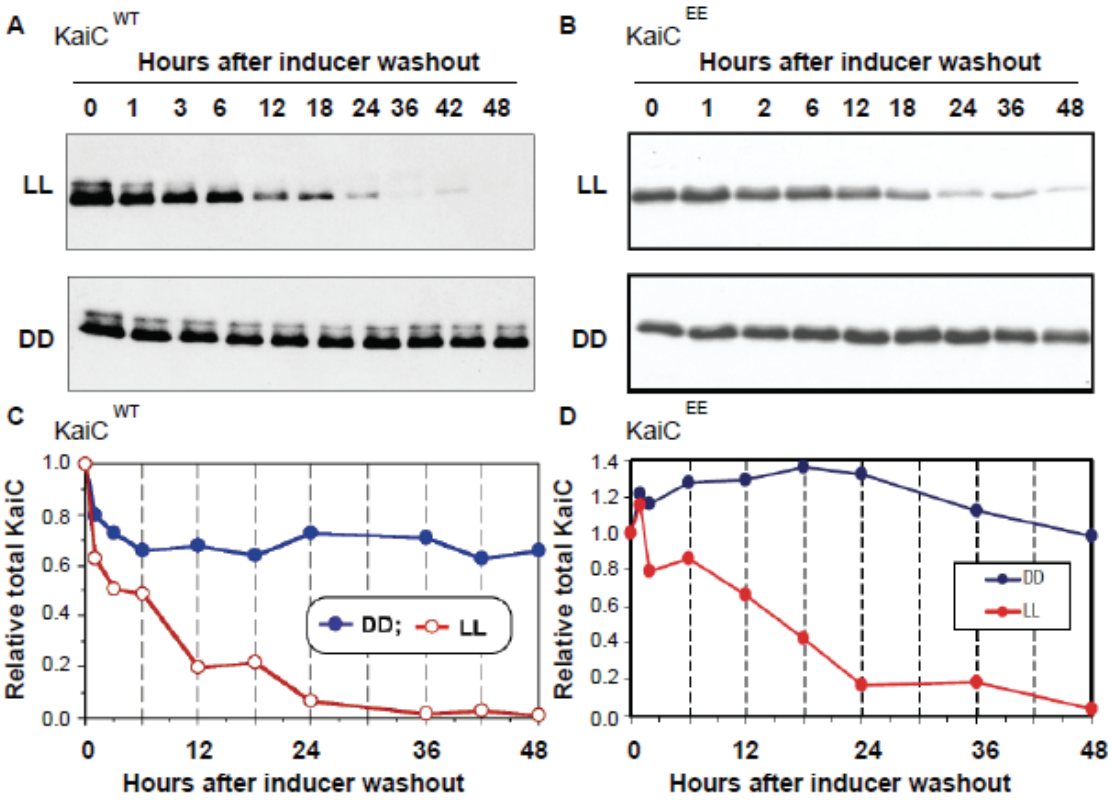

Figure S3-3. Degradation of KaiC protein is dependent upon light. A. $KaiC^{WT}$ expression was induced in the $KaiC^{OX}$ strain by 100 μM IPTG for 6 h, and then the inducer was washed out and the cells were placed in either LL or DD. Samples were collected at the times indicated and processed for SDS-PAGE and immunoblotting as described previously for this type of degradation assay (Xu et al., 2003). **B.** $KaiC^{EE}$ expression was examined as in panel A. **C&D**. Quantification of the immunoblot data in panel A&B by Image J, which shows that $KaiC^{WT}$ and $KaiC^{EE}$ proteins degradation in the cells proceeds in LL, but is strongly inhibited in DD.

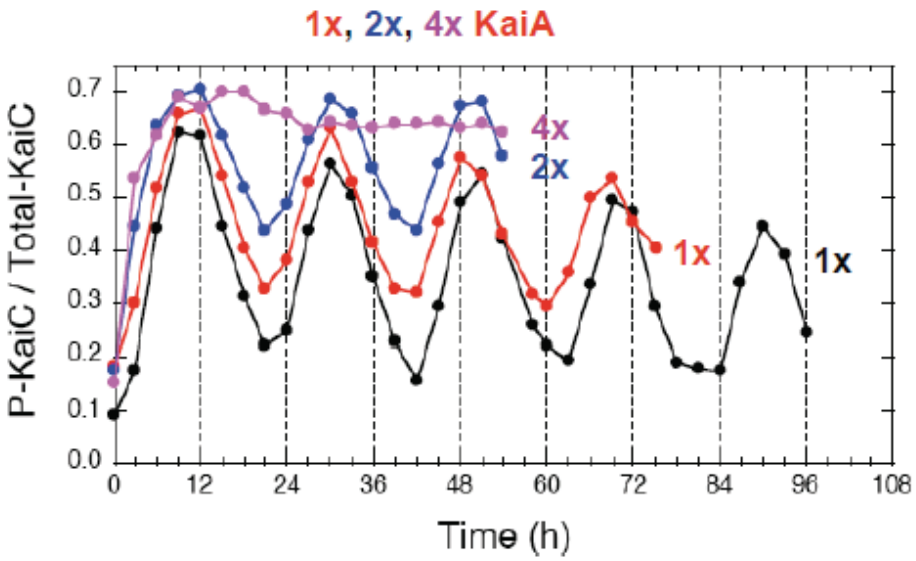

Figure S3-4. Elevated levels of KaiA in the *in vitro* reaction suppress the amplitude of the *in vitro* phosphorylation rhythm. 1X KaiA = 50 ng/µl KaiA (duplicate reactions shown in red and black)

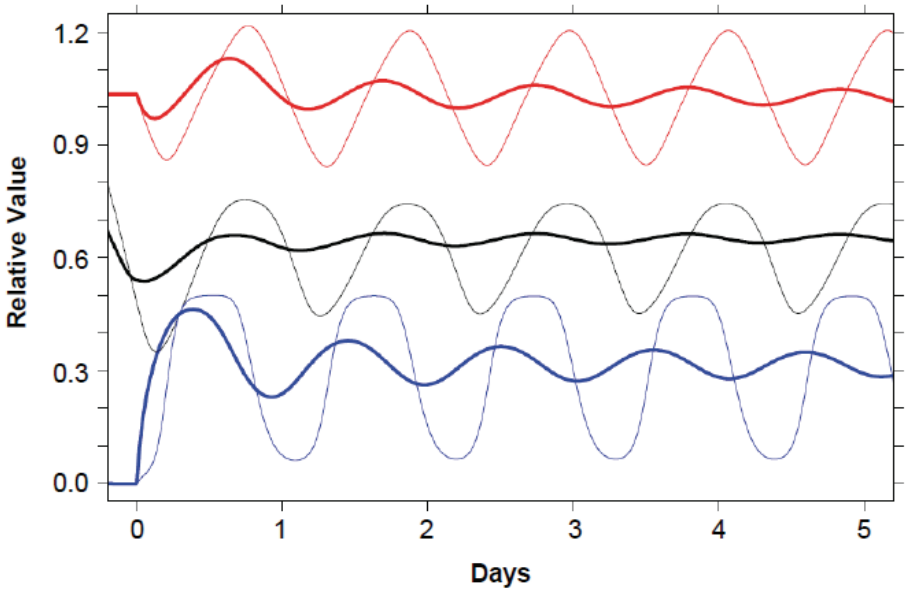

Figure S3-5. A simulated low amplitude KaiC phosphorylation rhythm (thick black trace) can be amplified into a larger amplitude rhythm in *kaiBC* mRNA (thick blue) and Kai C protein (thick red) abundance. The thin lines indicate the control simulation for the TTFL (**Fig 3-5B** in **Chapter III**).

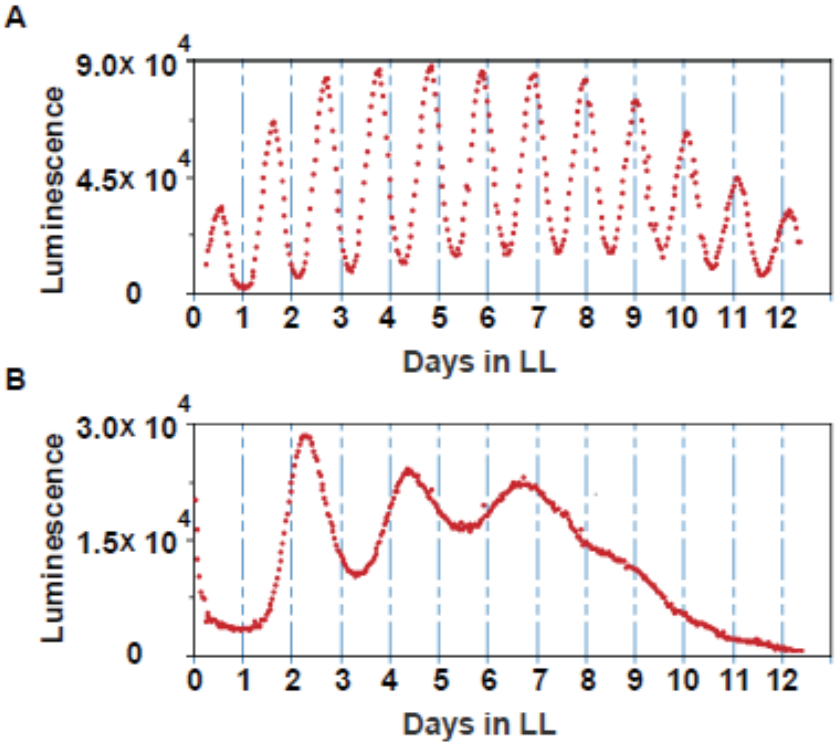

Figure S3-6. Another example of the rhythms expressed by KaiC^{EE} vs. KaiC^{WT} strains at 30°C that illustrates the obvious damping of the KaiC^{EE} strain.

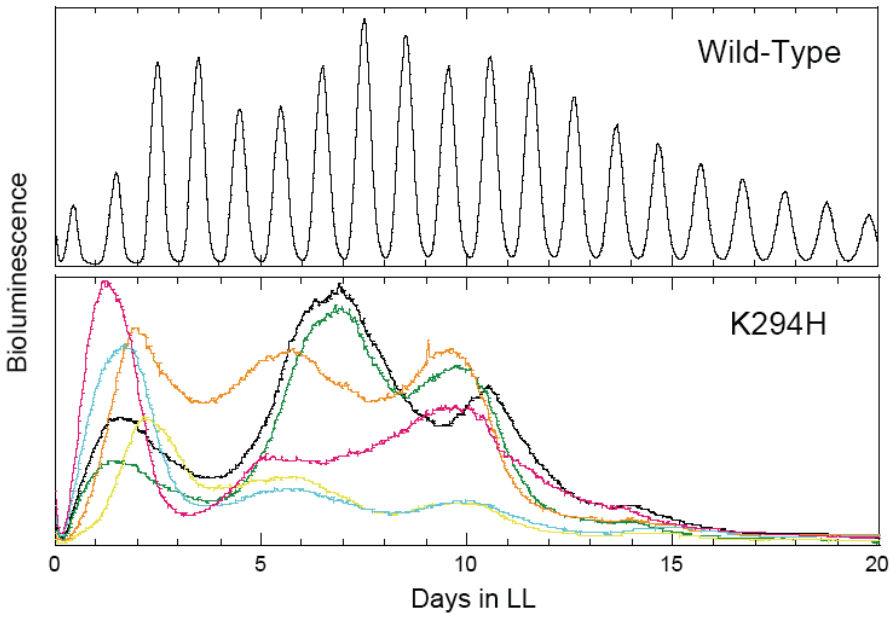

Figure S3-7. Strains expressing KaiC^{K294H} are unstable with respect to phase, amplitude and period. KaiC^{K294H} was constructed and expressed as in (Kitayama et al., 2008)

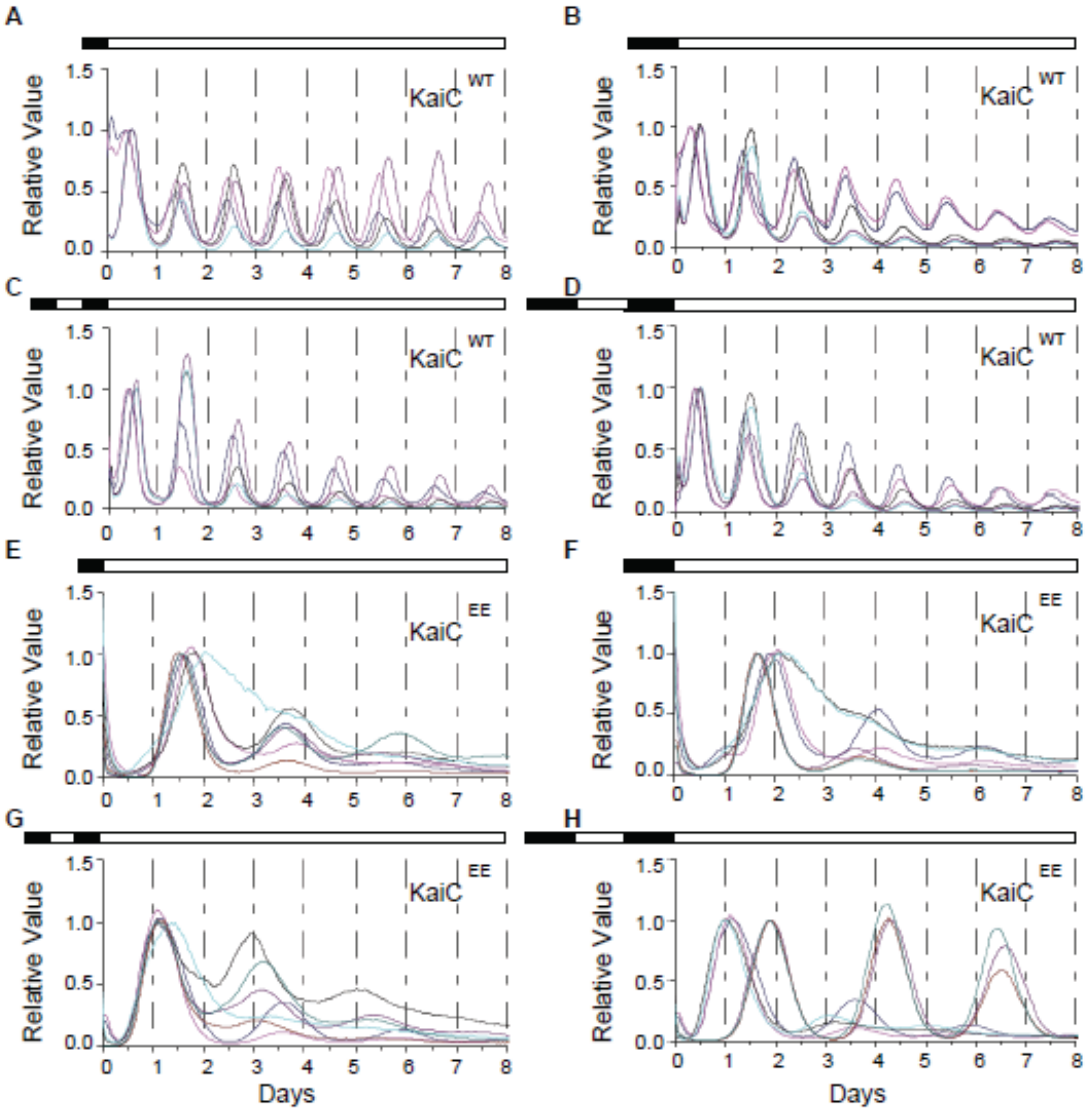

Figure S3-8. Raw data for Fig. 3-4 ("Prior entrainment conditions determine the rate of damping in cells expressing KaiC^{EE}"). Cells were in LL at 30°C before and after the following entrainment conditions: **(A & E)** One 12 h dark pulse; **(B & F)** One 24 h dark pulse; **(C & G)** Two 12 h dark pulses separated by one 12 h light pulse (i.e., 1.5 cycles of LD12:12); and **(D & H)** Two 24 h dark pulses separated by one 24 h light pulse (i.e., 1.5 cycles of LD24:24). Each differently colored trace is from an independent measurement; n = 5 for each of the KaiC^{WT} sample sets and n = 7 for each of the KaiC^{EE} sample sets.

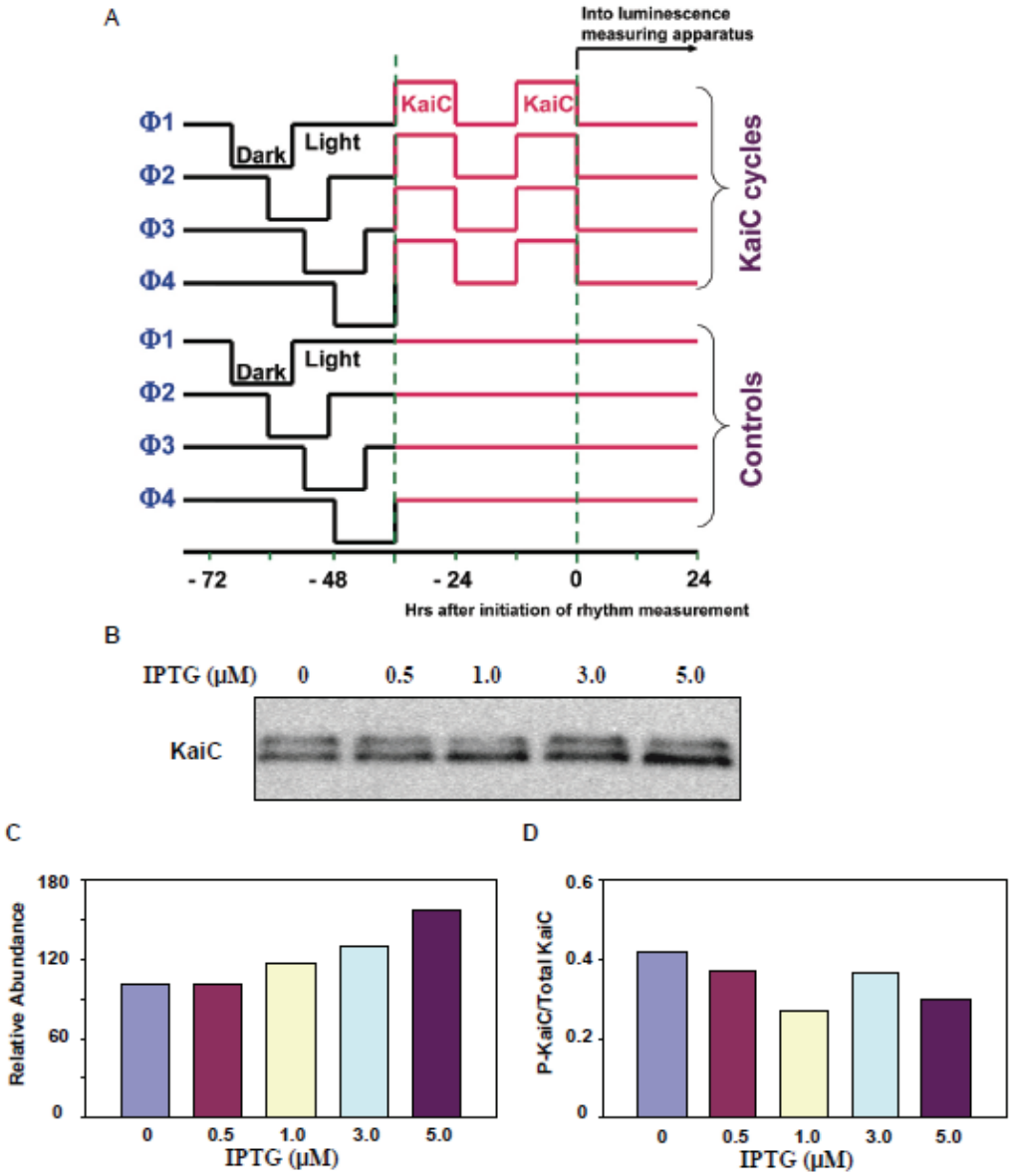

Figure S3-9. A. Protocol of the phase locking experiment depicted in **Fig. 3-6B**. **B.** Induction of new KaiC synthesis in strain KaiC^{OX} by various concentrations of IPTG leads to changes in KaiC phosphorylation status and abundance. **C.** densitometry of total KaiC abundance in the blot depicted in panel B. **D.** ratio of hyper-phosphorylated to total KaiC in the blot depicted in panel B. Data were analyzed by Image J.

Mathematical Model Description

I. Post-Translational Oscillator/Constant Darkness (PTO/DD) Model

The PTO model is described in the mathematical model in **Appendix A**.

II. *In Vivo* Model (LL)

The *in vivo* model consists of the PTO and a generic Transcription-Translation Feedback Loop (TTFL) in which KaiC negatively represses its own production as indicated experimentally by overexpression of KaiC and its effect on *kaiBC* promoter activity. The precise form of this repression in terms of the various states of KaiC (C_i, BC_i, AC_i, ABC_i) however, is not derivable from existing experimental data. The mRNA abundance is modeled as follows (a TTFL based on Goldbeter 1995 PER model (Goldbeter, 1995)) and includes a nonlinear repression term and a linear degradation rate:

1.17 * $dC_{mRNA}/dt = k_{+,mRNA}\ 1/(1 +(f(x)/K)^n)\ - k\text{-},_{mRNA}\, C_{mRNA}$

where n is the coefficient of cooperativity for repression, K is the dissociation constant and x represents hexamer states C_i, (AC_i), (BC_i), or (ABC_i). The function f(x) is assumed to be some linear combination of these states: $f(x) = S\ \{a_i\ C_i + b_i\ (BC_i) + c_i\,(ABC_i) + d_i\ (AC_i)\}$ parameterized by constant coefficients. An assumption consistent with current data is that KaiB•KaiC and KaiA•KaiB•KaiC (BC_i and ABC_i) complexes suppress promoter activity. The relative phase of mRNA, protein, and phosphorylation in LL is determined by the form(s) of KaiC that suppress(es) transcription. Simulations indicate that phase relationships of mRNA, protein, and phosphorylation consistent with previously published studies are obtained when hyper-phosphorylated KaiC states (including the KaiB•KaiC and KaiA•KaiB•KaiC complexes) are primarily responsible for mRNA suppression.

In LL the proteins $KaiC_0$ and KaiB are translated from mRNA and are also degraded so that Equations 1.1 and 1.14 are modified to include

1.18 $dC0/dt = ...+ k_{trans}\, C_{mRNA} - \ k_{deg}\, C0$
1.19 $dB/dt = ...+ k_{trans}\, C_{mRNA} - \ k_{deg}\, B$

The other complexes are likewise assumed to be degraded (which might be complex-dependent and phosphorylation-dependent). For simplicity we will assume constant and equal degradation rates for all forms of KaiC ($y = AC_i, ABC_i$):

1.20 $dy/dt = ... -k_{deg}\, y$

Since KaiA abundance shows little variation in abundance in LL we introduce an *ad hoc* production term for KaiA in the simplified model (modeled as if $KaiACi \rightarrow KaiA + KaiC_i$ and the $KaiC_i$ is degraded; this is not necessary in the full DD model as C_i states are included).

---

* The numeration systems of the equations in this appendix are following that in **Appendix A**

1.21 $dA/dt = ... + k_{deg}\, y$

III. KaiC^{EE} Model

The mutant protein KaiC^{EE} is a phosphomimetic for a constitutively hyperphosphorylated KaiC. Since there are no intermediate phosphorylation states nor a functional PTO the model simplifies considerably:

$$dC_{EE}/dt = k_{-B}\,(BC^{EE}) - k_B\, B{*}C^{EE} + k_{trans}\, C^{EE}{}_{,mRNA} - k_{deg}\, C^{EE}$$
$$dB/dt = -k_B\, B{*}C^{EE} + k_{-B}\,(BC^{EE}) + k_{trans}\, C^{EE}{}_{,mRNA} - k_{deg}\, B$$
$$dC^{EE}{}_{,mRNA}/dt = k_{+,mRNA}\, 1/(1 + (BC^{EE}/K)^n) - k_{-,mRNA}\, C^{EE}{}_{,mRNA}$$
$$d(BC^{EE})/dt = k_B\, B{*}C^{EE} - k_{-B}\,(BC^{EE}) - k_{deg}\,(BC^{EE})$$

Here the repression function f(x) is simply $B{\bullet}C^{EE}$ consistent with the simulation results for the wild type system simulations. We rescale as before to KaiC^{EE}(t=0) with all other variables relative to this scale and $B(0) = C^{EE}(0)$. This model does not show sustained oscillations (n = 4) but can produce long period decaying oscillations to a steady-state.

IV. Figure Rates and Parameters

Figures 3-5 (A, C and E) use the PTO parameters given below.
Figures 3-3C, **3-5** (B, D and F) and **Fig 3-6** use the PTO and TTFL parameters given below.

PTO/DD Simplified Model

	phosphorylation (hr^{-1})	dephosphorylation(hr^{-1})
+ KaiA	$k_3 = 0.6$	$k_4 = 0.0$
+ KaiB	$k_1 = 0.0$	$k_2 = 0.6$

KaiA Association $k_A = 5.0$ (M^{-1} hr^{-1})
KaiA Dissociation $k_{-A} = 0.0$ (hr^{-1})

KaiB Threshold N = 6

KaiB Association $k_B = 0.5$ (M^{-1} hr^{-1})
KaiB Dissociation $k_{-B} = 0.0$ (hr^{-1})

KaiA-KaiB-KaiC Dissociation: $k_d = 1.0$ (hr^{-1})

	phosphorylation	dephosphorylation
Monomer Exchange (hr^{-1})	k_{e1} =2.5	k_{e2} = 5.0

TTFL (rates are hr^{-1})

Concentrations scaled to initial $KaiC_0$ (t=0) concentration. $C_{mRNA}(t=0) = 1.0$

mRNA synthesis rate: $k_{+,mRNA} = 0.5$
mRNA degradation rate: $k_{-,mRNA} = 1.0$
$KaiC_0$ and KaiB synthesis rate: $k_{trans}= 0.5$,
KaiC/KaiA·KaiC/ KaiA·KaiB·KaiC degradation rate: $k_{deg} = 0.05$

Suppression: $dC_{mRNA}/dt = k_{+,mRNA}\ 1/(1 +(f(x)/K)^n) - k_{-,mRNA}\ C_{mRNA}$
K = 1
n = 4
$f(x) = \Sigma(ABC)_i$ (KaiA·KaiB·KaiC complexes suppress transcription)

Noise simulations (**Fig 3-5C&D**)

Noise was explicitly introduced by modifying the $KaiC_0$ concentration using Eqn (1.1) to include a term with production or degradation specified by a uniform random number on [-1,1] and suitably re-scaled.

Phase simulations (**Fig 3-5 D&E**, **Fig 3-6A**)

$KaiC_0$ concentration was varied by adding a pure oscillatory term to Eqn (1.1), $0.2\omega\cos(\omega t + \varphi)$ with an angular frequency of $\omega = (2\pi/24)\ hr^{-1}$, where φ is the phase.

KaiC-EE Simulation Rates: **Fig 3-3D**

TTFL (rates are hr^{-1})
TTFL Suppression: $dC_{mRNA}/dt = k_{+,mRNA}\ 1/(1 +(f(x)/K)^n)\ - k_{-,mRNA}\ C_{mRNA}$
K = 1
n = 4
$f(x) = BC_{EE}$ (KaiB·$KaiC^{EE}$ complexes suppress transcription)

BC_{EE} association ($\mu M^{-1}\ hr^{-1}$): 0.02
BC_{EE} dissociation (hr^{-1}): 0.01

Parameter Set #1 (black trace)
$C_{mRNA}(t=0) = 1.0$
B/C_{EE} (t=0)= 1.5

mRNA synthesis rate: $k_{+,mRNA} = 0.5$
mRNA degradation rate: $k_{-,mRNA} = 0.01$
$KaiC_0$ and KaiB synthesis rate: $k_{trans} = 0.2$,
KaiC/KaiA·KaiC/ KaiA·KaiB·KaiC degradation rate: $k_{deg} = 0.05$

Parameter Set #2 (red trace)
$C_{mRNA}(t=0) = 1.0$
$B/C_{EE}\ (t=0) = 1.0$

mRNA synthesis rate: $k_{+,mRNA} = 0.1$
mRNA degradation rate: $k_{-,mRNA} = 0.05$
$KaiC_0$ and KaiB synthesis rate: $k_{trans} = 0.2$,
KaiC/KaiA·KaiC/ KaiA·KaiB·KaiC degradation rate: $k_{deg} = 0.05$

APPENDIX C

THE CIRCADIAN PHENOTYPES OF *kaiA*, *kaiB*, AND *kaiC* cys-MUTANTS IN *S. elongatus*

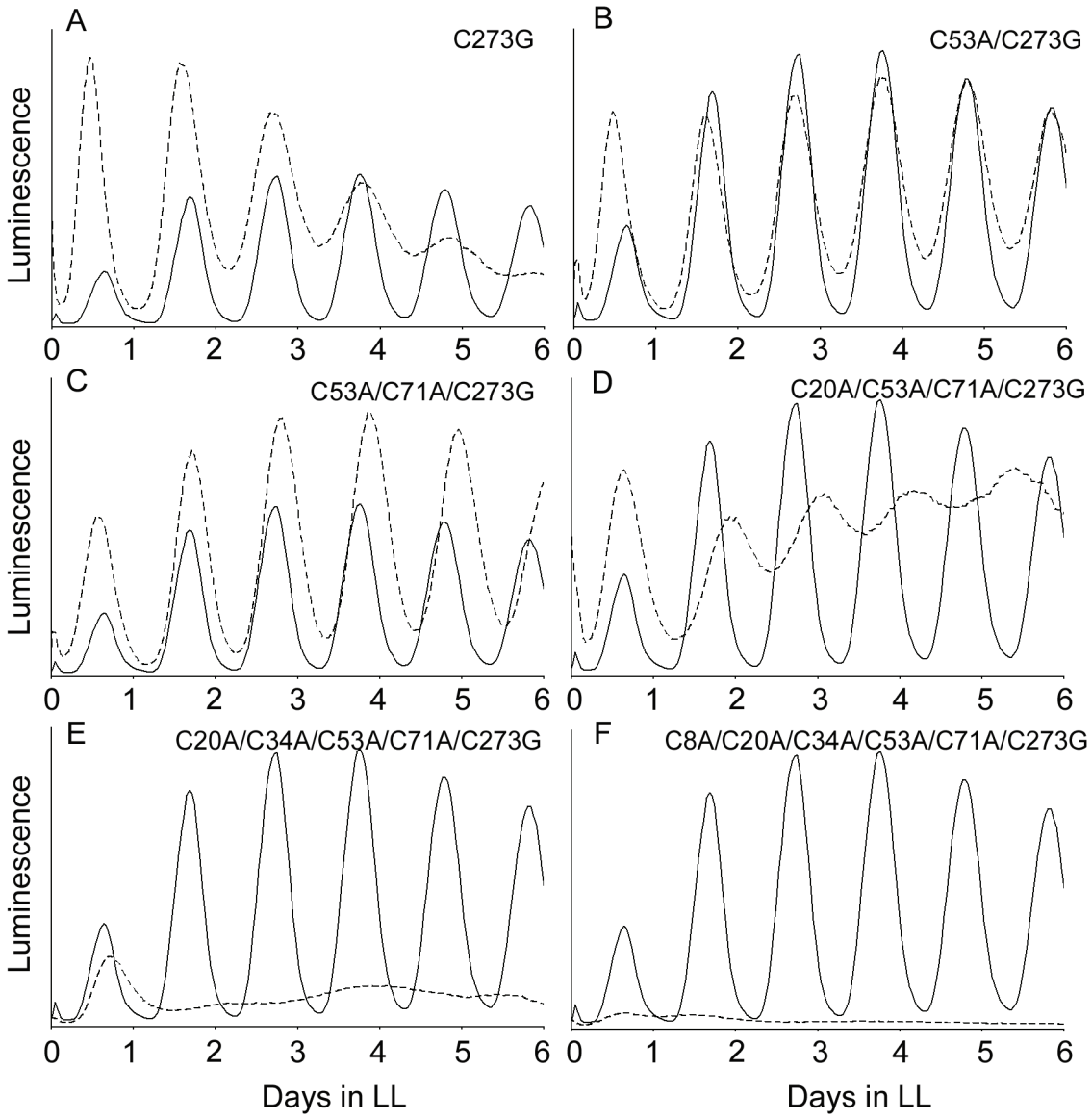

Figure S5-1. Phenotypes of different cys-*kaiA* mutant cyanobacterial strains. KaiA from *S. elongatus* has 6 intrinsic cysteines: C8, C20, C34, C53, C71, and C273. In each panel, a representative curve (dashed line) shows a cyanobacterial strain carrying the mutated *kaiA* allele (mutation is indicated in each panel). The solid line represents a wild-type strain. Panel F shows the strain with a cys-null *kaiA* allele.

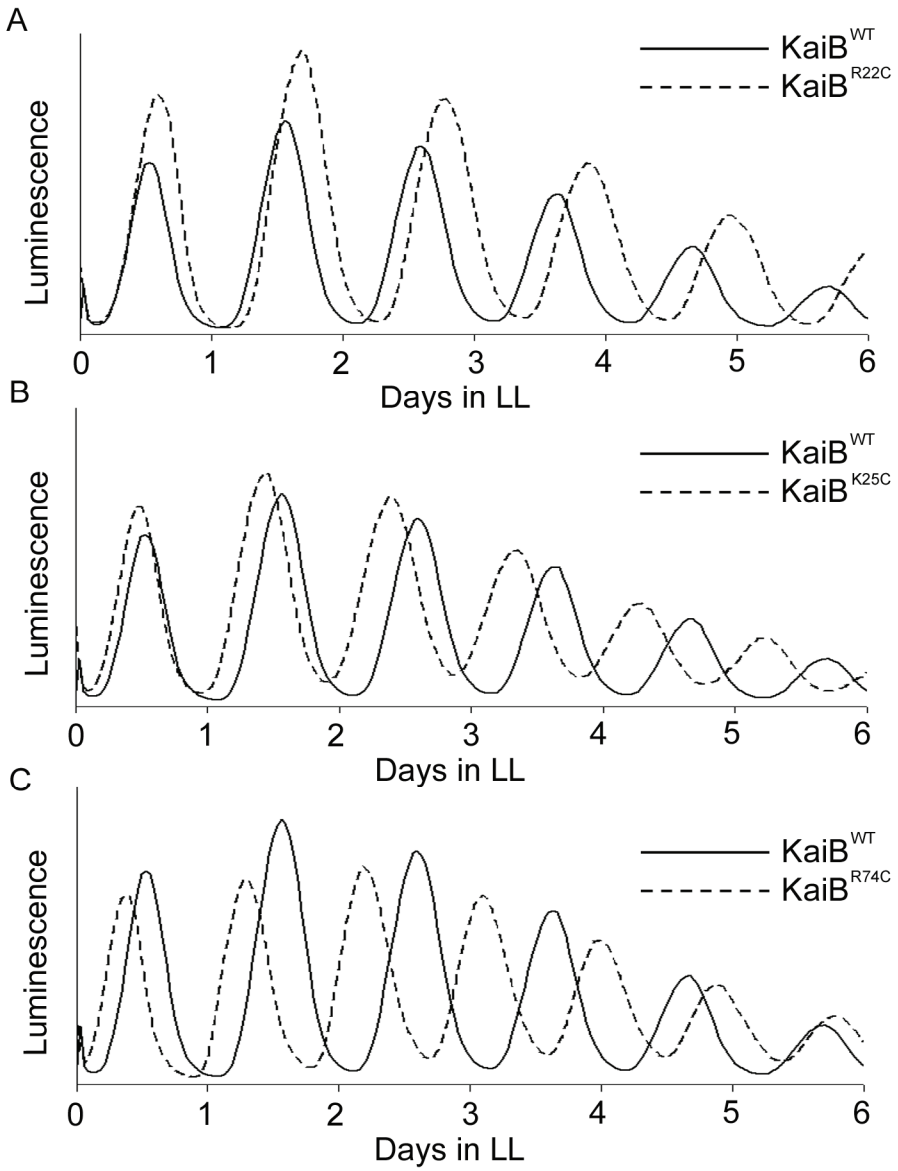

Figure S5-2. Phenotypes of different cys-*kaiB* mutant cyanobacterial strains. KaiB from S. elongatus does not contain cysteine residues, therefore the wild-type *kaiB* is a cys-null allele. Three single-cys-KaiB proteins were constructed and the cyanobacterial strains expressing these mutant KaiB proteins were shown with representatives in panels **(A)** $KaiB^{R22C}$, **(B)** $KaiB^{K25C}$, and **(C)** $KaiB^{R74C}$. In each panel, the trace of the solid line represents the WT.

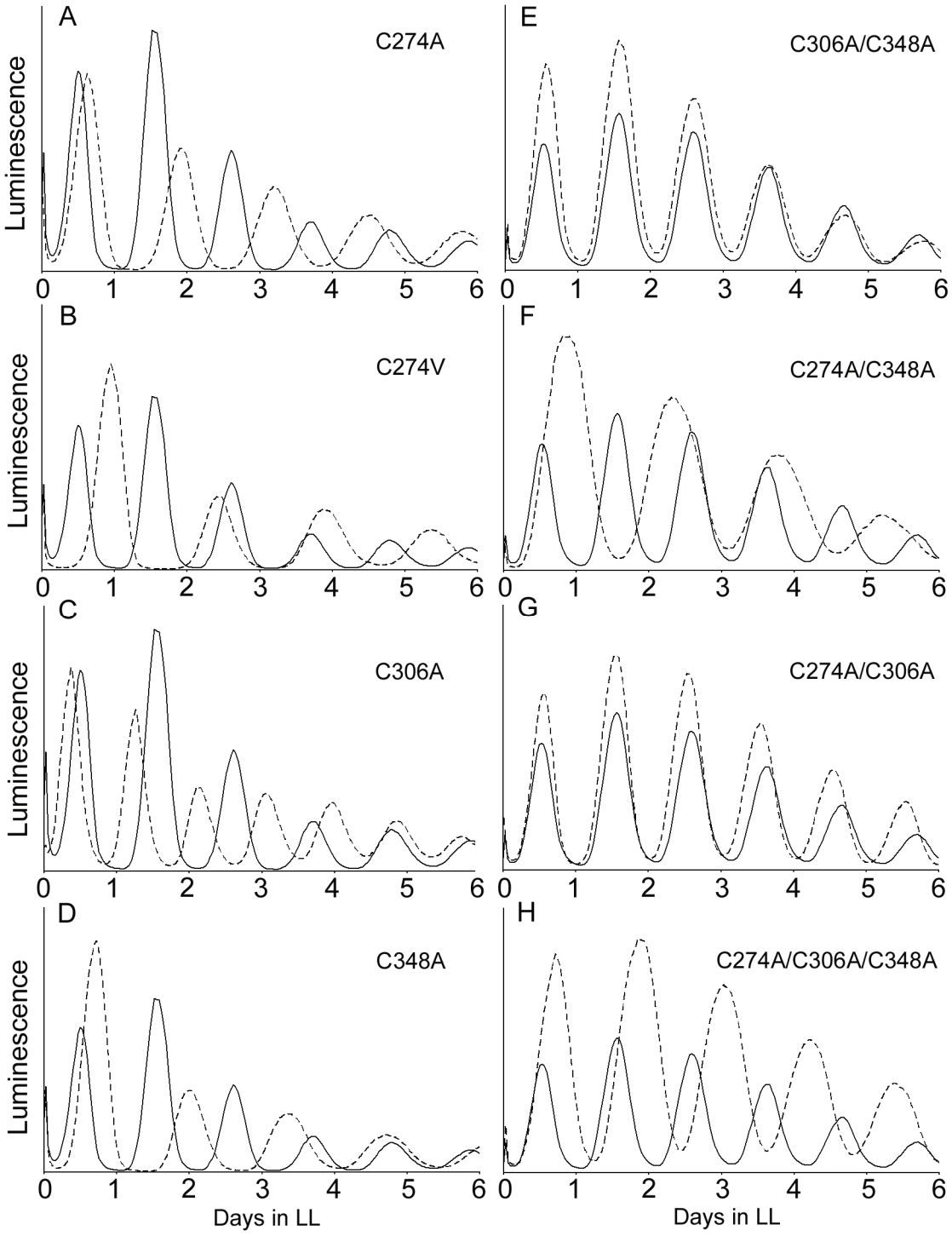

Figure S5-3. Phenotypes of different cys-*kaiC* mutant cyanobacterial strains. KaiC from *S. elongatus* has 3 intrinsic cysteines: C274, C306, and C348. In each panel, a representative curve (dashed line) shows a cyanobacterial strain carrying the mutated *kaiC* allele (the single, or double, or triple cysteine mutation is indicated in each panel). In each panel, the solid line represents a wild-type strain. Panel H shows the strain with a cys-null *kaiC* allele.

REFERENCES

Abrahams JP, Leslie AGW, Lutter R, Walker JE (1994) Structure at 2.8 Å resolution of F1 ATPase from bovine heart mitochondria. *Nature* 370: 621-628

Angermayr SA, Hellingwerf KJ, Lindblad P, de Mattos MJ (2009) Energy biotechnology with cyanobacteria. *Curr Opin Biotechnol* 20: 257-263.

Akiyama S, Nohara A, Ito K, Maéda Y (2008) Assembly and disassembly dynamics of the cyanobacterial periodosome. *Mol Cell* 29: 703-716.

Bova MP, Huang Q, Ding L, Horwitz J (2002) Subunit exchange, conformational stability, and chaperone-like function of the small heat shock protein 16.5 from *Methanococcus jannaschii*. *J Biol Chem* 277: 38468-38475.

Bustos SA, Golden SS (1991) Expression of the psbDII gene in Synechococcus sp. strain PCC7942 requires sequences downstream of the transcription start site. *J Bacteriol* 173: 7525-7533.

Chen TH, Chen TL, Hung LM, Huang TC (1991) Circadian rhythm in amino acid uptake by *Synechococcus* RF-1. *Plant Physiol* 97: 55-59.

Cheng P, Yang Y, Gardner KH, Liu Y (2002) PAS domain-mediated WC-1/WC-2 interaction is essential for maintaining the steady-state level of WC-1 and the function of both proteins in circadian clock and light responses of *Neurospora*. *Mol Cell Biol* 22: 517-524.

Clegg RM (1995) Fluorescence resonance energy transfer. *Curr Opin Biotechnol* 6: 103–110.

Clodong S, Dühring U, Kronk L, Wilde A, Axmann I, Herzel H, Kollmann M (2007) Functioning and robustness of a bacterial circadian clock. *Mol Syst Biol* 3: 90.

Dibner C, Sage D, Unser M, Bauer C, d'Eysmond T, Naef F, Schibler U (2009) Circadian gene expression is resilient to large fluctuations in overall transcription rates. *EMBO J* 28: 123-134.

Ditty JL, Canales SR, Anderson BE, Williams SB, Golden SS (2005) Stability of the *Synechococcus elongatus* PCC 7942 circadian clock under directed anti-phase expression of the *kai* genes. *Microbiology* 151: 2605-2613.

Ditty JL, Mackey SR, Johnson CH, eds (2009) *Bacterial Circadian Programs* (Springer, Heidelberg), 333 pages.

Dong G, Yang Q, Wang Q, Kim YI, Wood TL, Osteryoung KW, van Oudenaarden A, Golden SS (2010) Elevated ATPase activity of KaiC applies a circadian checkpoint on cell division in *Synechococcus elongatus*. *Cell* 140: 529-539.

Dunlap JC, Loros JJ, DeCoursey PJ, Eds. (2004) *Chronobiology: Biological Timekeeping*. Sinauer, Sunderland, MA.

Dvomyk V, Vinogradova O, Nevo E (2003) Origin and evolution of circadian clock genes in prokaryotes. *Proc Natl Acad Sci USA* 100: 2495-2500.

Edery I, Zwiebel LJ, Dembinska ME, Rosbash M (1994) Temporal phosphorylation of the Drosophila period protein. *Proc Natl Acad Sci USA* 91: 2260-2264.

Elowitz MB, Leibler S (2000) A synthetic oscillatory network of transcriptional regulators. *Nature* 403: 335-338.

Fan Y, Hida A, Anderson DA, Izumo M, Johnson CH (2007) Cycling of CRYPTOCHROME proteins is not necessary for circadian-clock function in mammalian fibroblasts. *Curr Biol* 17: 1091-1100.

Garces RG, Wu N, Gillon W, Pai EF (2004) *Anabaena* circadian clock proteins KaiA and KaiB reveal a potential common binding site to their partner KaiC. *EMBO J* 23: 1688-1698.

Gekakis N, Saez L, Delahaye-Brown AM, Myers MP, Sehgal A, Young MW, Weitz CJ (1995) Isolation of *timeless* by PER protein interaction: defective interaction between *timeless* protein and long-period mutant PER^{L}. *Science* 270: 811-815.

Gillespie DT (1977) Exact stochastic simulation of coupled chemical reactions. *J Phys Chem* 81: 2340-2361.

Goldbeter A (1995) A Model for Circadian Oscillations in the Drosophila Period Protein (PER). *Proc Biol Sci* 261: 319-324.

Golden SS, Ishiura M, Johnson CH, Kondo T (1997) Cyanobacterial circadian rhythms. *Annu Rev Plant Physiol Plant Mol Biol* 48: 327–354.

Green J, Paget MS (2004) Bacterial redox sensors. *Nat Rev Microbiol* 2: 954-966.

Grobbelaar N, Huang TC, Lin HY, Chow TJ (1986) Dinitrogen-fixing endogenous rhythm in *Synechococcus* RF-1. *FEMS Microbiol Lett* 37: 173-177.

Hardin PE, Hall JC, Rosbash M (1990) Feedback of the Drosophila period gene product on circadian

cycling of its messenger RNA levels. *Nature* 343: 536-540.

Hastings MH, Maywood ES, O'Neill JS (2008) Cellular circadian pacemaking and the role of cytosolic rhythms. *Curr Biol* 18: R805-R815.

Hastings JW (2001) Cellular and molecular mechanisms of circadian regulation in the unicellular dinoflagellate *Gonyaulax polyedra.* In: *Handbook of Behavioral Neurobiology,vol 12: Circadian Clocks.* (J. Takahashi, F. Turek & R.Y. Moore, eds.) Plenum Press NY, pp. 321-334.

Hayashi F, Suzuki H, Iwase R, Uzumaki T, Miyake A, Shen JR, Imada K, Furukawa Y, Yonekura K, Namba K, Ishiura M (2003) ATP-induced hexameric ring structure of the cyanobacterial circadian clock protein KaiC. *Genes Cells* 8: 287-296.

Hayashi F, Ito H, Fujita M, Iwase R, Uzumaki T, Ishiura M (2004) Stoichiometric interactions between cyanobacterial clock proteins KaiA and KaiC. *Biochem Biophys Res Commun* 316:195-202.

Hitomi K, Oyama T, Han S, Arvai AS, Getzoff ED (2005) Tetrameric architecture of the circadian clock protein KaiB. A novel interface for intermolecular interactions and its impact on the circadian rhythm. *J Biol Chem* 280: 19127-19135.

Holtman CK, Chen Y, Sandoval P, Gonzales A, Nalty MS, Thomas TL, Youderian P, Golden SS (2005) High-throughput functional analysis of the *Synechococcus elongatus* PCC 7942 genome. *DNA Res* 12: 103-115.

Huang TC, Wang ST, Grobbelaar N (1993a) Circadian rhythm mutants of the prokaryotic *Synechococcus* RF-1. *Curr Microbil* 27: 249-254.

Huang ZJ, Edery I, Rosbash M (1993b) PAS is a dimerization domain common to *Drosophila* period and several transcription factors. *Nature* 364: 259-262.

Imai K, Nishiwaki T, Kondo T, Iwasaki H (2004) Circadian rhythms in the synthesis and degradation of a master clock protein KaiC in cyanobacteria. *J Biol Chem* 279: 36534-36539.

Ishiura M, et al. (1998) Expression of a gene cluster kaiABC as a circadian feedback process in cyanobacteria. *Science* 281: 1519-1523.

Isin EM, Guengerich FP (2006) Kinetics and thermodynamics of ligand binding by cytochrome P450 3A4. *J Biol Chem* 281: 9127-9136.

Ito H, et al. (2007) Autonomous synchronization of the circadian KaiC phosphorylation rhythm. *Nat Struct Mol Biol* 14:1084-1088.

Ivleva NB, Gao T, LiWang AC, Golden SS (2006) Quinone sensing by the circadian input kinase of the cyanobacterial circadian clock. *Proc Natl Acad Sci USA* 103: 17468-17473.

Iwasaki H, Taniguchi Y, Ishiura M, Kondo T (1999) Physical interactions among circadian clock proteins KaiA, KaiB and KaiC in cyanobacteria. *EMBO J* 18: 1137-1145.

Iwasaki H, Williams SB, Kitayama Y, Ishiura M, Golden SS, Kondo T (2000) A kaiC-interacting sensory histidine kinase, SasA, necessary to sustain robust circadian oscillation in cyanobacteria. *Cell* 101: 223-233.

Iwasaki H, Nishiwaki T, Kitayama Y, Nakajima M, Kondo T (2002) KaiA-stimulated KaiC phosphorylation in circadian timing loops in cyanobacteria. *Proc Natl Acad Sci USA* 99: 15788-15793.

Iwase R, Imada K, Hayashi F, Uzumaki T, Morishita M, Onai K, Furukawa Y, Namba K, Ishiura M (2005) Functionally important substructures of circadian clock protein KaiB in a unique tetramer complex. *J Biol Chem* 280: 43141-43149.

Johnson, CH (2004) Precise circadian clocks in prokaryotic cyanobacteria. *Curr Issues Mol Biol* 6: 103-110.

Johnson CH, Egli M, Stewart PL (2008a) Structural Insights into a Circadian Oscillator. *Science* 322: 697-701.

Johnson CH, Xu Y, Mori T (2008b) A Cyanobacterial Circadian Clockwork. *Current Biology* 18: R816–R825.

Kageyama H, Kondo T, Iwasaki H. (2003) Circadian formation of clock protein complexes by KaiA, KaiB, KaiC, and SasA in cyanobacteria. *J Biol Chem* 278: 2388-2395.

Kageyama H, Nishiwaki T, Nakajima M, Iwasaki H, Oyama T, Kondo T (2006) Cyanobacterial circadian pacemaker: Kai protein complex dynamics in the KaiC phosphorylation cycle in vitro. *Mol Cell* 23: 161-171.

Kim YI, Dong G, Carruthers CW Jr, Golden SS, LiWang A (2008) The day/night switch in KaiC, a central oscillator component of the circadian clock of cyanobacteria. *Proc Natl Acad Sci USA* 105: 12825-12830.

Kitayama Y, Iwasaki H, Nishiwaki T, Kondo T (2003) KaiB functions as an attenuator of KaiC phosphorylation in the cyanobacterial circadian clock system. *EMBO J* 22: 2127-2134.

Kitayama Y, Nishiwaki T, Terauchi K, Kondo T (2008) Dual KaiC-based oscillations constitute the

circadian system of cyanobacteria. *Genes Dev* 22: 1513-1521.

Kloss B, Price JL, Saez L, Blau J, Rothenfluh A, Wesley CS, Young MW (1998) The *Drosophila* clock gene *double-time* encodes a protein closely related to human casein kinase I epsilon. *Cell* 94: 97-107.

Kondo T, Strayer CA, Kulkarni RD, Taylor W, Ishiura M, Golden SS, Johnson CH (1993) Circadian rhythms in prokaryotes: luciferase as a reporter of circadian gene expression in cyanobacteria. *Proc Natl Acad Sci USA* 90: 5672-5676.

Kondo T, Ishiura M (1994) Circadian rhythms of cyanobacteria: monitoring the biological clocks of individual colonies by bioluminescence. *J Bacteriol* 176: 1881-1885.

Kondo T, Tsinoremas NF, Golden SS, Johnson CH, Kutsuna S, Ishiura M (1994) Circadian clock mutants of cyanobacteria. *Science* 266: 1233-1236.

Kondo T, Mori T, Lebedeva NV, Aoki S, Ishiura M, Golden SS (1997) Circadian rhythms in rapidly dividing cyanobacteria. *Science* 275: 224-227.

Kovaleski BJ, Kennedy R, Hong MK, Datta SA, Kleiman L, Rein A, Musier-Forsyth K (2006) In vitro characterization of the interaction between HIV-1 Gag and human lysyl-tRNA synthetase. *J Biol Chem* 281: 19449-19456.

Kutsuna S, Kondo T, Ikegami H, Uzumaki T, Katayama M, Ishiura M (2007) The circadian clock-related gene pex regulates a negative cis element in the kaiA promoter region. *J Bacteriol* 189: 7690-7696.

Lakin-Thomas PL (2006) Transcriptional feedback oscillators: maybe, maybe not.... *J Biol Rhythms* 21: 83-92.

Lee C, Bae K, Edery I (1999) PER and TIM inhibit the DNA binding activity of a *Drosophila* CLOCK-CYC/dBMAL1 heterodimer without disrupting formation of the heterodimer: a basis for circadian transcription. *Mol Cell Biol* 19: 5316-5325.

Leipe DD, Aravind L, Grishin NV, Koonin EV (2000) The bacterial replicative helicase DnaB evolved from a RecA duplication. *Genome Res* 10: 5-16.

Liu Y, Tsinoremas NF, Johnson CH, Lebedeva NV, Golden SS, Ishiura M, Kondo T (1995) Circadian orchestration of gene expression in cyanobacteria. *Genes Dev* 9: 1469-1478.

Lome J, Scheffer J, Lee A, Painter M, Miao VP (2000) Genes controlling circadian rhythm are widely distributed in cyanobacteria. *FEMS Microbiol Lett* 189: 129-133.

Malpica R, Franco B, Rodriguez C, Georgellis D (2004) Identification of a quinone- sensitive redox switch in the ArcB sensor kinase. *Proc Natl Acad Sci USA* 101: 13318–13323.

Markov DA, Swinney K, Bornhop DJ (2004) Label-free molecular interaction determinations with nanoscale interferometry. *J Am Chem Soc* 126: 16659-16664.

McAdams HH, Arkin A (1999) It's a noisy business! Genetic regulation at the nanomolar scale. *Trends Genet* 15: 65-69.

Merrow M, Roenneberg T (2007) Circadian clock: time for a phase shift of ideas? *Curr Biology* 17: R636-R638.

Mihalcescu I, Hsing W, Leibler S (2004) Resilient circadian oscillator revealed in individual cyanobacteria. *Nature* 430: 81-85.

Mitsui A, Kumazawa S, Takahashi A, Ikemoto H, Cao S, Arai, T (1986) Strategy by which nitrogen-fixing unicellular cyanobacteria grow photoautotrophically. Nature 323: 720-722.

Mori T, Binder B, Johnson CH (1996) Circadian gating of cell division in cyanobacteria growing with average doubling times of less than 24 hours. *Proc Natl Acad Sci USA* 93: 10183-10188.

Mori T, Saveliev SV, Xu Y, Stafford WF, Cox MM, Inman RB, Johnson CH (2002) Circadian clock protein KaiC forms ATP-dependent hexameric rings and binds DNA. *Proc Natl Acad Sci USA* 99: 17203-17208.

Mori T, Williams DR, Byrne MO, Qin X, Egli M, Mchaourab HS, Stewart PL, Johnson CH (2007) Elucidating the ticking of an in vitro circadian clockwork. *PLoS Biol* 5: e93. doi:10.1371/journal.pbio. 0050093

Müller B, Restle T, Reinstein J, Goody RS (1991) Interaction of fluorescently labeled dideoxynucleotides with HIV-1 reverse transcriptase. *Biochemistry* 30: 3709-3715.

Nagoshi E, Saini C, Bauer C, Laroche T, Naef F, Schibler U (2004) Circadian gene expression in individual fibroblasts: cell-autonomous and self-sustained oscillators pass time to daughter cells. *Cell* 119: 693-705.

Nakahira Y, Katayama M, Miyashita H, Kutsuna S, Iwasaki H, Oyama T, Kondo T (2004) Global gene repression by KaiC as a master process of prokaryotic circadian system. *Proc Natl Acad Sci USA* 101: 881-885.

Nakajima M, Imai K, Ito H, Nishiwaki T, Murayama Y, Iwasaki H, Oyama T, Kondo T (2005)

Reconstitution of circadian oscillation of cyanobacterial KaiC phosphorylation *in vitro*. *Science* 308: 414-415.

Nishiwaki T, Iwasaki H, Ishiura M, Kondo T (2000) Nucleotide binding and autophosphorylation of the clock protein KaiC as a circadian timing process of cyanobacteria. *Proc Natl Acad Sci USA* 97: 495–499.

Nishiwaki T, Satomi Y, Nakajima M, Lee C, Kiyohara R, Kageyama H, Kitayama Y, Temamoto M, Yamaguchi A, Hijikata A, Go M, Iwasaki H, Takao T, Kondo T (2004) Role of KaiC phosphorylation in the circadian clock system of *Synechococcus elongatus* PCC 7942. *Proc Natl Acad Sci USA* 101: 13927-13932.

Nishiwaki T, Satomi Y, Kitayama Y, Terauchi K, Kiyohara R, Takao T, Kondo T (2007) A sequential program of dual phosphorylation of KaiC as a basis for circadian rhythm in cyanobacteria. *EMBO J* 26: 4029-4037.

Ouyang Y, Andersson CR, Kondo T, Golden SS, Johnson CH (1998) Resonating circadian clocks enhance fitness in cyanobacteria. *Proc Natl Acad Sci USA* 95: 8660-8664.

Ozbudak EM, Thattai M, Kurtser I, Grossman AD, van Oudenaarden A (2002) Regulation of noise in the expression of a single gene. *Nat Genet* 31: 69-73.

Partensky F, Hess WR, Vaulot D (1999) Prochlorococcus, a marine photosynthetic prokaryote of global significance. *Microbiol Mol Biol Rev* 63: 106-127.

Pattanayek R, Wang J, Mori T, Xu Y, Johnson CH, Egli M (2004) Visualizing a circadian clock protein: crystal structure of KaiC and functional insights. *Mol Cell* 15: 375-388.

Pattanayek R, Williams DR, Pattanayek S, Xu Y, Mori T, Johnson CH, Stewart PL, Egli M (2006) Analysis of KaiA-KaiC protein interactions in the cyanobacterial circadian clock using hybrid structural methods. *EMBO J* 25: 2017-2028.

Pattanayek R, Williams DR, Pattanayek S, Mori T, Johnson CH, Stewart PL, Egli M (2008) Structural model of the circadian clock KaiB-KaiC complex and mechanism for modulation of KaiC phosphorylation. *EMBO J* 27: 1767-1778.

Pattanayek R, Mori T, Xu Y, Pattanayek S, Johnson CH, Egli M (2009) Structures of KaiC circadian clock mutant proteins: a new phosphorylation site at T426 and mechanisms of kinase, ATPase and phosphatase. *PLoS One* 4: e7529.

Qin X, Byrne M, Xu Y, Mori T, Johnson CH (2010a) Coupling of a core post-translational pacemaker to a

slave transcription/translation feedback loop in a circadian system. *PLoS Biol* 8: e1000394. doi:10.1371/journal.pbio.1000394

Qin X, Byrne M, Mori T, Zou P, Williams DR, McHaourab H, Johnson CH (2010b) Intermolecular associations determine the dynamics of the circadian KaiABC oscillator. Proc Natl Acad Sci U S A. [Epub ahead of print]

Reddy P, Zehring WA, Wheeler DA, Pirrotta V, Hadfield C, Hall JC, Rosbash M (1984) Molecular analysis of the *period* locus in *Drosophila* melanogaster and identification of a transcript involved in biological rhythms. *Cell* 38: 701-710.

Reid SL, Parry D, Liu HH, and Connolly BA (2001) Binding and recognition of GATATC target sequences by the EcoRV restriction endonuclease: a study using fluorescent oligonucleotides and fluorescence polarization. *Biochemistry* 40: 2484-2494.

Reppert SM, Weaver DR (2001) Molecular analysis of mammalian circadian rhythms. *Annu Rev Physiol* 63: 647-676.

Ripperger JA, Schibler U (2006) Rhythmic CLOCK-BMAL1 binding to multiple E-box motifs drives circadian Dbp transcription and chromatin transitions. *Nat Genet* 38: 369-374.

Rust MJ, Markson JS, Lane WS, Fisher DS, O'Shea EK (2007) Ordered phosphorylation governs oscillation of a three-protein circadian clock. *Science* 318: 809-812.

Schmitz O, Katayama M, Williams SB, Kondo T, Golden SS (2000) CikA, a bacteriophytochrome that resets the cyanobacterial circadian clock. *Science* 289: 765-768.

Shestakov SV and Khyen NT (1970) Evidence for genetic transformation in bluegreen alga *Anacystis nidulans*. *Mol Gen Genet* 107: 372.

Smith RM, Williams SB (2006) Circadian rhythms in gene transcription imparted by chromosome compaction in the cyanobacterium Synechococcus elongatus. *Proc Natl Acad Sci USA* 103:8564-8569.

Stal LJ and Krumbein WE (1985) Nitrogenase activity in the non-heterocystous cyanobacterium *Oscillatoria* sp. grown under alternating light-dark cycles. *Arch Microbiol* 143: 67-71.

Sweeney BM, Haxo FT (1961) Persistence of a Photosynthetic Rhythm in Enucleated Acetabularia. *Science* 134: 1361-1363.

Takai N, Nakajima M, Oyama T, Kito R, Sugita C, Sugita M, Kondo T, Iwasaki H (2006) A KaiC-associating SasA-RpaA two-component regulatory system as a major circadian timing mediator

in cyanobacteria. *Proc Natl Acad Sci USA* 103: 12109-12114.

Terauchi K, Kitayama Y, Nishiwaki T, Miwa K, Murayama Y, Oyama T, Kondo T (2007) ATPase activity of KaiC determines the basic timing for circadian clock of cyanobacteria. *Proc Natl Acad Sci USA* 104:16377-16381.

Taniguchi Y, Yamaguchi A, Hijikata A, Iwasaki H, Kamagata K, Ishiura M, Go M, Kondo T (2001) Two KaiA-binding domains of cyanobacterial circadian clock protein KaiC. *FEBS Lett* 496:86-90.

Taniguchi Y, Katayama M, Ito R, Takai N, Kondo T, Oyama T (2007) *labA*: a novel gene required for negative feedback regulation of the cyanobacterial circadian clock protein KaiC. *Genes Dev* 21: 60-70.

Taniguchi Y, Takai N, Katayama M, Kondo T, Oyama T (2010) Three major output pathways from the KaiABC-based oscillator cooperate to generate robust circadian *kaiBC* expression in cyanobacteria. *Proc Natl Acad Sci USA* 107: 3263-3268.

Tigges M, Marquez-Lago TT, Stelling J, Fussenegger M (2009) A tunable synthetic mammalian oscillator. *Nature* 457: 309-312.

Tigges M, Dénervaud N, Greber D, Stelling J, Fussenegger M (2010) A synthetic low-frequency mammalian oscillator. *Nucleic Acids Res* 38: 2702-2711.

Tomita J, Nakajima M, Kondo T, Iwasaki H (2005) No transcription-translation feedback in circadian rhythm of KaiC phosphorylation. *Science* 307:251-254.

Uzumaki T, et al. (2004) Crystal structure of the C-terminal clock-oscillator domain of the cyanobacterial KaiA protein. *Nat Struct Mol Biol* 11: 623-631.

Vakonakis I, LiWang AC (2004) Structure of the C-terminal domain of the clock protein KaiA in complex with a KaiC-derived peptide: implications for KaiC regulation. *Proc Natl Acad Sci USA* 101:10925-10930.

van Zon JS, Lubensky DK, Altena PR, ten Wolde PR (2007) An allosteric model of circadian KaiC phosphorylation. *Proc Natl Acad Sci USA* 104: 7420-7425.

Vielhaber E, Eide E, Rivers A, Gao ZH, Virshup DM (2000) Nuclear entry of the circadian regulator mPER1 is controlled by mammalian casein kinase I epsilon. *Mol Cell Biol* 20: 4888-4899.

Vijayan V, Zuzow R, O'Shea EK (2009) Oscillations in supercoiling drive circadian gene expression in cyanobacteria. *Proc Natl Acad Sci USA* 106: 22564-22568.

Walter NG, Huang CY, Manzo AJ, Sobhy MA (2008) Do-it-yourself guide: how to use the modern single-molecule toolkit. *Nat Methods* 5: 475-489.

Welsh DK, Yoo SH, Liu AC, Takahashi JS, Kay SA (2004) Bioluminescence imaging of individual fibroblasts reveals persistent, independently phased circadian rhythms of clock gene expression. *Curr Biol* 14: 2289-2295.

Williams SB, Vakonakis I, Golden SS, LiWang AC (2002) Structure and function from the circadian clock protein KaiA of *Synechococcus elongatus*: a potential clock input mechanism. *Proc Natl Acad Sci USA* 99: 15357-15362.

Wood TL, Bridwell-Rabb J, Kim YI, Gao T, Chang YG, LiWang A, Barondeau DP, Golden SS (2010) The KaiA protein of the cyanobacterial circadian oscillator is modulated by a redox-active cofactor. *Proc Natl Acad Sci USA* 107: 5804-5809.

Woelfle MA, Ouyang Y, Phanvijhitsiri K, Johnson CH (2004) The adaptive value of circadian clocks: an experimental assessment in cyanobacteria. *Current Biol* 14: 1481-1486.

Woelfle MA, Xu Y, Qin X, Johnson CH (2007) Circadian rhythms of superhelical status of DNA in cyanobacteria. *Proc Natl Acad Sci USA* 104:18819-18824.

Woolum JC (1991) A re-examination of the role of the nucleus in generating the circadian rhythm in *Acetabularia*. *J. Biol. Rhythms* 6: 129-136.

Xu Y, Mori T, Johnson CH (2000) Circadian clock-protein expression in cyanobacteria: rhythms and phase setting. *EMBO J* 19: 3349-3357.

Xu Y, Mori T, Johnson CH (2003) Cyanobacterial circadian clockwork: roles of KaiA, KaiB and the kaiBC promoter in regulating KaiC. *EMBO J* 22: 2117-2126.

Xu Y, Mori T, Pattanayek R, Pattanayek S, Egli M, Johnson CH (2004) Identification of key phosphorylation sites in the circadian clock protein KaiC by crystallographic and mutagenetic analyses. *Proc Natl Acad Sci USA* 101: 13933-13938.

Xu Y, Mori T, Qin X, Yan H, Egli M, Johnson CH (2009) Intramolecular regulation of phosphorylation status of the circadian clock protein kaiC. *PLoS ONE* 4:e7509.

Ye S, Vakonakis I, Ioerger TR (2004) Crystal structure of circadian clock protein KaiA from *Synechococcus elongatus*. *J Biol Chem* 279: 20511-20518.

Yildiz O, Doi M, Yujnovsky I, Cardone L, Berndt A, Hennig S, Schulze S, Urbanke C, Sassone-Corsi P,

Wolf E. (2005) Crystal structure and interactions of the PAS repeat region of the Drosophila clock protein PERIOD. *Mol Cell* 17: 69-82.